Supplementary Information

Facile Tuning of the Aggregation Induced Emission Wavelength in a Common Framework of a Cyclometalated Iridium(III) Complex : Micellar Encapsulated Probe in Celluler Imaging

Parvej Alam[a], Pradip Das[b], Clàudia Climent[c], Maheswararao Karanam[d], Pere Alemany[c]*, Angshuman Roy Choudhury[d]*, Nikhil R. Jana[b]*, Inamur Rahaman Laskar[a]*

[a]Department of Chemistry, Birla Institute of Technology and Science, Pilani Campus, Pilani, Rajasthan, India, ir_laskar@bits-pilani.ac.in; [b]Centre For Advanced Materials, Indian Association for the Cultivation of Science, Kolkata-32, India, camnrj@iacs.res.in; [c]Departament de Química Física and Institut de Química Teòrica i Computacional (IQTCUB), Universitat de Barcelona. Martí i Franquès 1-11, 08028 Barcelona, Spain, Email: p.alemany@ub.edu; [d]Department of Chemical Sciences, Indian Institute of Science Education and Research (IISER), Mohali, Sector 81, S. A. S. Nagar, Manauli PO, Mohali, Punjab, 140306, India, angshurc@iisermohali.ac.in

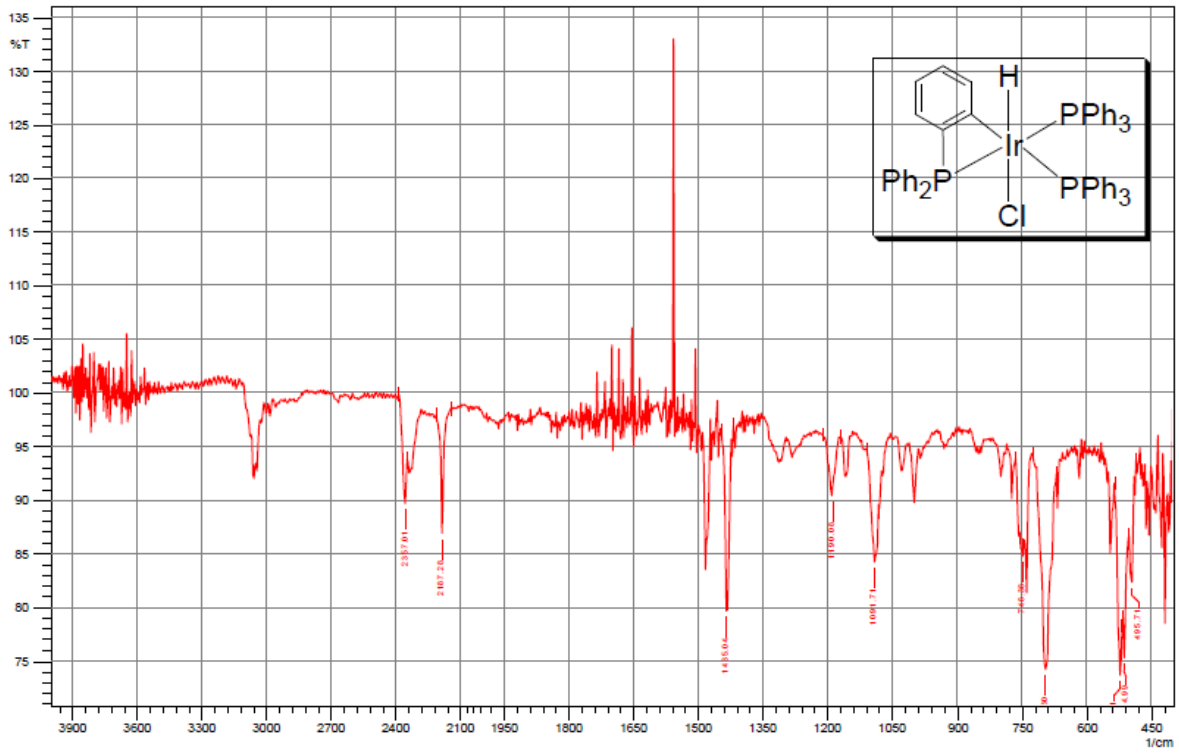

a

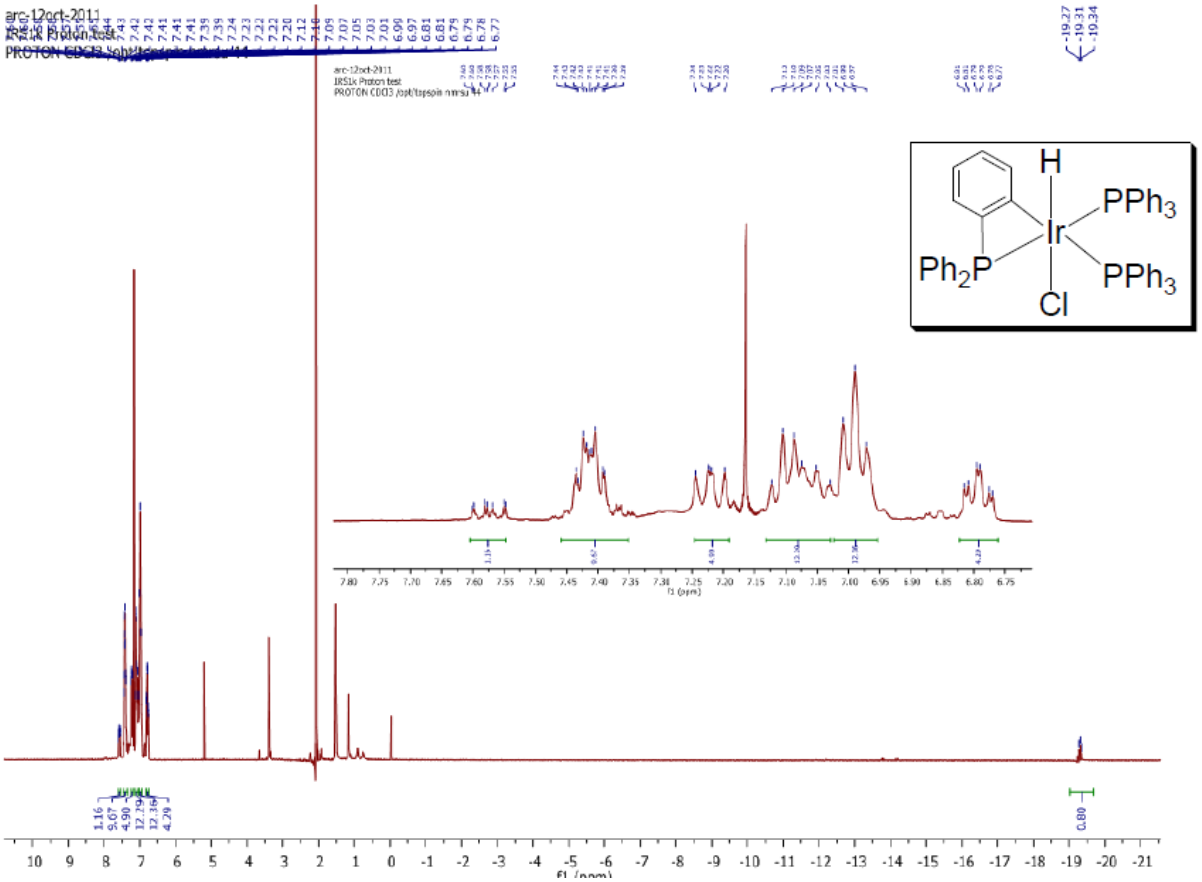
arc-12oct-2011
IR51k Proton test
PROTON CDCl3
H
PPh3
Ir
Ph2P
PPh3
Cl
f1 (ppm)

b

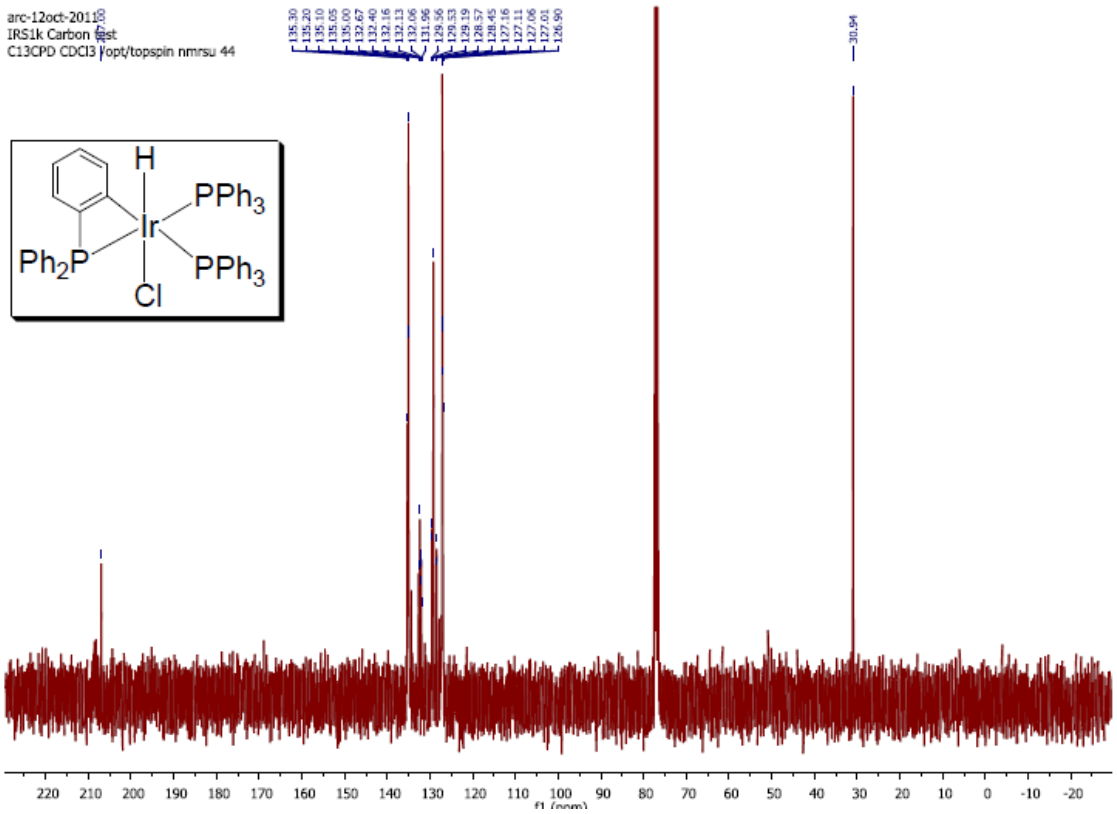
arc-12oct-2011
IRS1k Carbon test
C13CPD CDCl3 /opt/topspin nmrsu 44
H
PPh3
Ir
Ph2P
PPh3
Cl
135.30
135.20
135.10
135.05
135.00
132.67
132.40
132.16
132.13
132.06
131.96
129.56
129.53
129.19
128.57
128.45
127.16
127.11
127.06
127.01
126.90
30.94
220 210 200 190 180 170 160 150 140 130 120 110 100 90 80 70 60 50 40 30 20 10 0 -10 -20
f1 (ppm)

c

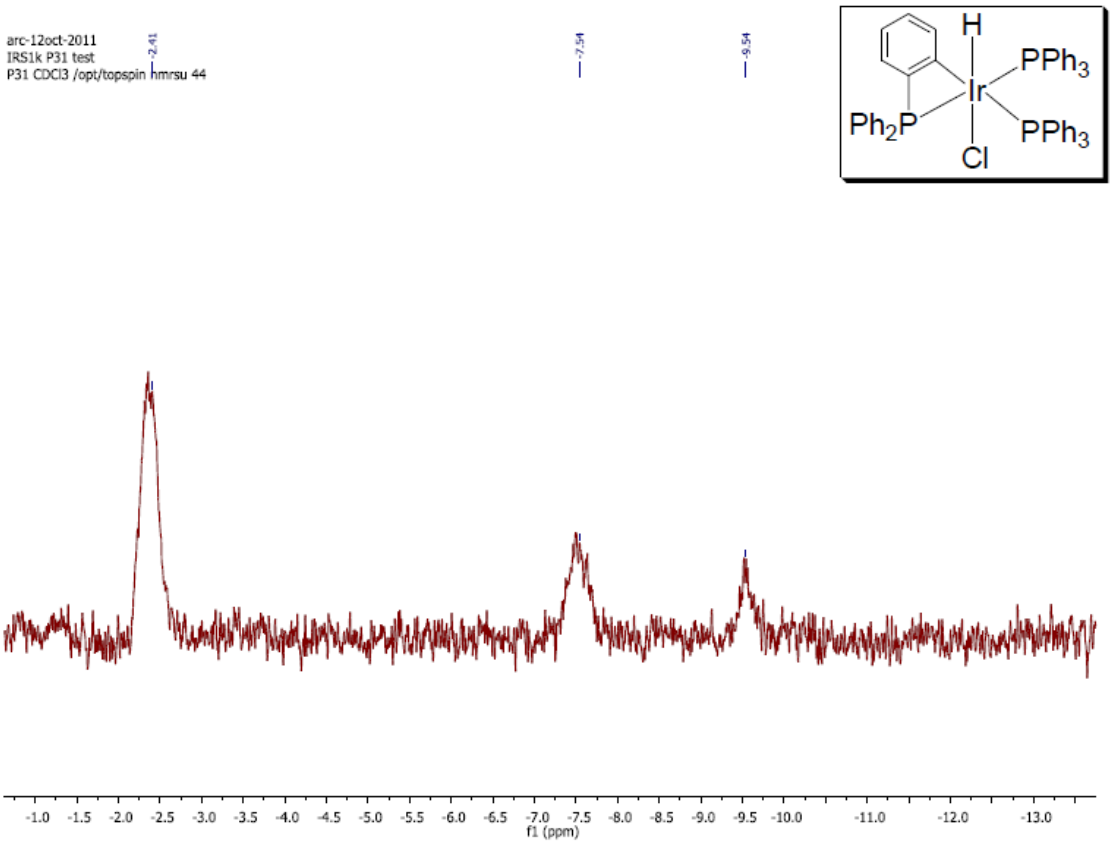

d

Fig. S1. IR and (^{1}H,^{13}C,^{31}P) NMR spectra are shown in a, b, c, d, respectively for the intermediate, A(i).

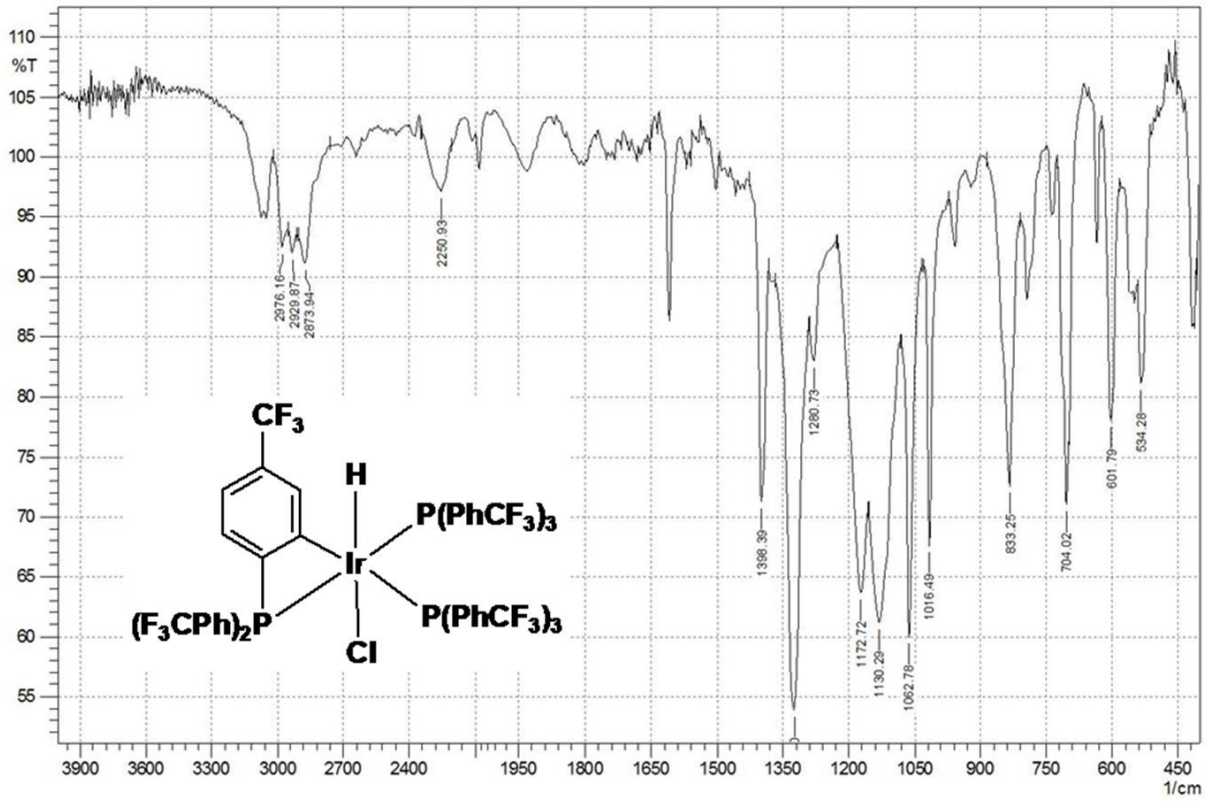
%T
110
105
100
95
90
85
80
75
70
65
60
55
2976.16
2929.87
2873.94
2250.93
1398.39
1280.73
1172.72
1130.29
1062.78
1016.49
833.25
704.02
601.79
534.28
3900
3600
3300
3000
2700
2400
1950
1800
1650
1500
1350
1200
1050
900
750
600
450
1/cm
CF3
H
P(PhCF3)3
Ir
(F3CPh)2P
P(PhCF3)3
Cl

a

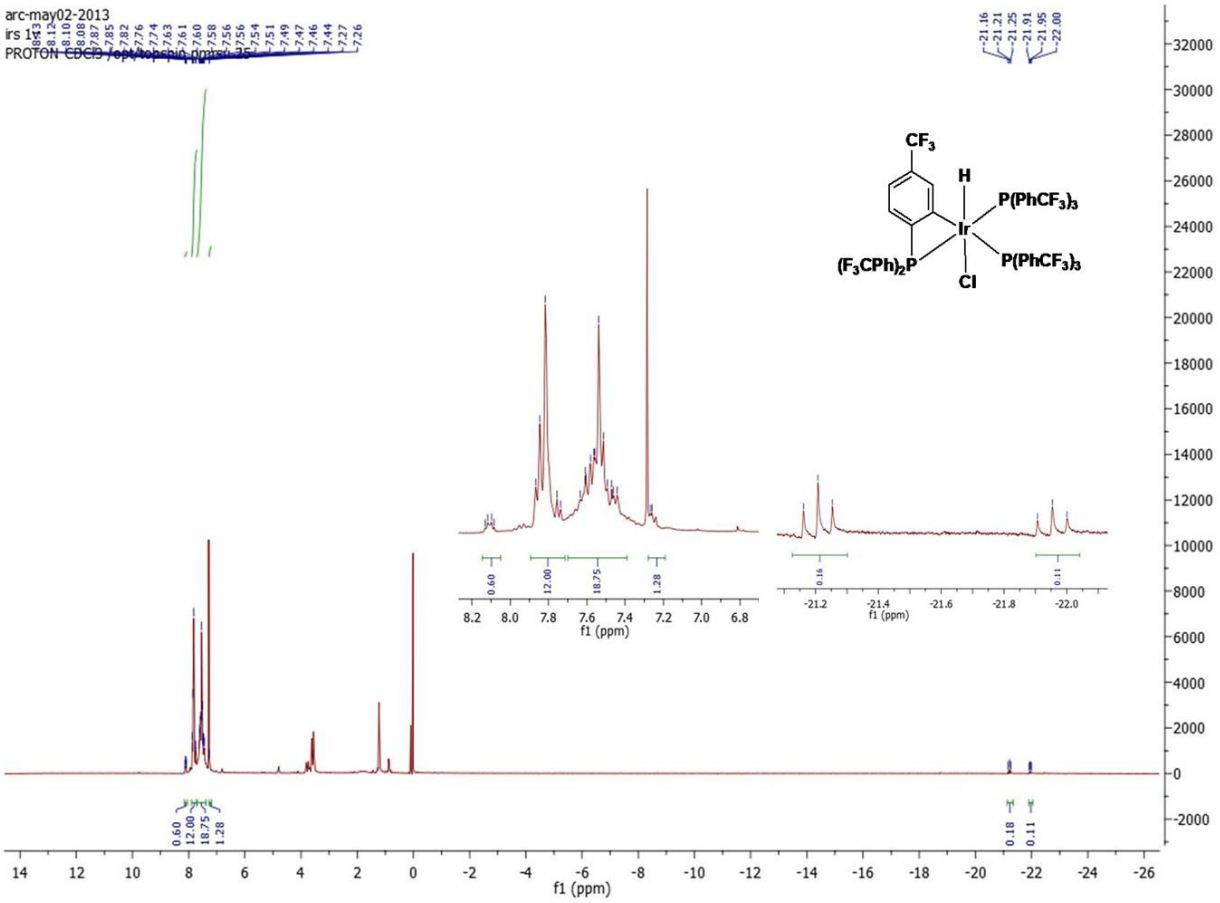
arc-may02-2013
irs 1H
PROTON CDCl3 /opt/topspin
CF3
H
P(PhCF3)3
Ir
(F3CPh)2P
P(PhCF3)3
Cl
f1 (ppm)

b

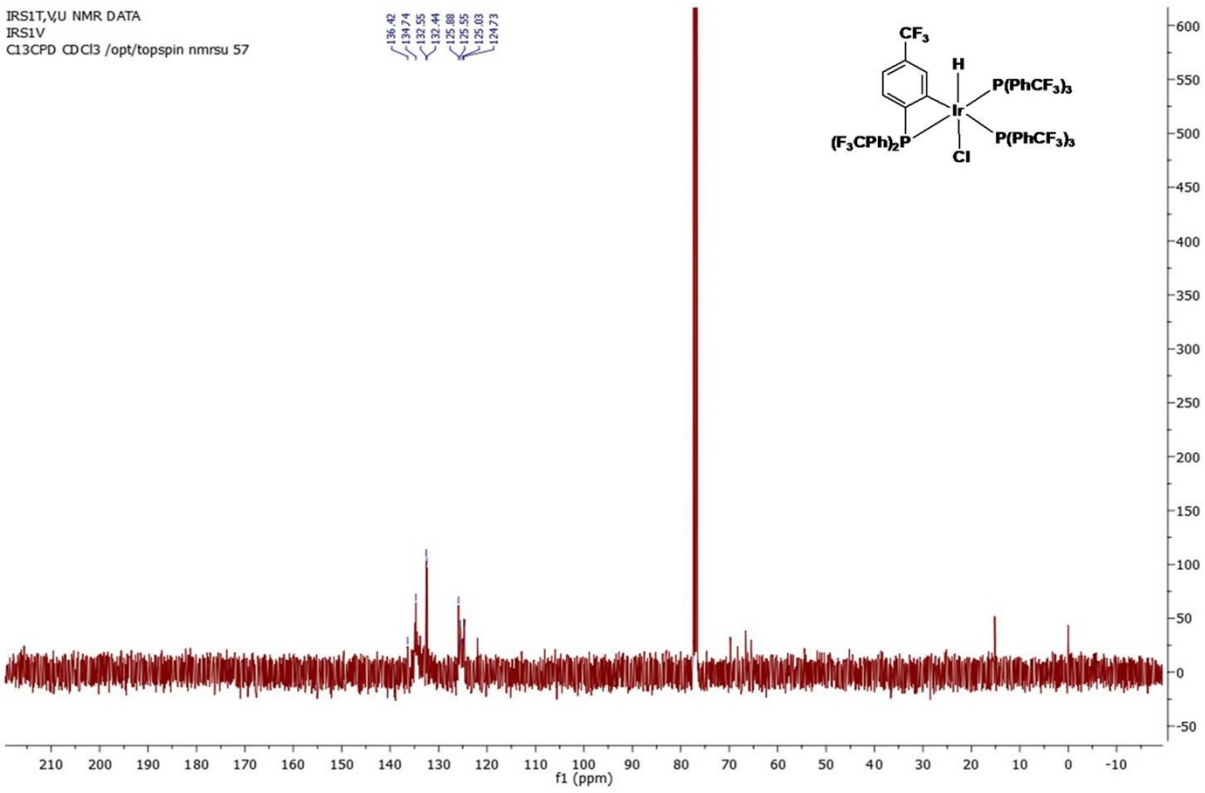
IRS1T,V,U NMR DATA
IRS1V
C13CPD CDCl3 /opt/topspin nmrsu 57
136.42
134.74
132.55
132.44
125.88
125.55
125.03
124.73
CF3
H
P(PhCF3)3
Ir
(F3CPh)2P
P(PhCF3)3
Cl
f1 (ppm)

c

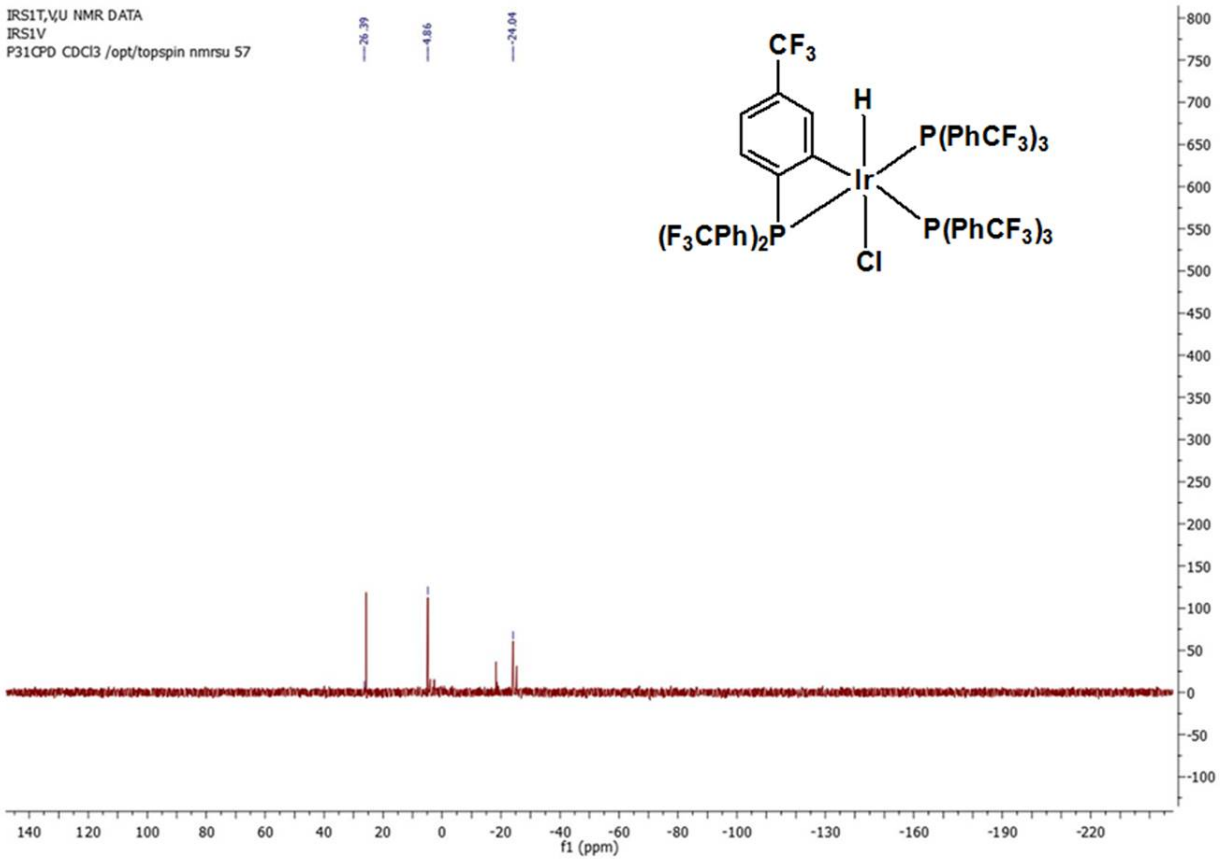

d

Fig. S2. IR and (^{1}H,^{13}C,^{31}P) NMR spectra are shown in a, b, c, d, respectively for the intermediate, A(j).

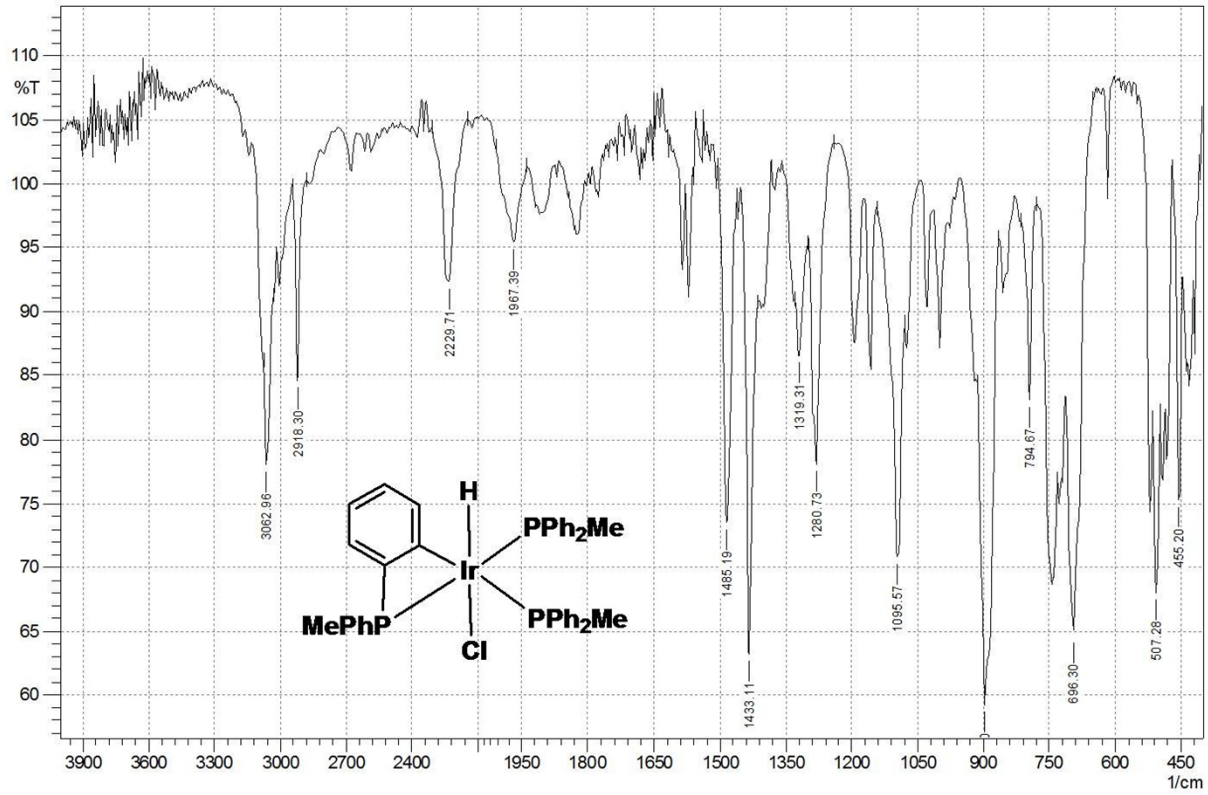
%T
110
105
100
95
90
85
80
75
70
65
60
3062.96
2918.30
2229.71
1967.39
1485.19
1433.11
1319.31
1280.73
1095.57
794.67
696.30
507.28
455.20
H
PPh2Me
Ir
PPh2Me
MePhP
Cl
3900
3600
3300
3000
2700
2400
1950
1800
1650
1500
1350
1200
1050
900
750
600
450
1/cm

a

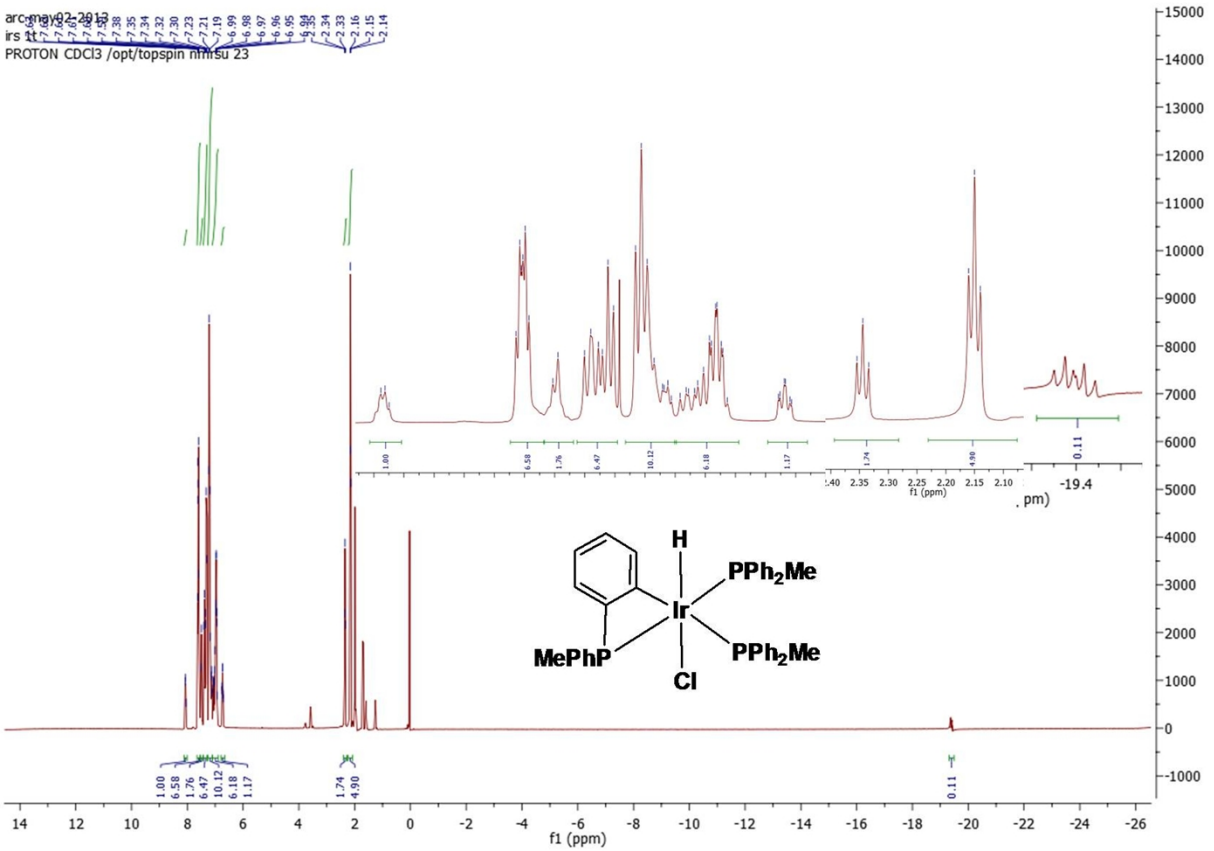
PROTON CDCl3 /opt/topspin nmrsu 23
H
PPh2Me
Ir
MePhP
PPh2Me
Cl
f1 (ppm)
-19.4

b

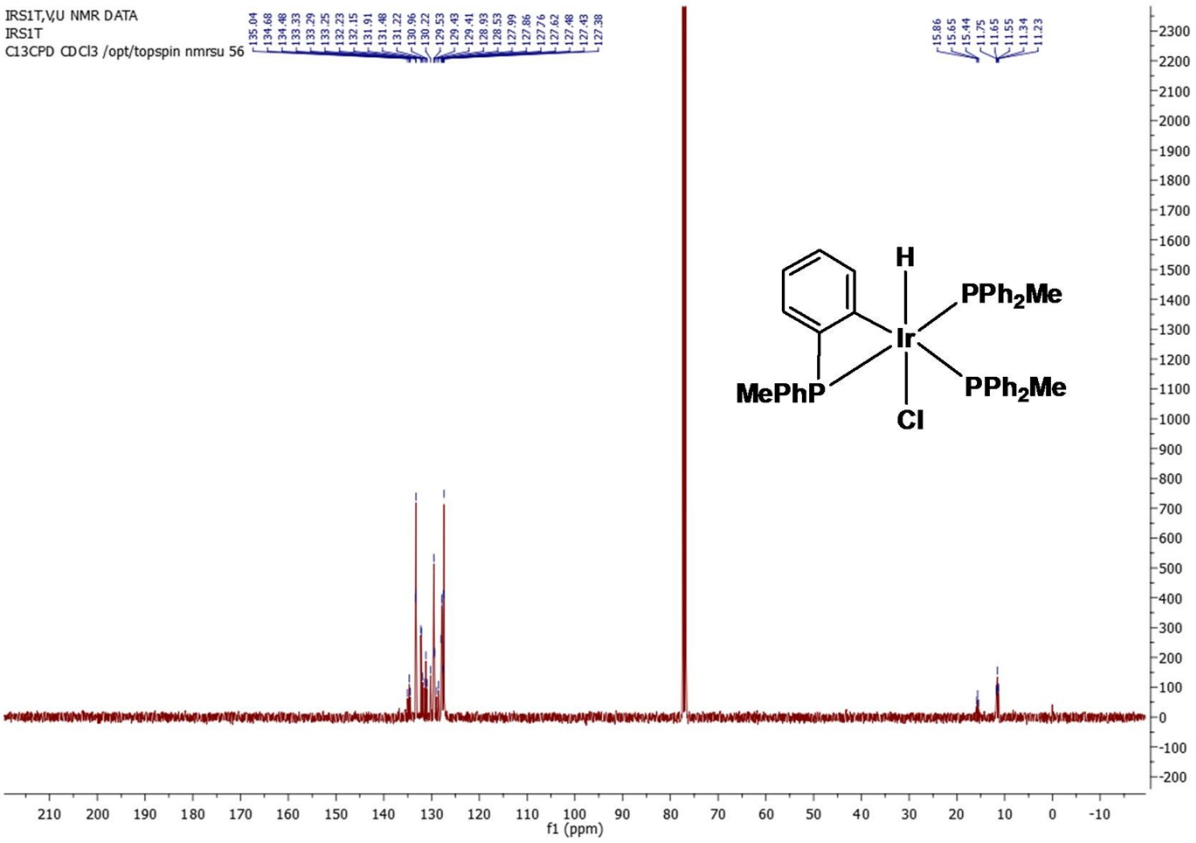
IRS1T,V,U NMR DATA
IRS1T
C13CPD CDCl3 /opt/topspin nmrsu 56
H
PPh2Me
Ir
MePhP
PPh2Me
Cl
f1 (ppm)

c

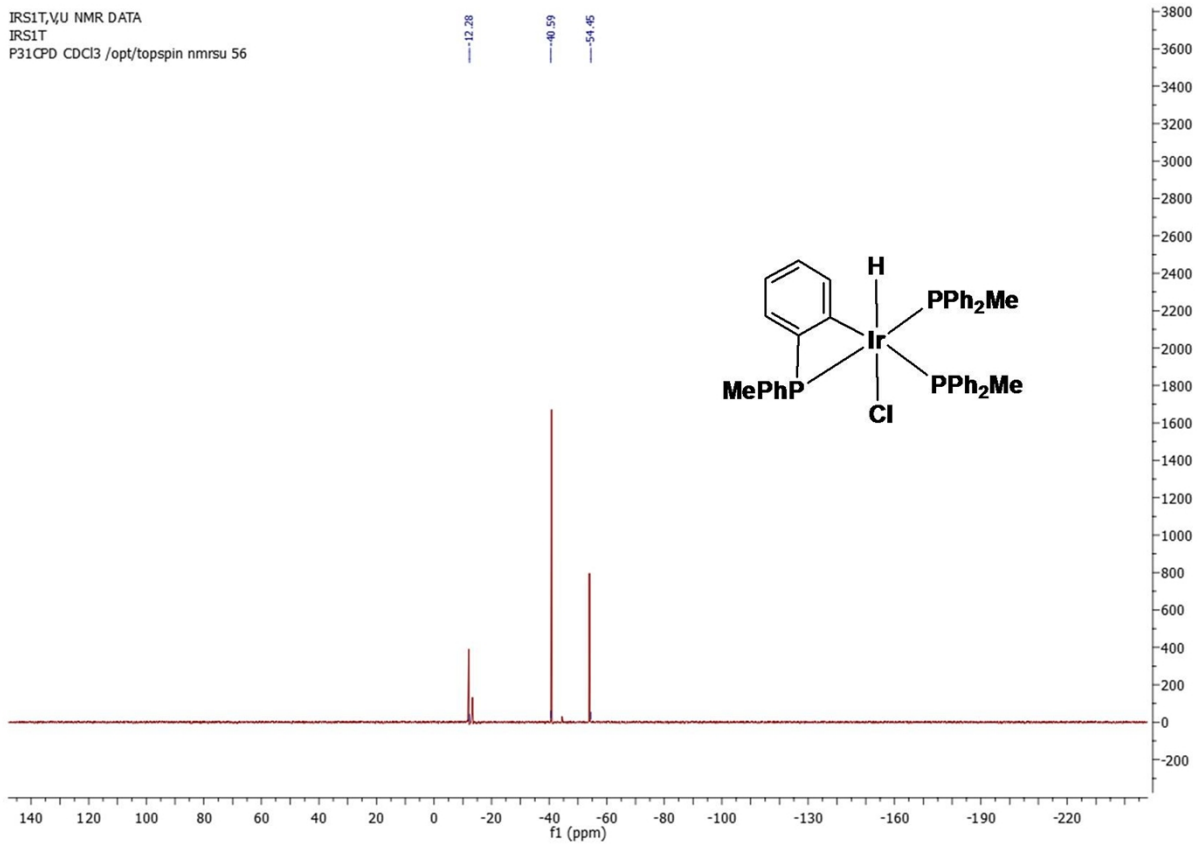

d

Fig. S3. IR and (^{1}H,^{13}C,^{31}P) NMR spectra are shown in a, b, c, d, respectively for the intermediate, A(k).

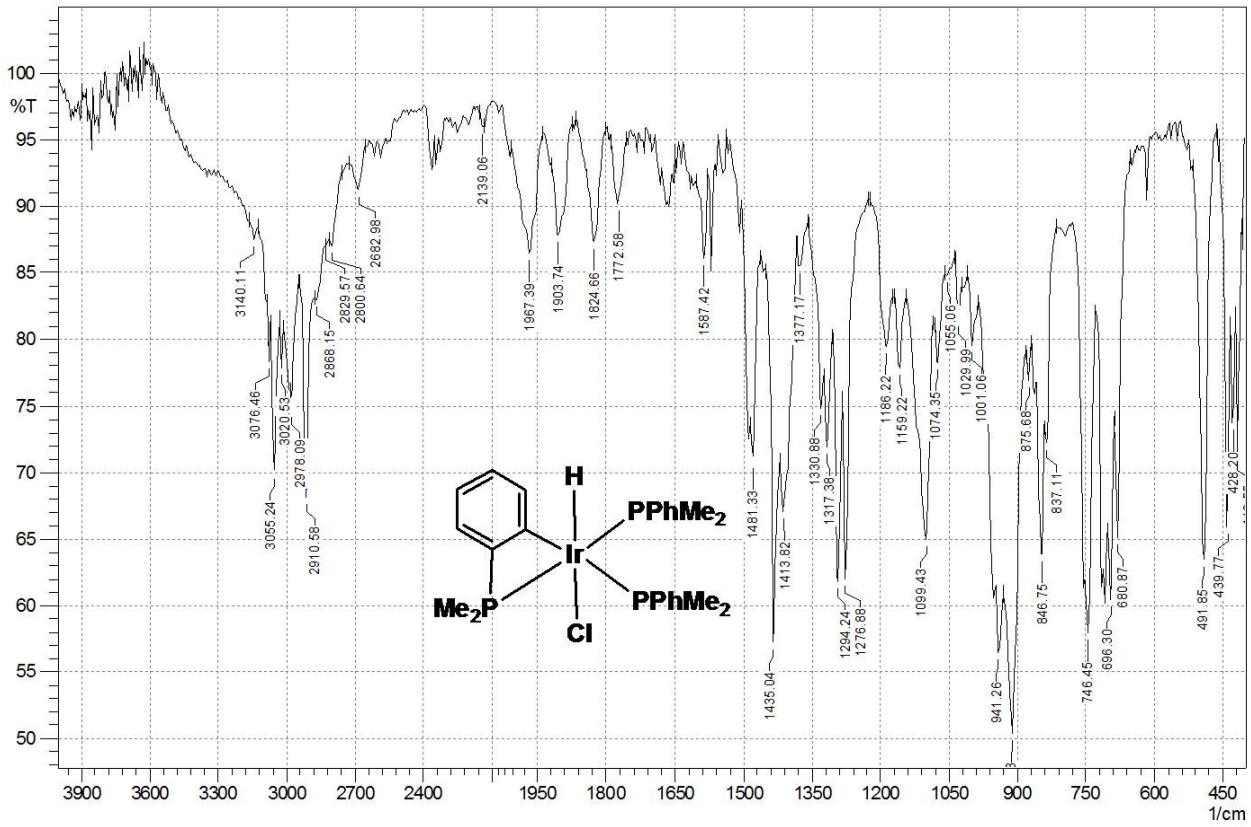
100
%T
95
90
85
80
75
70
65
60
55
50
3900
3600
3300
3000
2700
2400
1950
1800
1650
1500
1350
1200
1050
900
750
600
450
1/cm
3140.11
3076.46
3055.24
3020.53
2978.09
2910.58
2868.15
2829.57
2800.64
2682.98
2139.06
1967.39
1903.74
1824.66
1772.58
1587.42
1481.33
1435.04
1413.82
1377.17
1330.88
1317.38
1294.24
1276.88
1186.22
1159.22
1099.43
1074.35
1055.06
1029.99
1001.06
941.26
875.68
846.75
837.11
746.45
696.30
680.87
491.85
439.77
428.20
H
PPhMe2
Ir
Me2P
PPhMe2
Cl

a

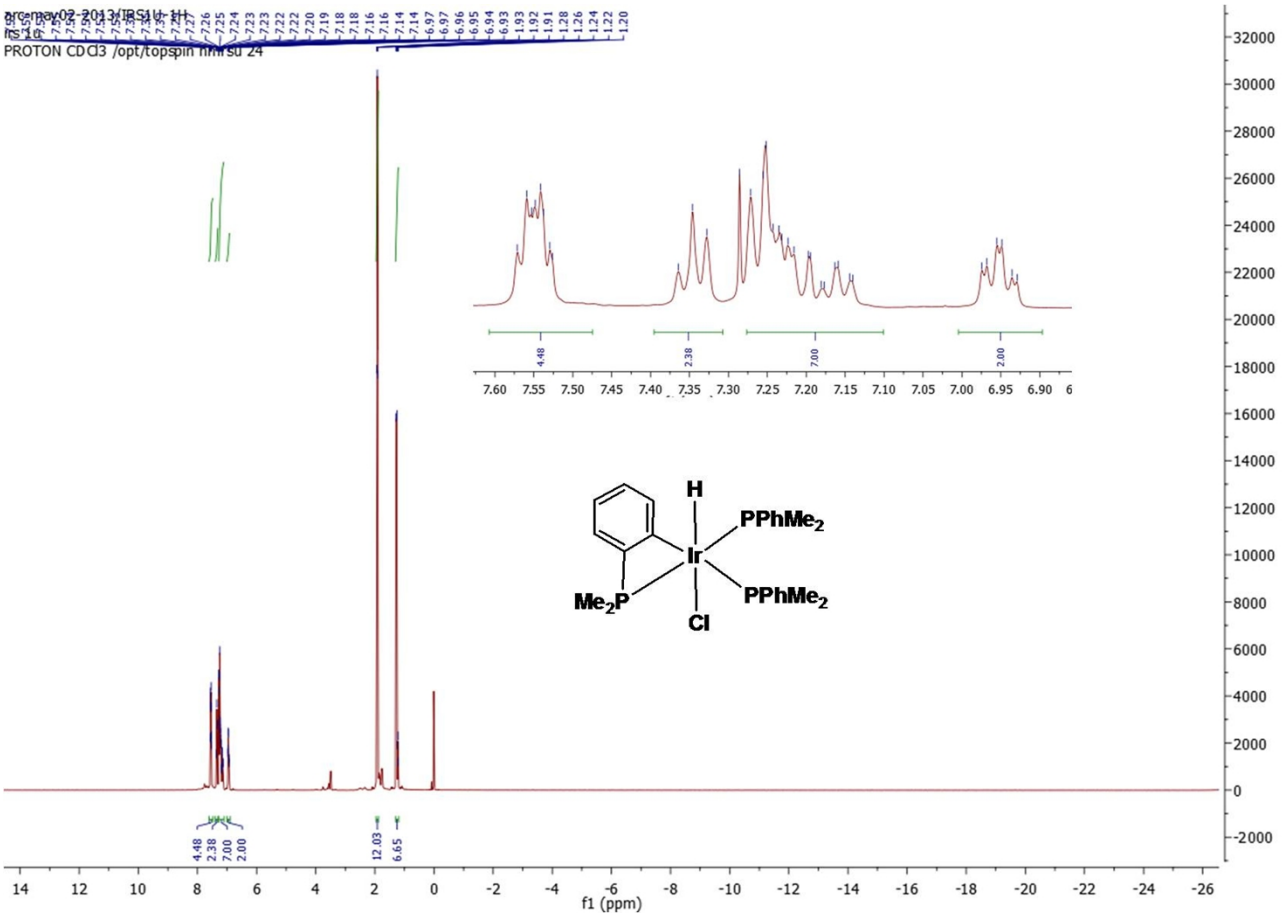
PROTON CDCl3 /opt/topspin nmrsu 24
4.48
2.38
7.00
2.00
12.03
6.65
f1 (ppm)
H
PPhMe2
Ir
PPhMe2
Me2P
Cl

b

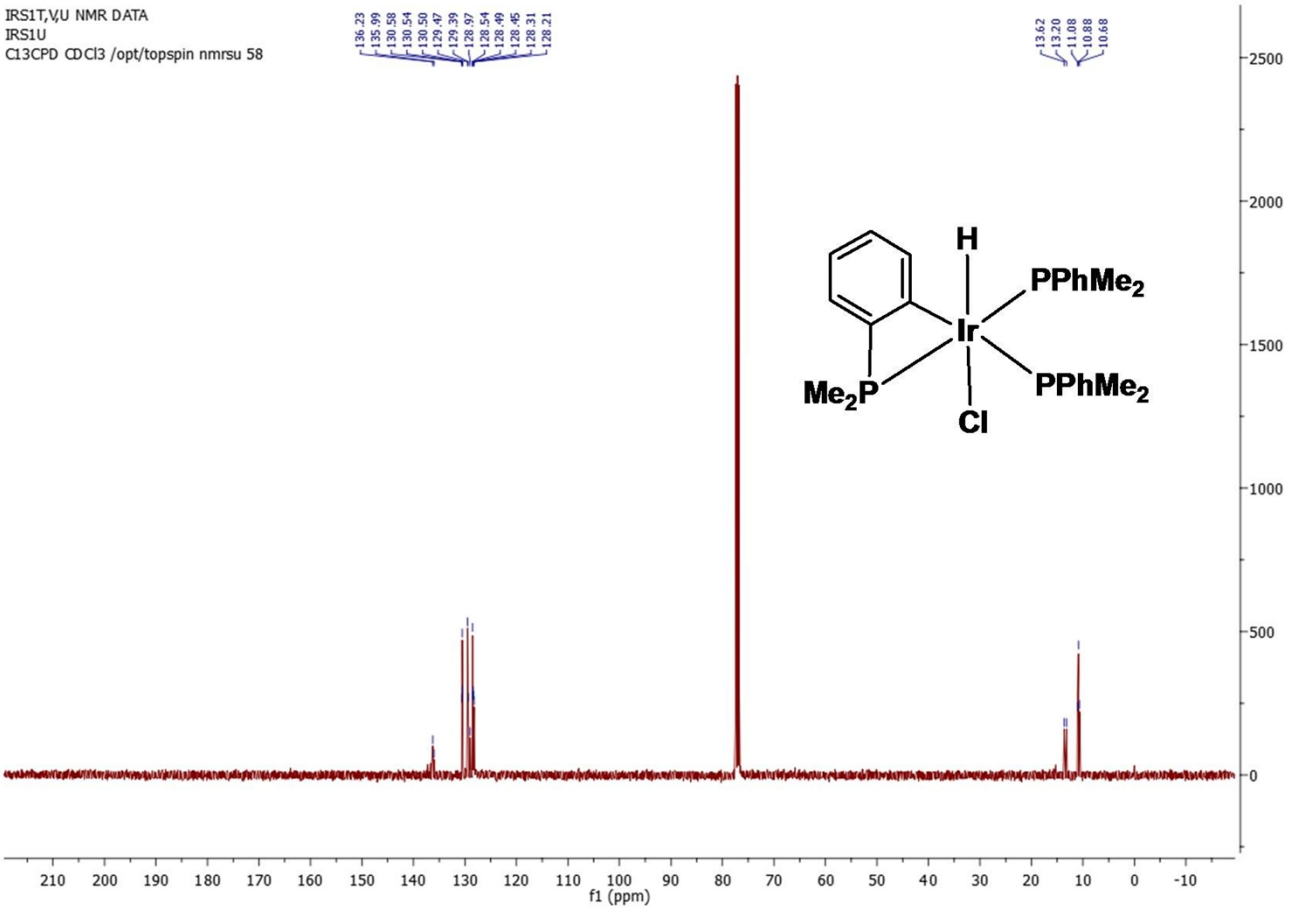
IRS1T,V,U NMR DATA
IRS1U
C13CPD CDCl3 /opt/topspin nmrsu 58
136.23
135.99
130.58
130.54
130.50
129.47
129.39
128.97
128.54
128.49
128.45
128.31
128.21
13.62
13.20
11.08
10.88
10.68
H
PPhMe2
Ir
Me2P
PPhMe2
Cl
2500
2000
1500
1000
500
0
210 200 190 180 170 160 150 140 130 120 110 100 90 80 70 60 50 40 30 20 10 0 -10
f1 (ppm)

c

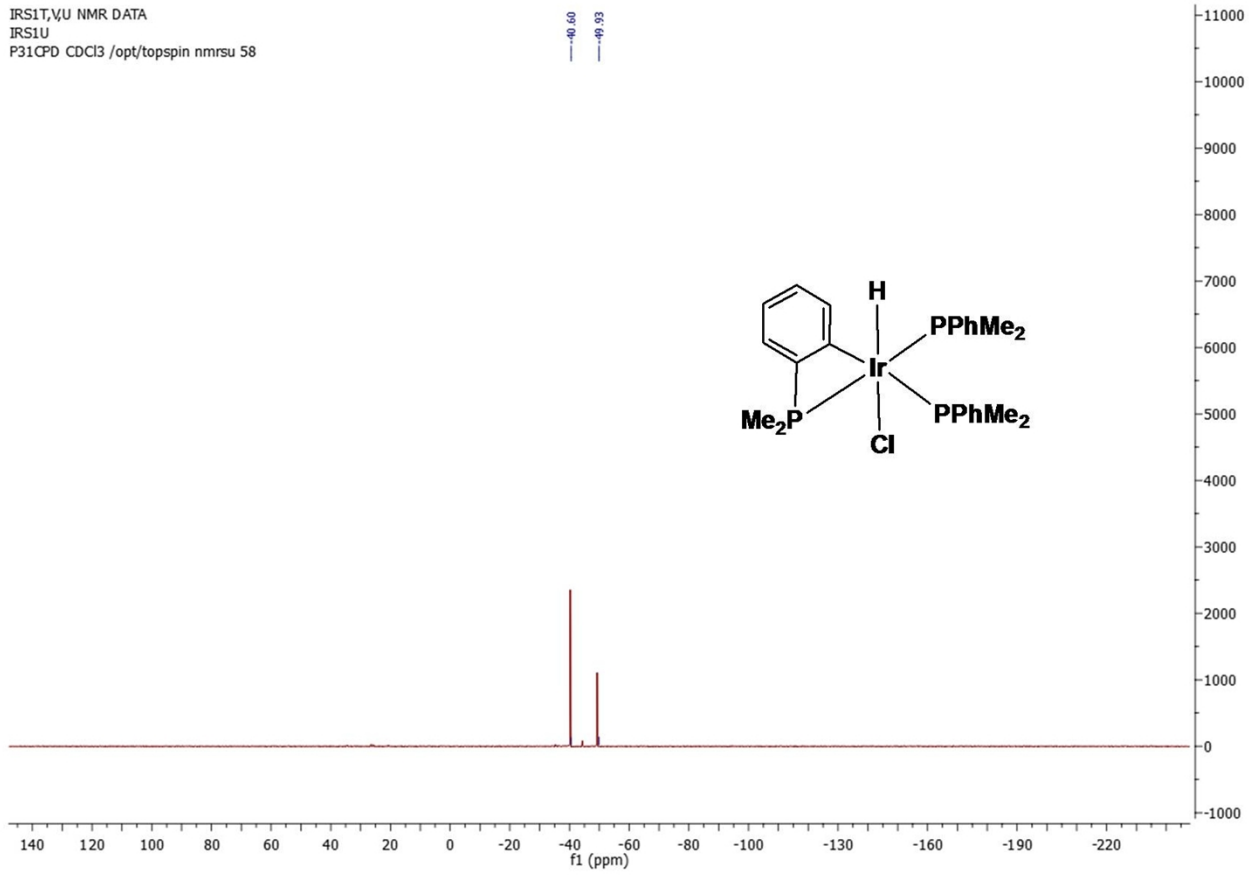

d

Fig. S4. IR and (^{1}H,^{13}C,^{31}P) NMR spectra are shown in a, b, c, d, respectively for the intermediate, A(l).

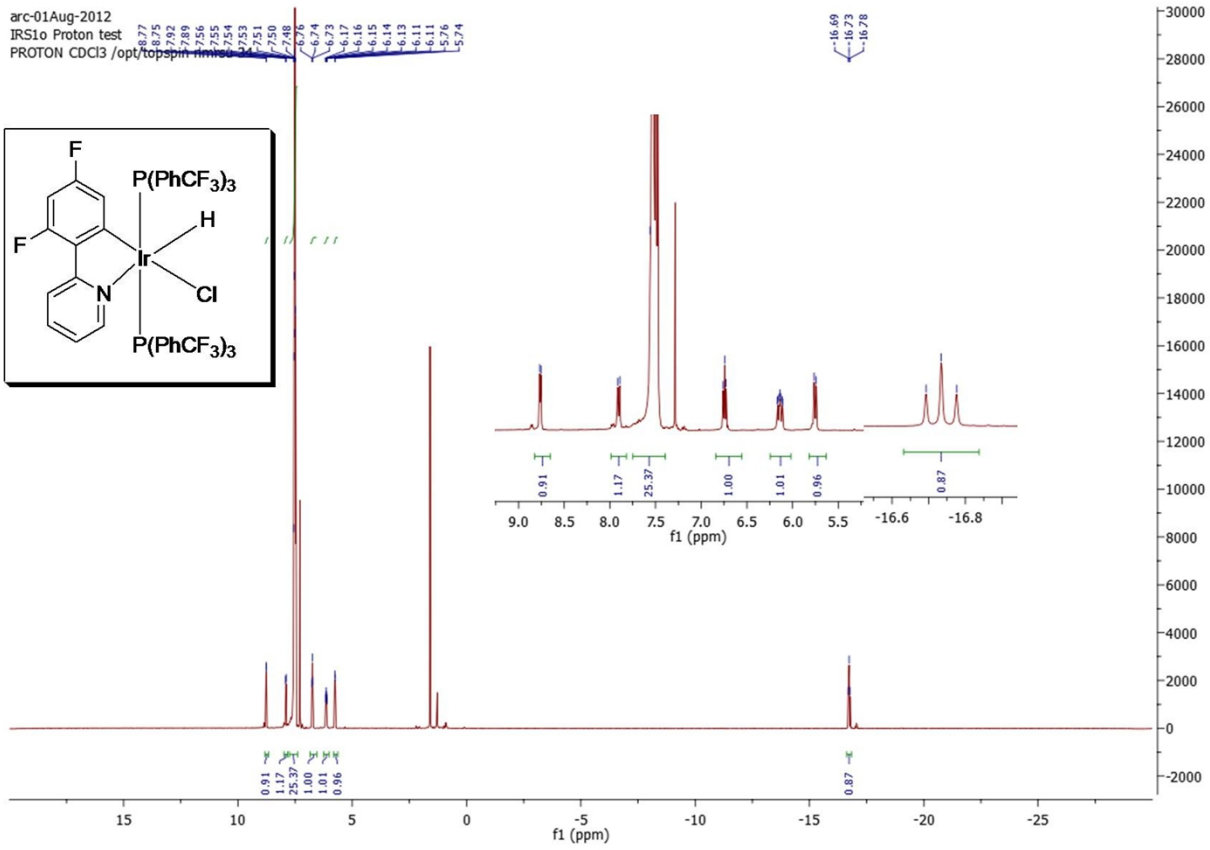
arc-01Aug-2012
IRS1o Proton test
PROTON CDCl3 /opt/topspin
F
P(PhCF3)3
H
F
Ir
N
Cl
P(PhCF3)3
f1 (ppm)

a

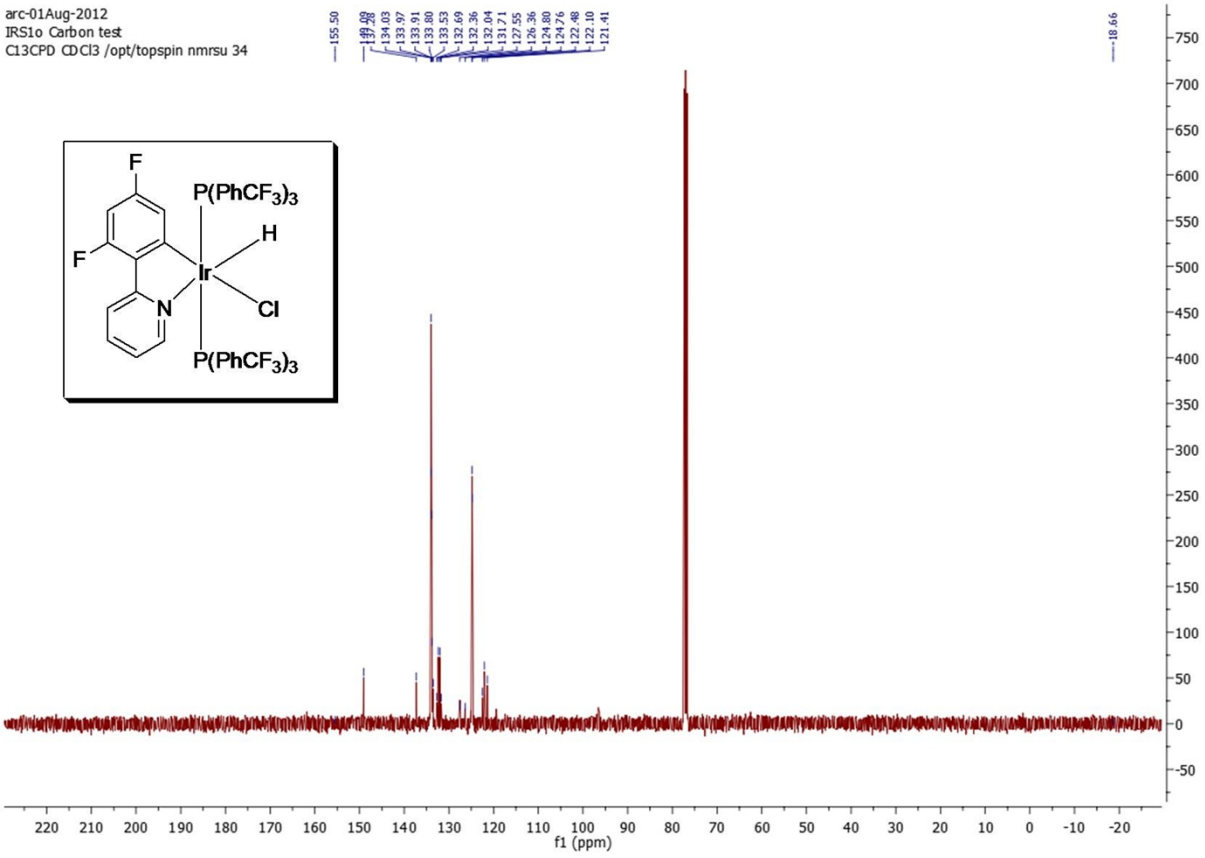
arc-01Aug-2012
IRS1o Carbon test
C13CPD CDCl3 /opt/topspin nmrsu 34
F
P(PhCF3)3
H
F
Ir
N
Cl
P(PhCF3)3
f1 (ppm)

b

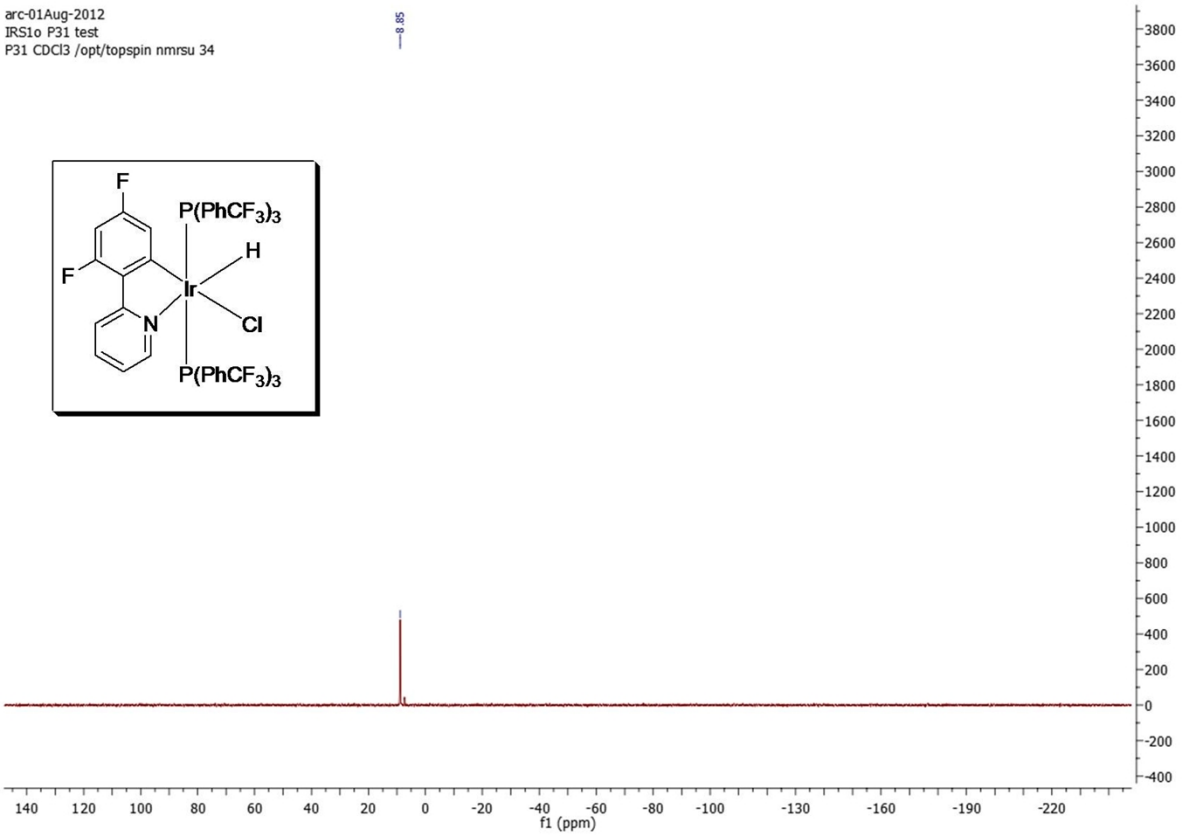
arc-01Aug-2012
IRS1o P31 test
P31 CDCl3 /opt/topspin nmrsu 34
8.85
F
P(PhCF3)3
H
F
Ir
N
Cl
P(PhCF3)3
3800
3600
3400
3200
3000
2800
2600
2400
2200
2000
1800
1600
1400
1200
1000
800
600
400
200
0
-200
-400
140
120
100
80
60
40
20
0
-20
-40
-60
-80
-100
-130
-160
-190
-220
f1 (ppm)

c

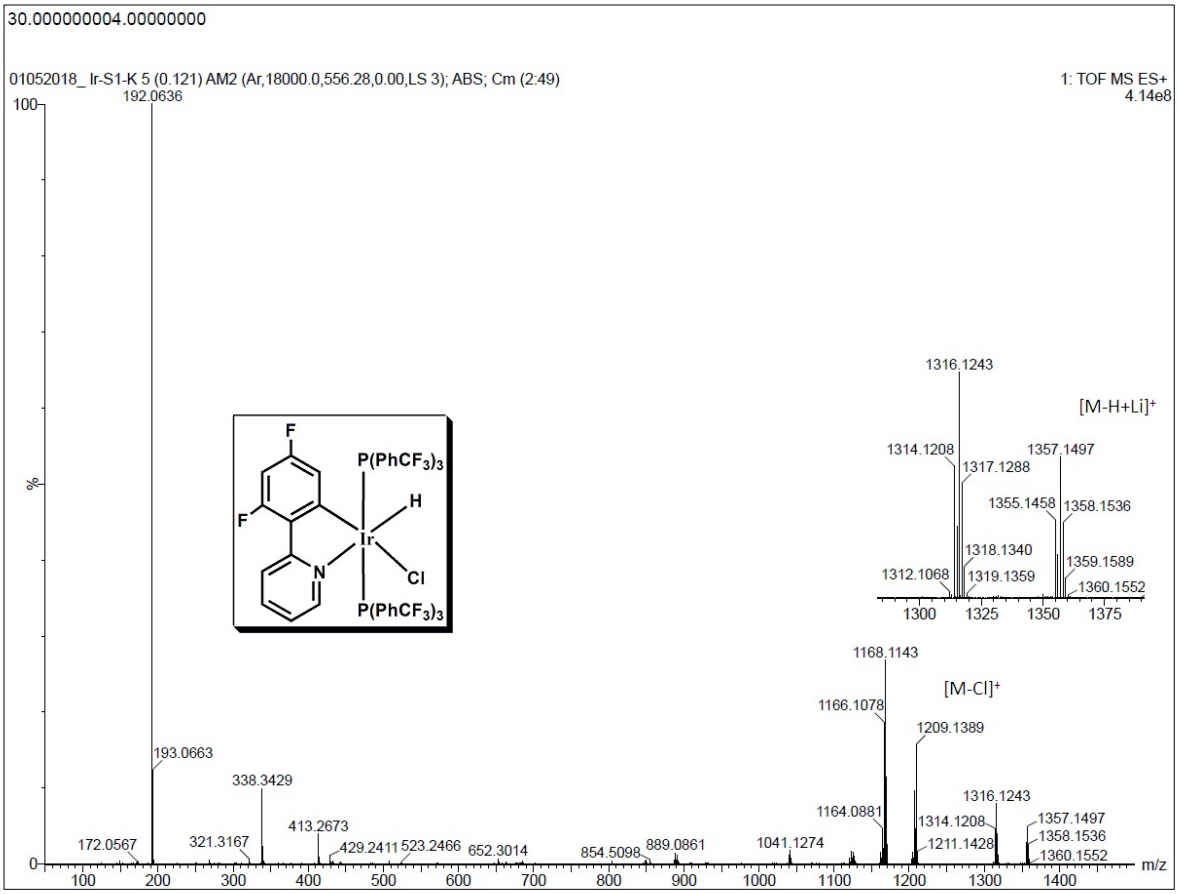

d

Fig. 5S. (^{1}H,^{13}C,^{31}P) NMR spectra are shown in a, b, c and HRMS data in d respectively for **1**

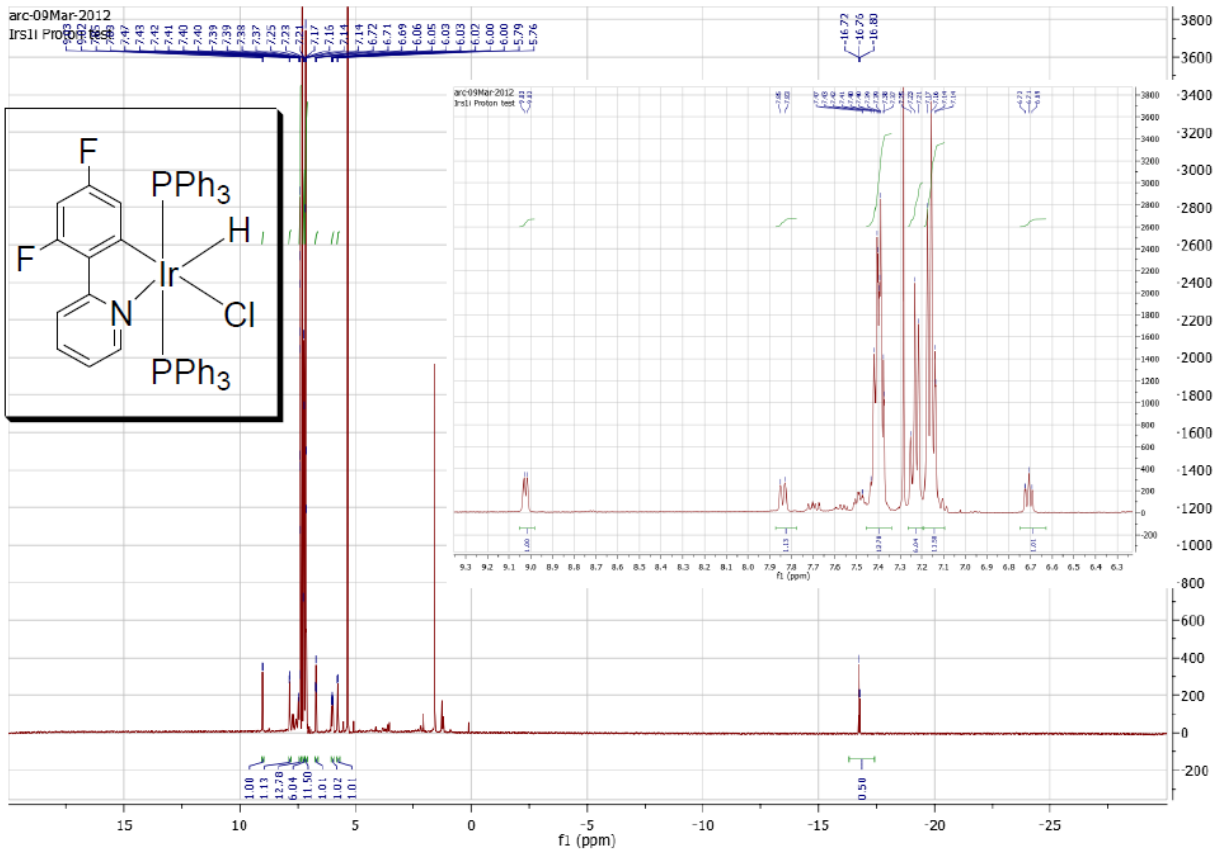

a

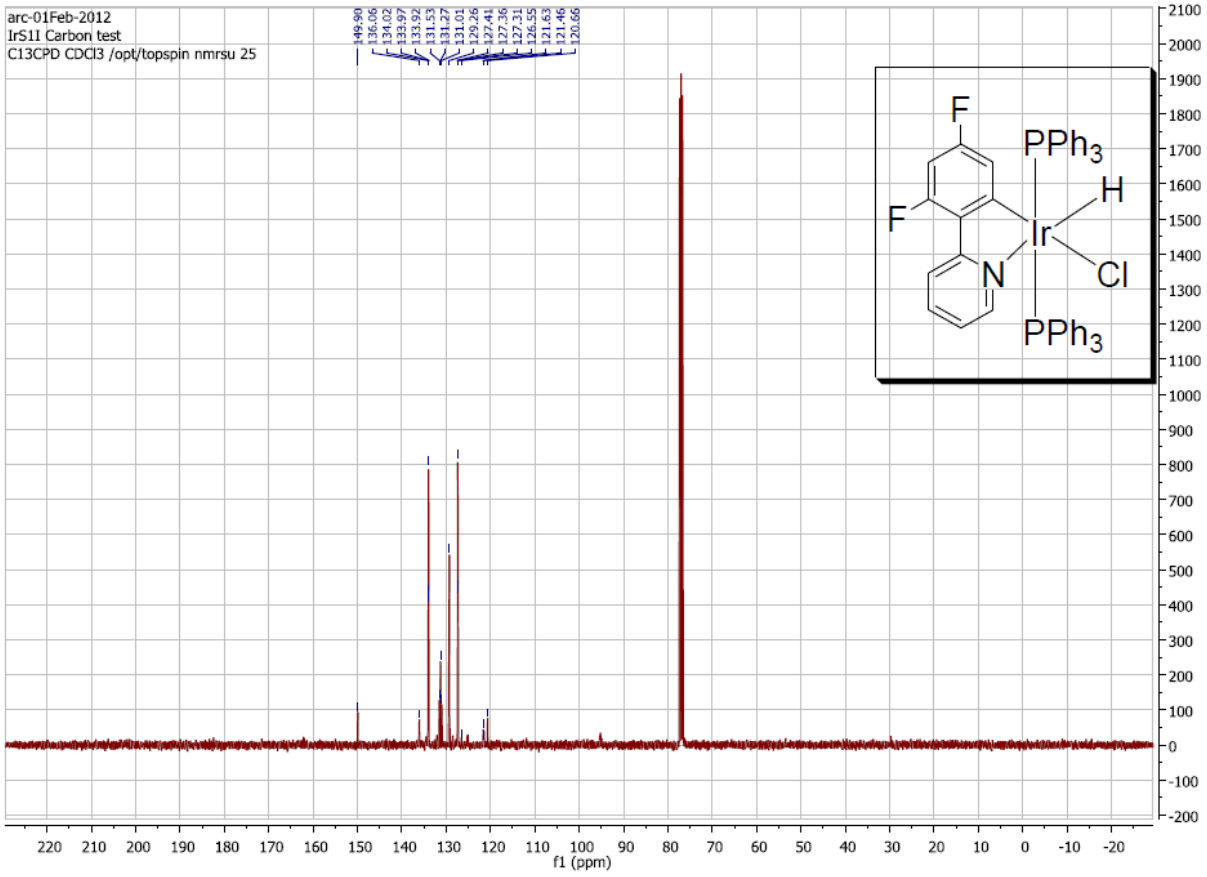
arc-01Feb-2012
IrS1I Carbon test
C13CPD CDCl3 /opt/topspin nmrsu 25
149.90
136.06
134.02
133.97
133.92
131.53
131.27
131.01
129.26
127.41
127.36
127.31
126.55
121.63
121.46
120.66
F
PPh3
H
F
Ir
N
Cl
PPh3
f1 (ppm)

b

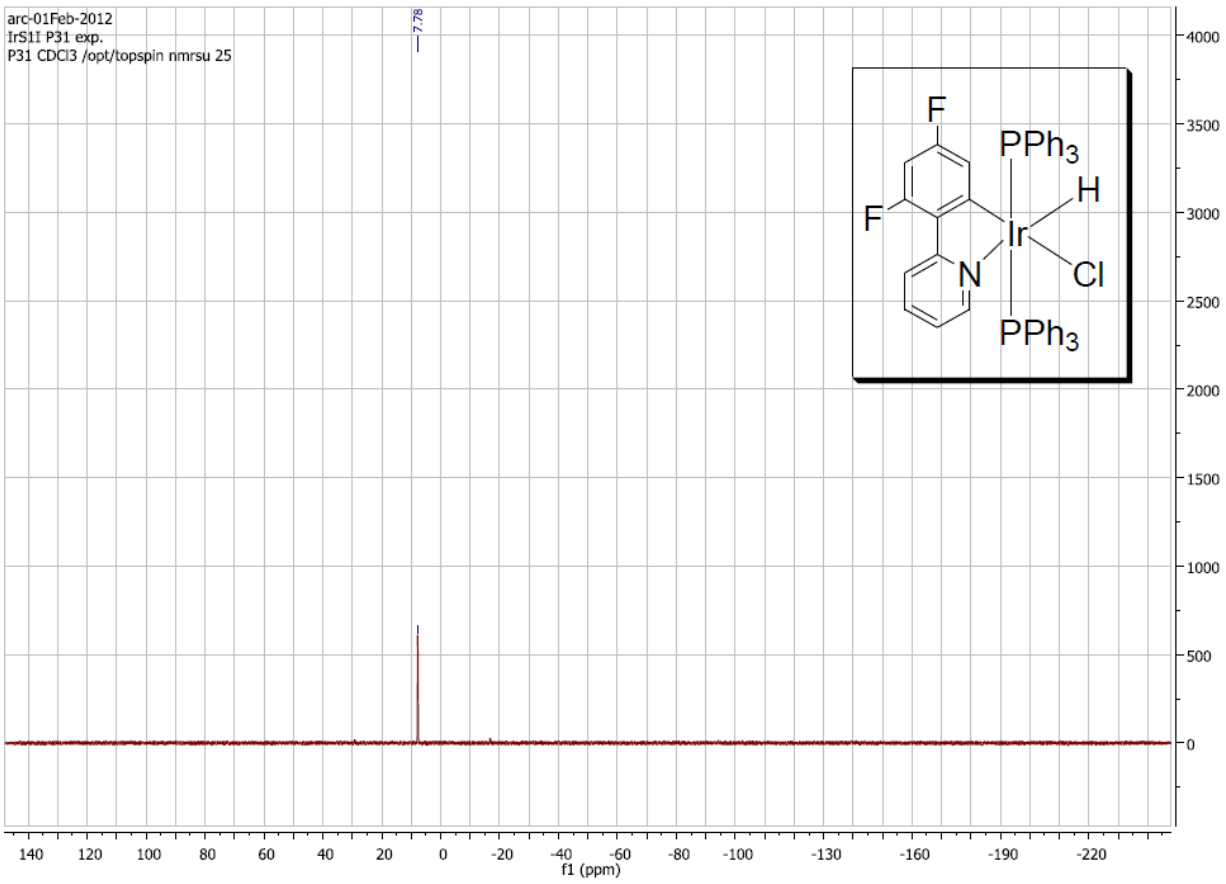

c

Acquisition Parameter

Source Type	ESI	Ion Polarity	Positive	Set Nebulizer	0.3 Bar
Focus	Active	Set Capillary	3700 V	Set Dry Heater	180 °C
Scan Begin	50 m/z	Set End Plate Offset	-500 V	Set Dry Gas	4.0 l/min
Scan End	1500 m/z	Set Collision Cell RF	1500.0 Vpp	Set Divert Valve	Source

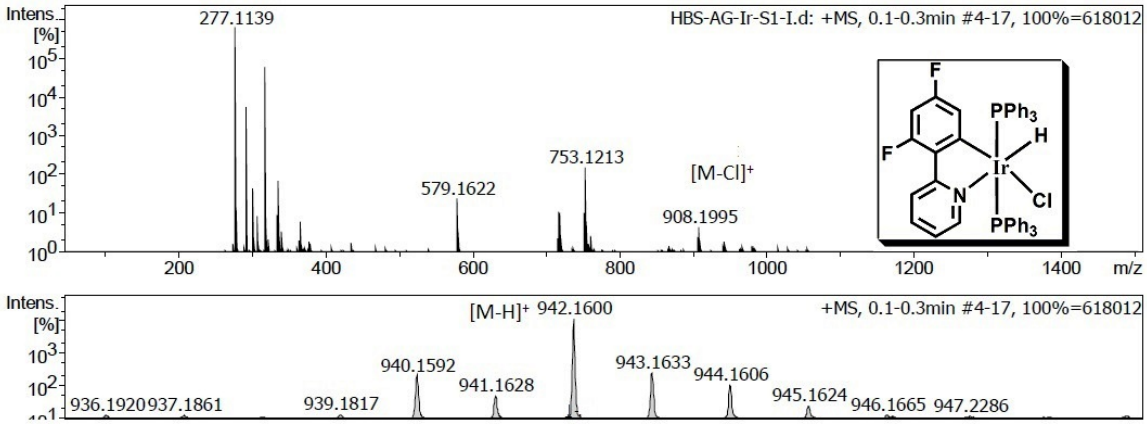

d

Fig. 6S. (^{1}H,^{13}C,^{31}P) NMR spectra are shown in a, b, c and HRMS data in d respectively for **2**

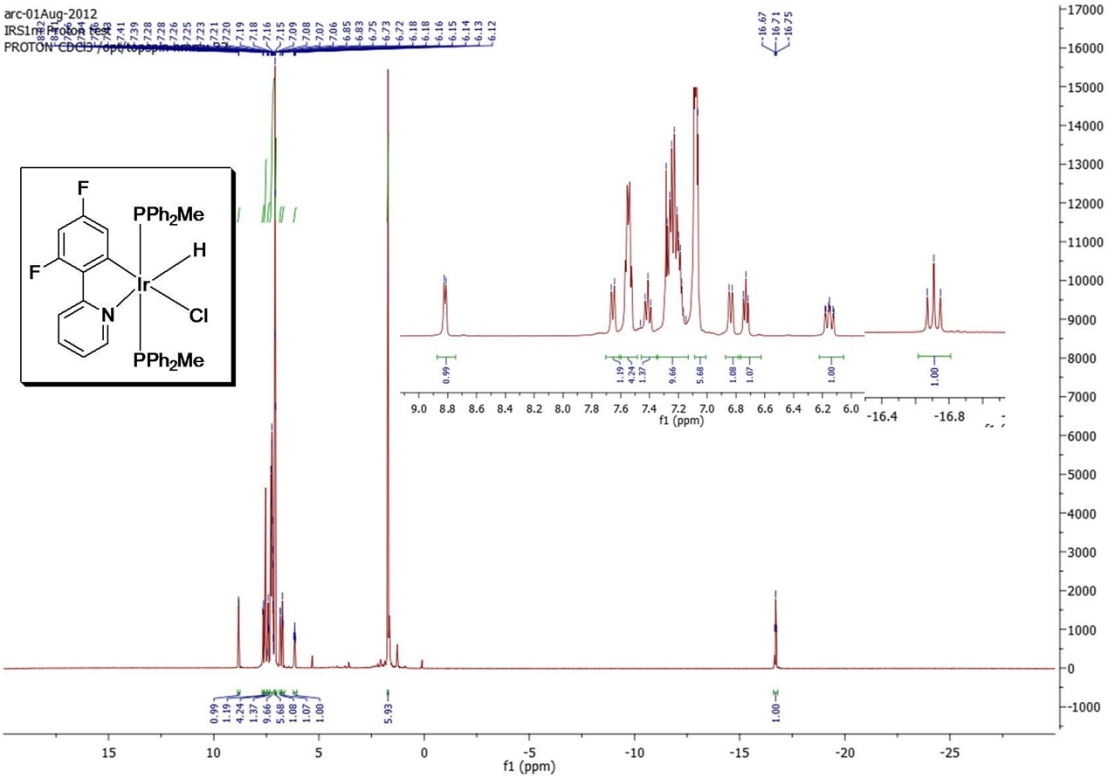

a

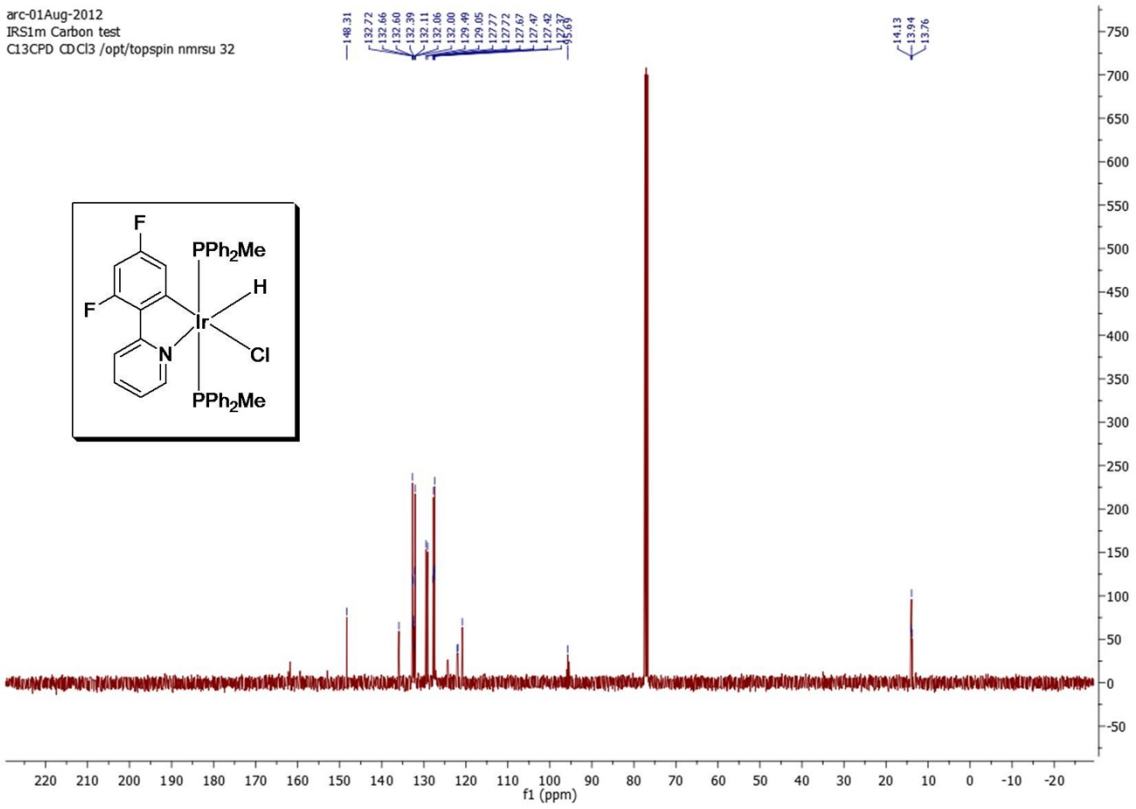
arc-01Aug-2012
IRS1m Carbon test
C13CPD CDCl3 /opt/topspin nmrsu 32
F
PPh2Me
H
F
Ir
N
Cl
PPh2Me
f1 (ppm)

b

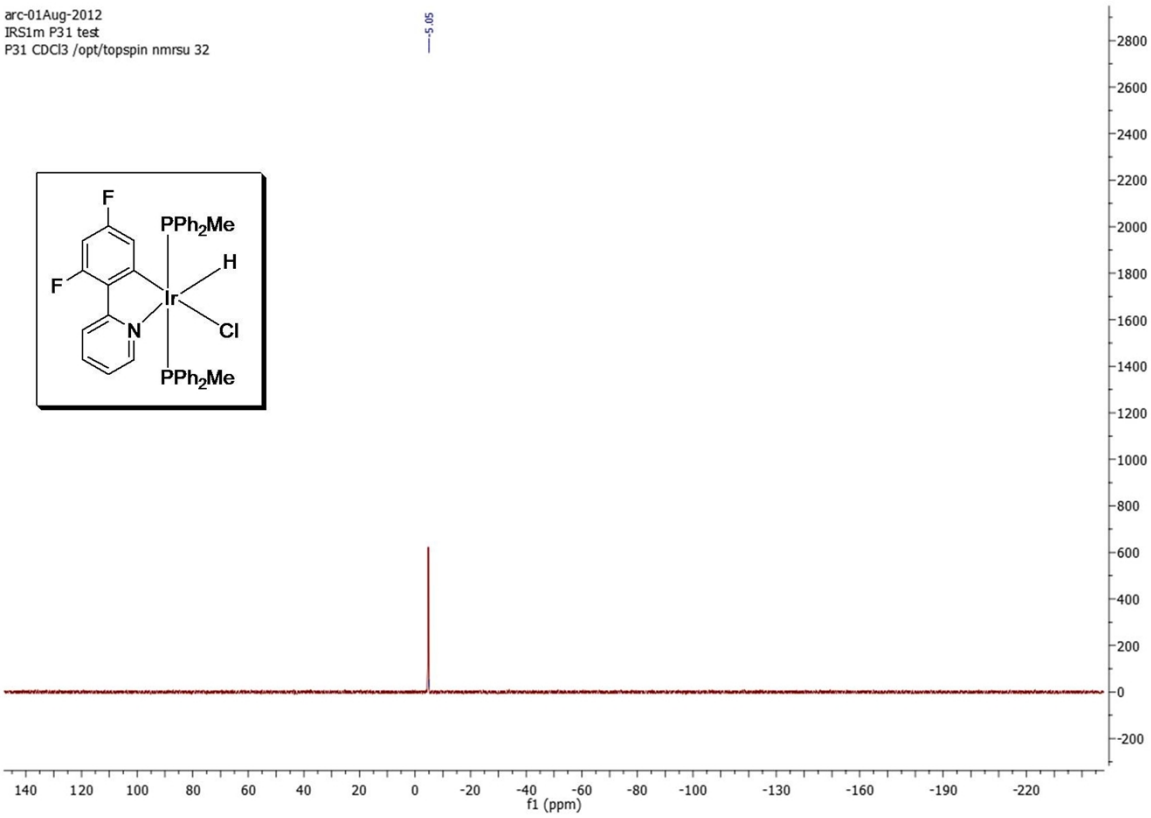
arc-01Aug-2012
IRS1m P31 test
P31 CDCl3 /opt/topspin nmrsu 32
5.05
F
PPh2Me
H
F
Ir
N
Cl
PPh2Me
2800
2600
2400
2200
2000
1800
1600
1400
1200
1000
800
600
400
200
0
-200
140 120 100 80 60 40 20 0 -20 -40 -60 -80 -100 -130 -160 -190 -220
f1 (ppm)

c

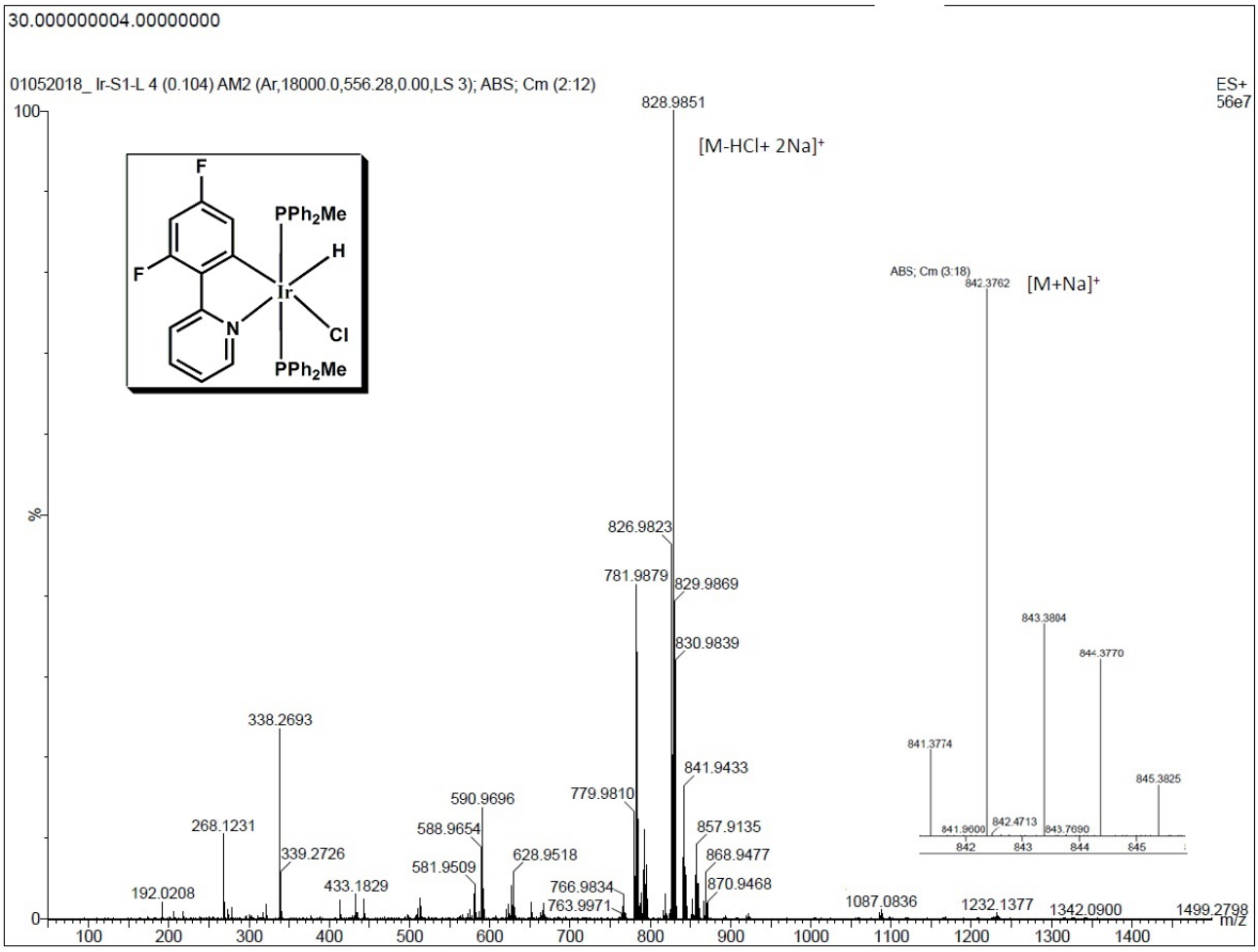

Fig.S7. (^{1}H,^{13}C,^{31}P) NMR spectra are shown in a, b, c and HRMS data in d respectively for **3**.

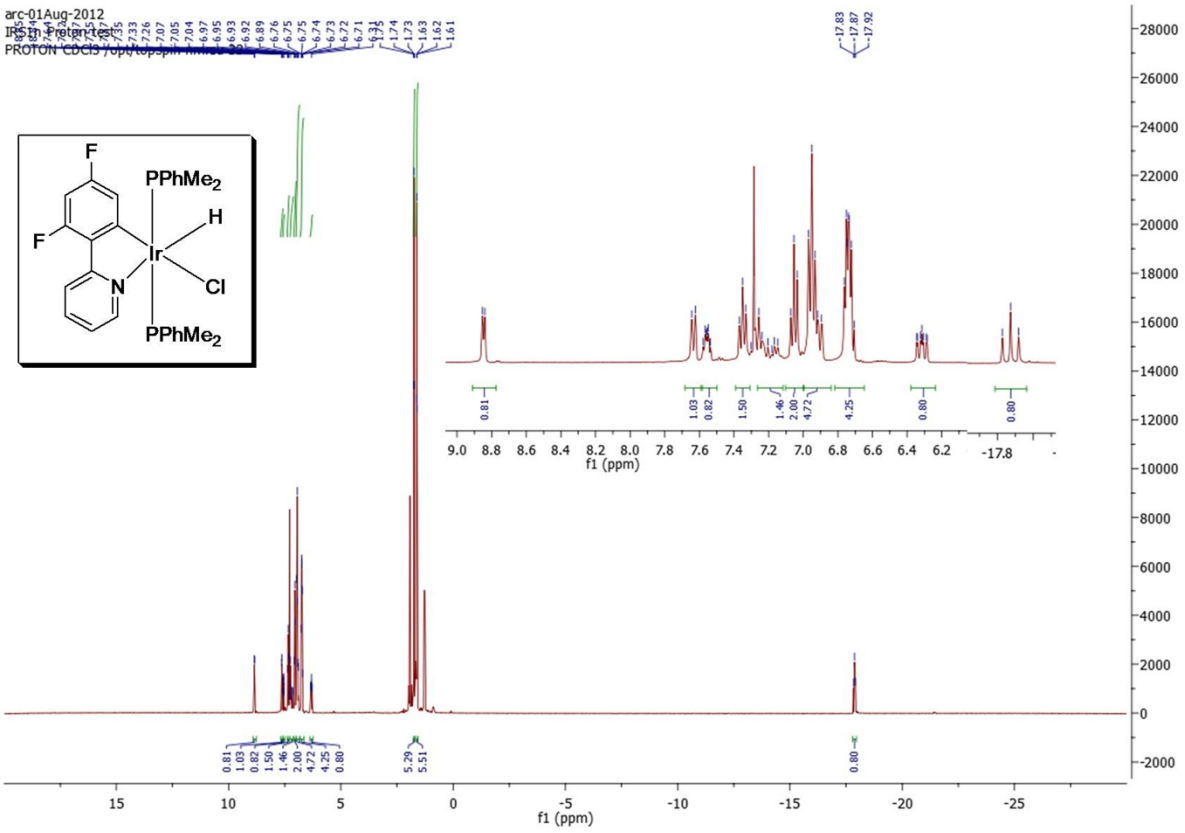
arc-01Aug-2012
IRSTn Proton-test
PROTON CDCl3
F
PPhMe2
H
F
Ir
N
Cl
PPhMe2
f1 (ppm)

a

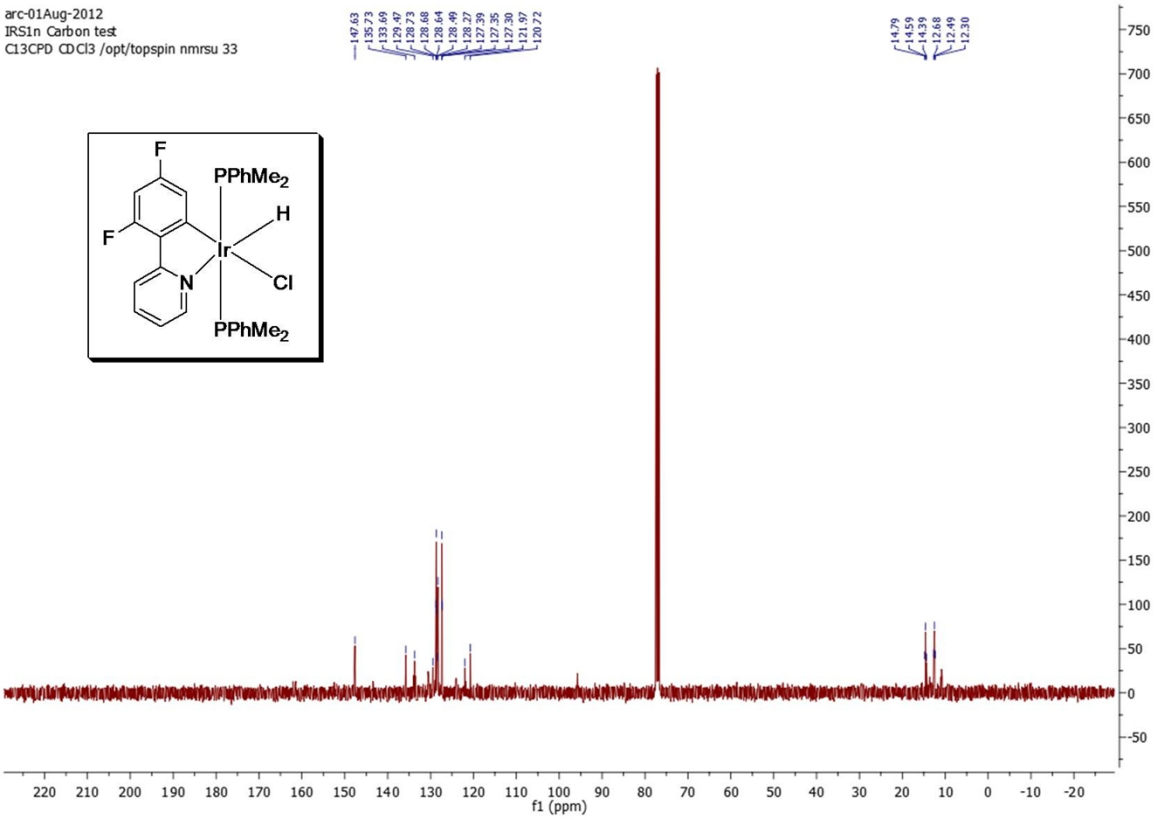
arc-01Aug-2012
IRS1n Carbon test
C13CPD CDCl3 /opt/topspin nmrsu 33
147.63
135.73
133.69
129.47
128.73
128.68
128.64
128.49
128.27
127.39
127.35
127.30
121.97
120.72
14.79
14.59
14.39
12.68
12.49
12.30
F
PPhMe2
H
F
Ir
N
Cl
PPhMe2
f1 (ppm)

b

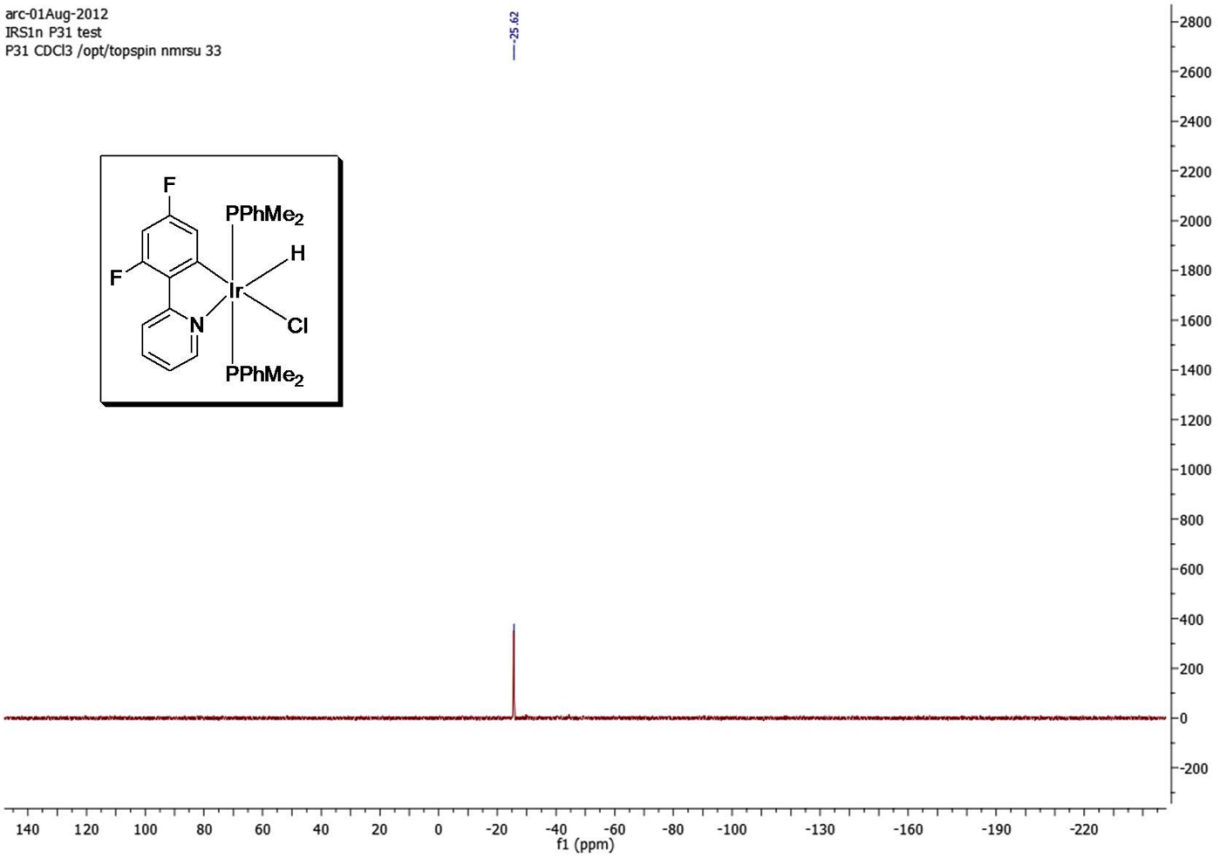
arc-01Aug-2012
IRS1n P31 test
P31 CDCl3 /opt/topspin nmrsu 33
-25.62
F
PPhMe2
H
F
Ir
N
Cl
PPhMe2
2800
2600
2400
2200
2000
1800
1600
1400
1200
1000
800
600
400
200
0
-200
140
120
100
80
60
40
20
0
-20
-40
-60
-80
-100
-130
-160
-190
-220
f1 (ppm)

c

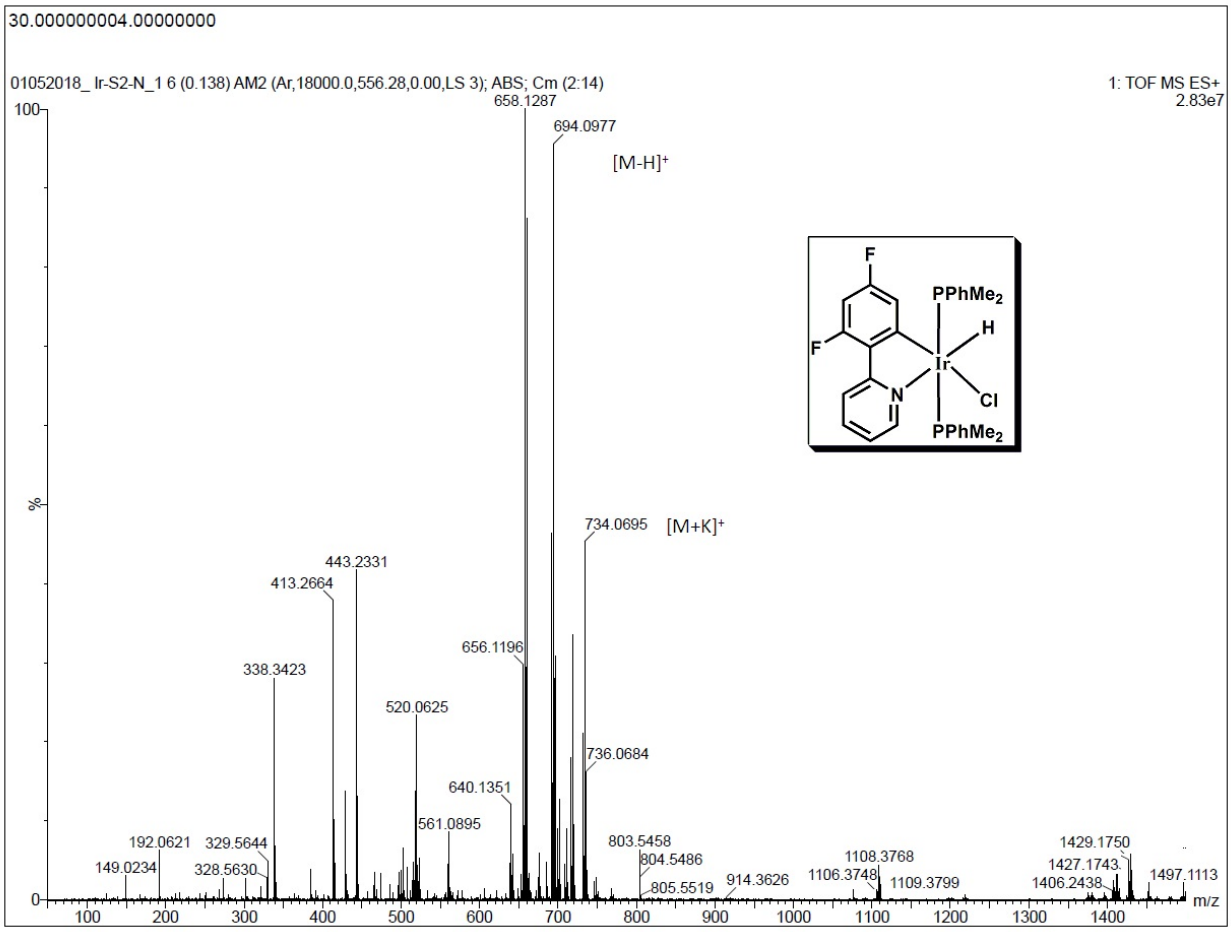

Fig. S8. (^{1}H,^{13}C,^{31}P) NMR spectra are shown in a, b, c and HRMS data in d respectively for **4**.

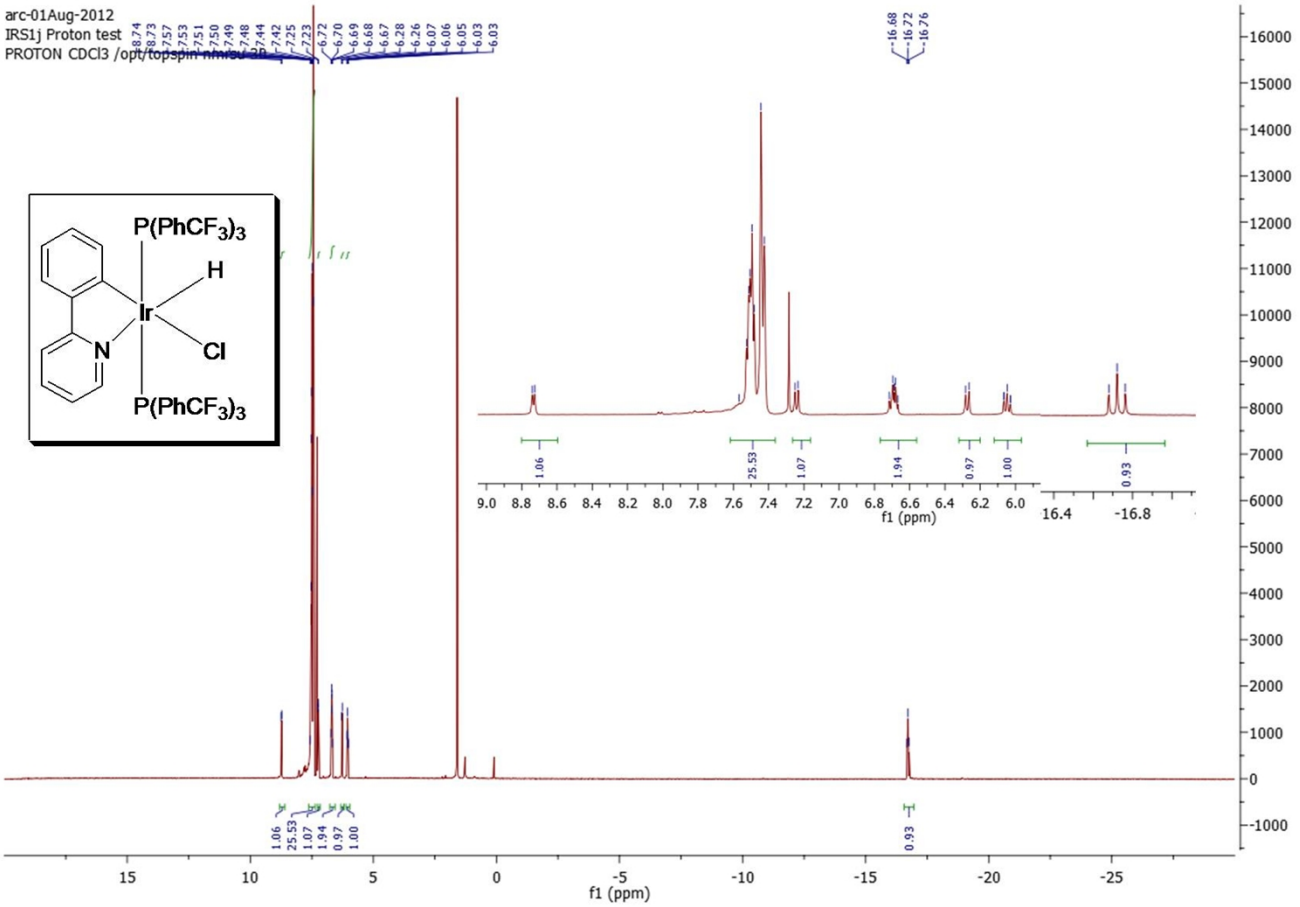
arc-01Aug-2012
IRS1j Proton test
PROTON CDCl3 /opt/topspin nmrsu 2P
P(PhCF3)3
H
Ir
N
Cl
P(PhCF3)3
f1 (ppm)

a

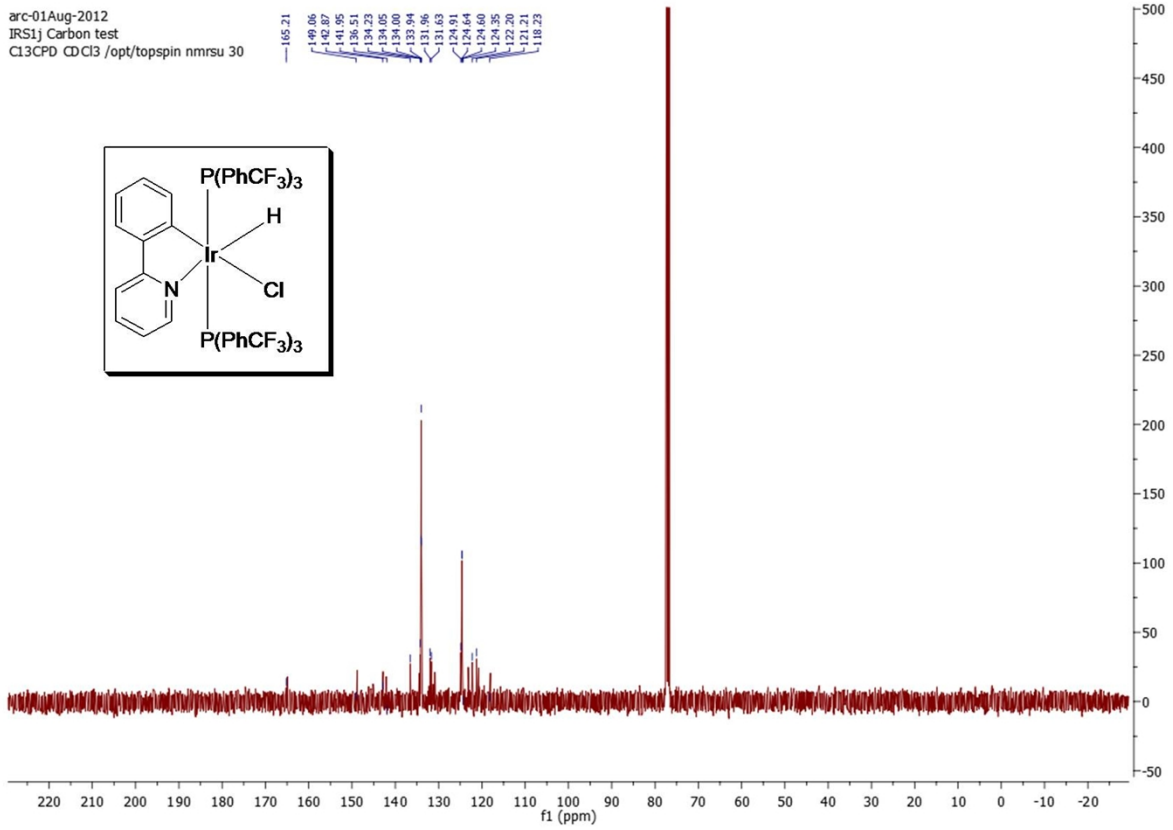
arc-01Aug-2012
IRS1j Carbon test
C13CPD CDCl3 /opt/topspin nmrsu 30
165.21
149.06
142.87
141.95
136.51
134.23
134.05
134.00
133.94
131.96
131.63
124.91
124.64
124.60
124.35
122.20
121.21
118.23
P(PhCF3)3
H
Ir
N
Cl
P(PhCF3)3
f1 (ppm)

b

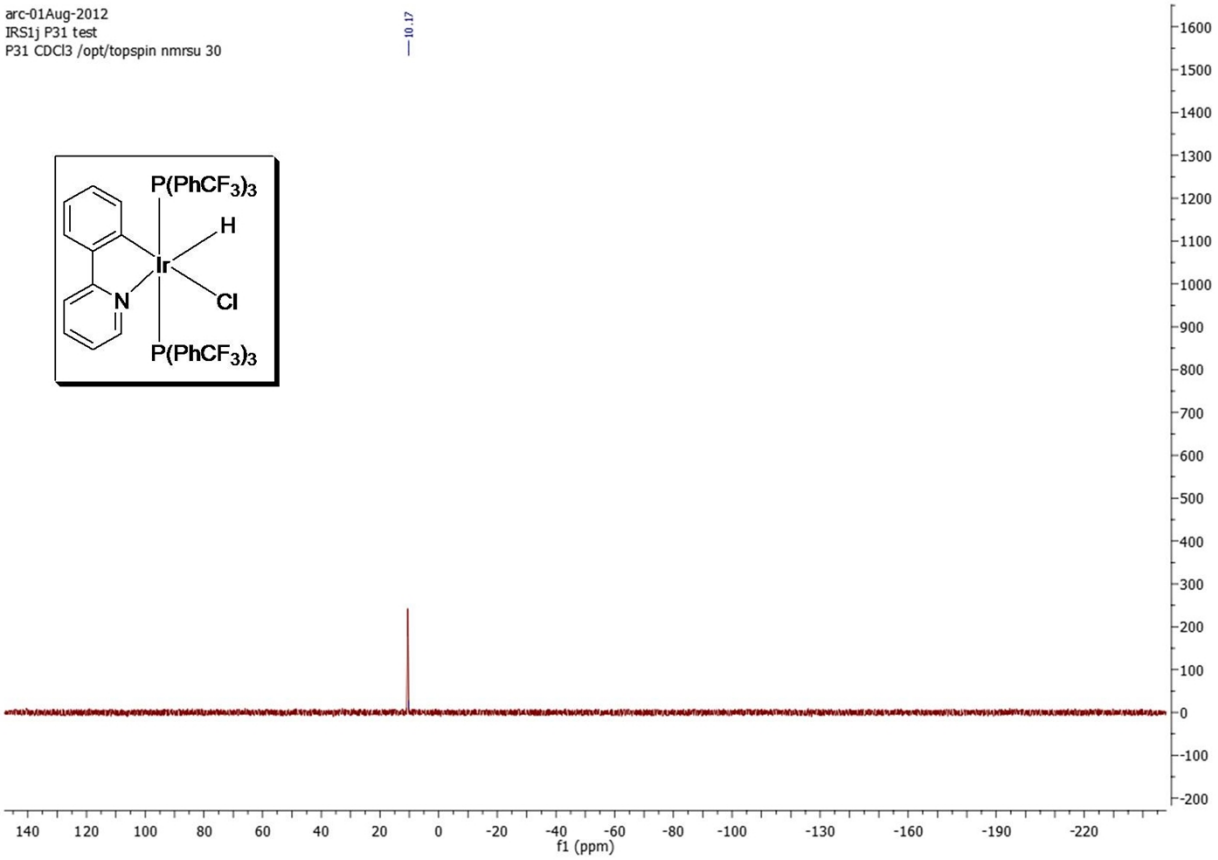

c

Acquisition Parameter

Source Type	ESI	Ion Polarity	Positive	Set Nebulizer	0.3 Bar
Focus	Active	Set Capillary	3700 V	Set Dry Heater	180 °C
Scan Begin	50 m/z	Set End Plate Offset	-500 V	Set Dry Gas	4.0 l/min
Scan End	1500 m/z	Set Collision Cell RF	1500.0 Vpp	Set Divert Valve	Source

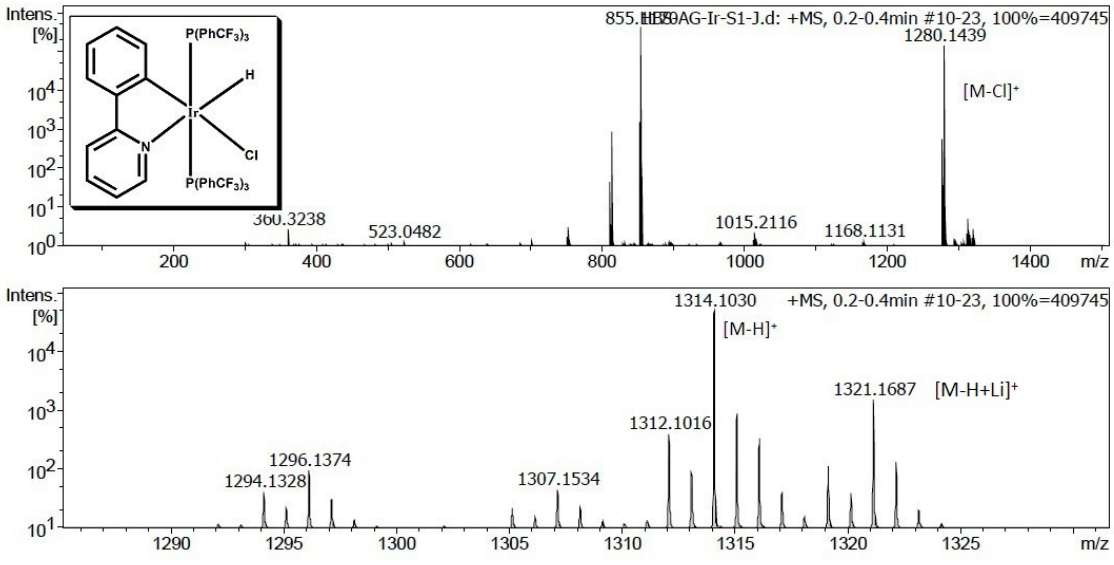

d

Fig. S9. (^{1}H,^{13}C,^{31}P) NMR spectra are shown in a, b, c and HRMS data in d respectively for **5**.

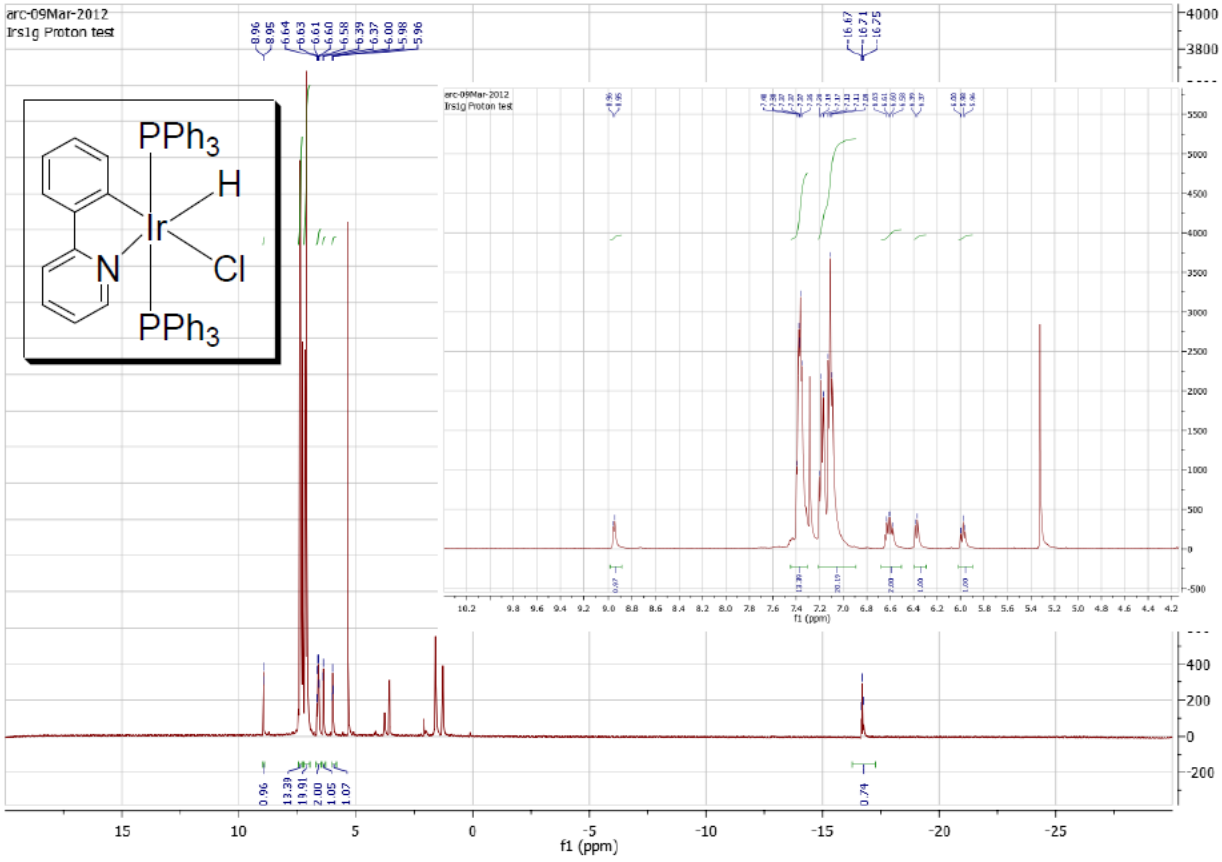

a

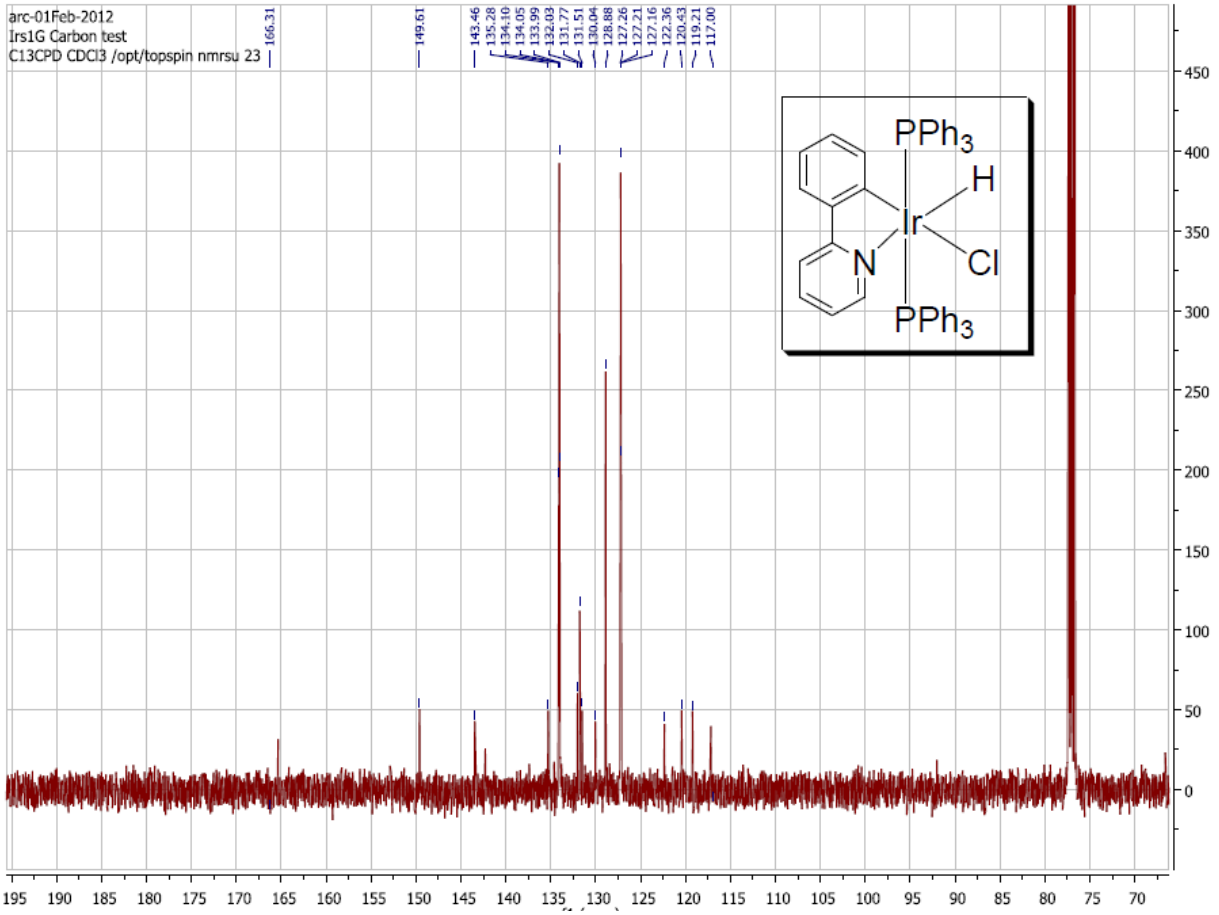
arc-01Feb-2012
Irs1G Carbon test
C13CPD CDCl3 /opt/topspin nmrsu 23
166.31
149.61
143.46
135.28
134.16
134.05
133.99
132.03
131.77
131.51
130.04
128.88
127.26
127.21
127.16
122.36
120.43
119.21
117.00
PPh3
H
Ir
N
Cl
PPh3

b

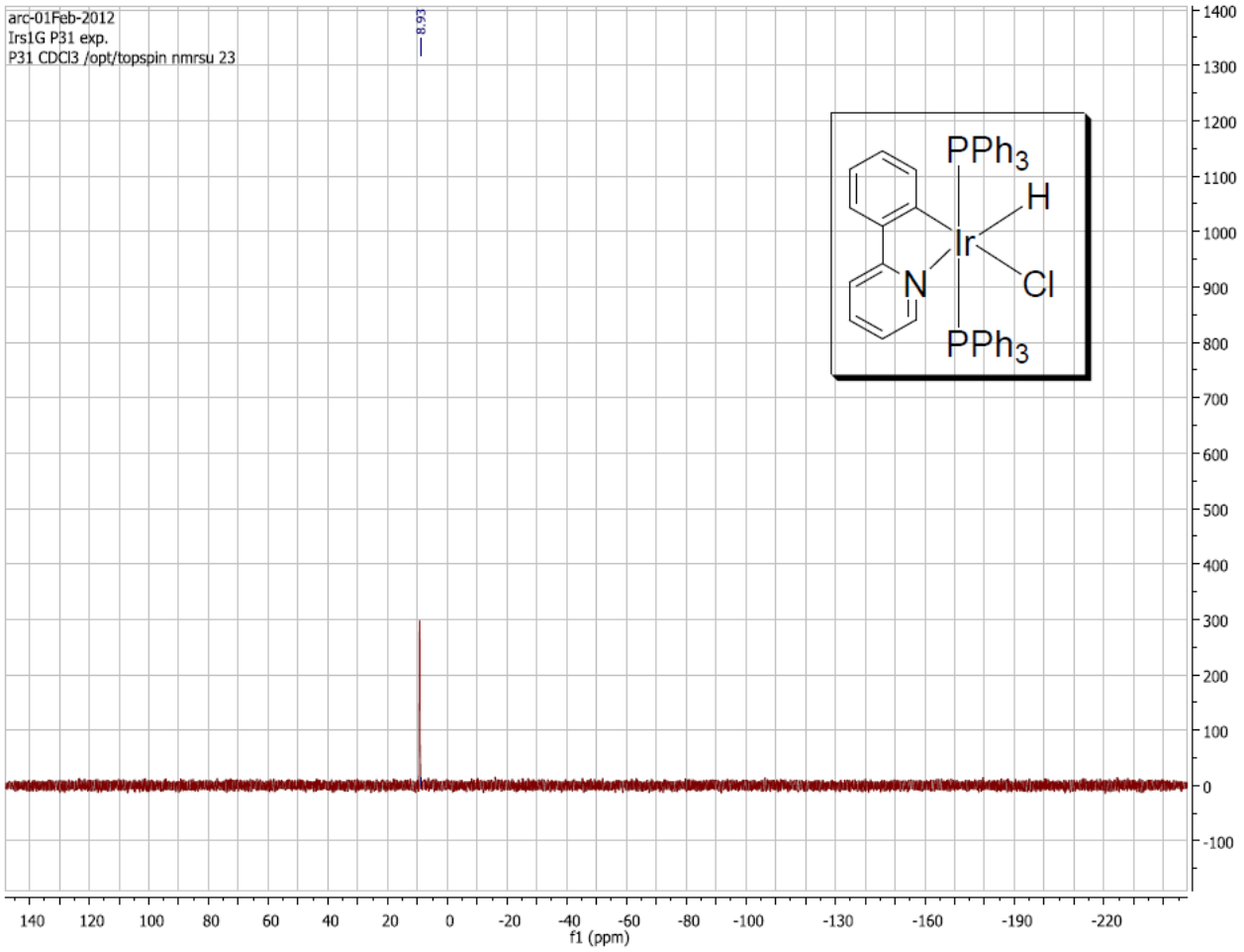
arc-01Feb-2012
Irs1G P31 exp.
P31 CDCl3 /opt/topspin nmrsu 23
8.93
PPh3
H
Ir
N
Cl
PPh3
1400
1300
1200
1100
1000
900
800
700
600
500
400
300
200
100
0
-100
140
120
100
80
60
40
20
0
-20
-40
-60
-80
-100
-130
-160
-190
-220
f1 (ppm)

c

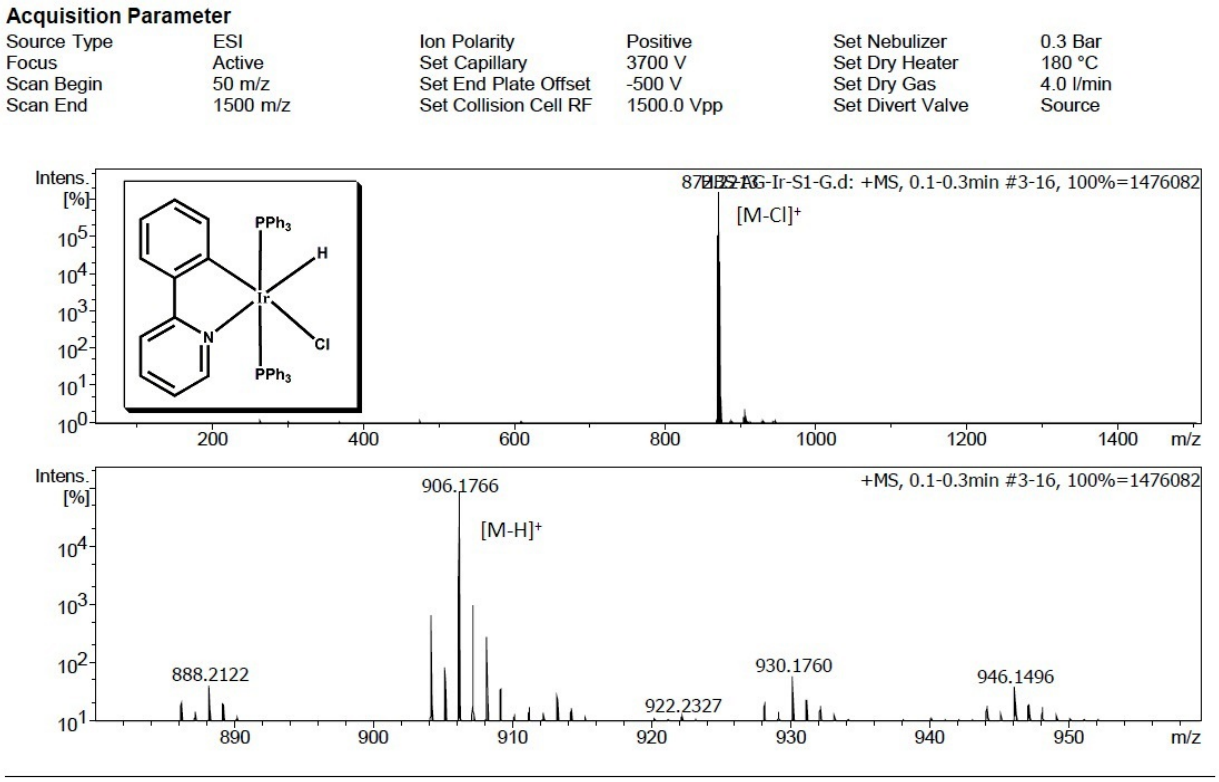

d

Fig. S10. (^{1}H,^{13}C,^{31}P) NMR spectra are shown in a, b, c and HRMS data in d respectively for **6**.

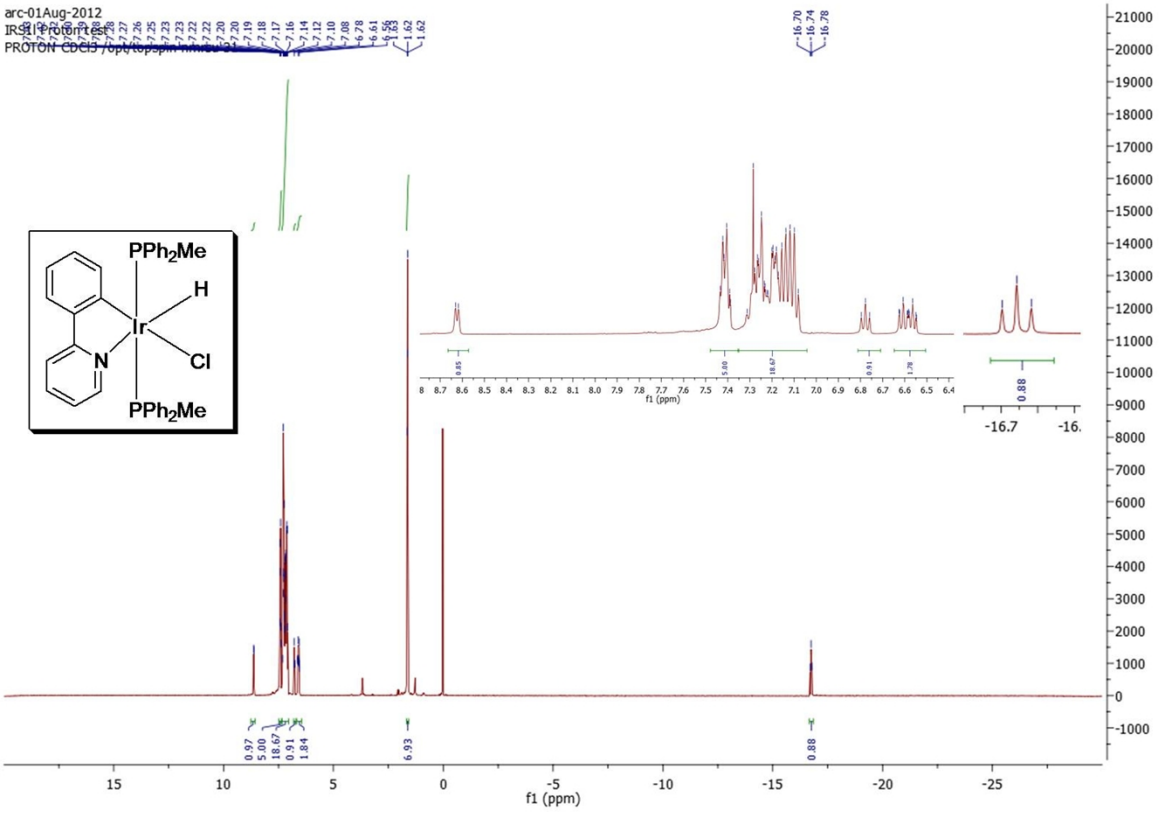
arc-01Aug-2012
IRSII Proton test
PROTON CDCl3
PPh2Me
H
Ir
N
Cl
PPh2Me
f1 (ppm)

a

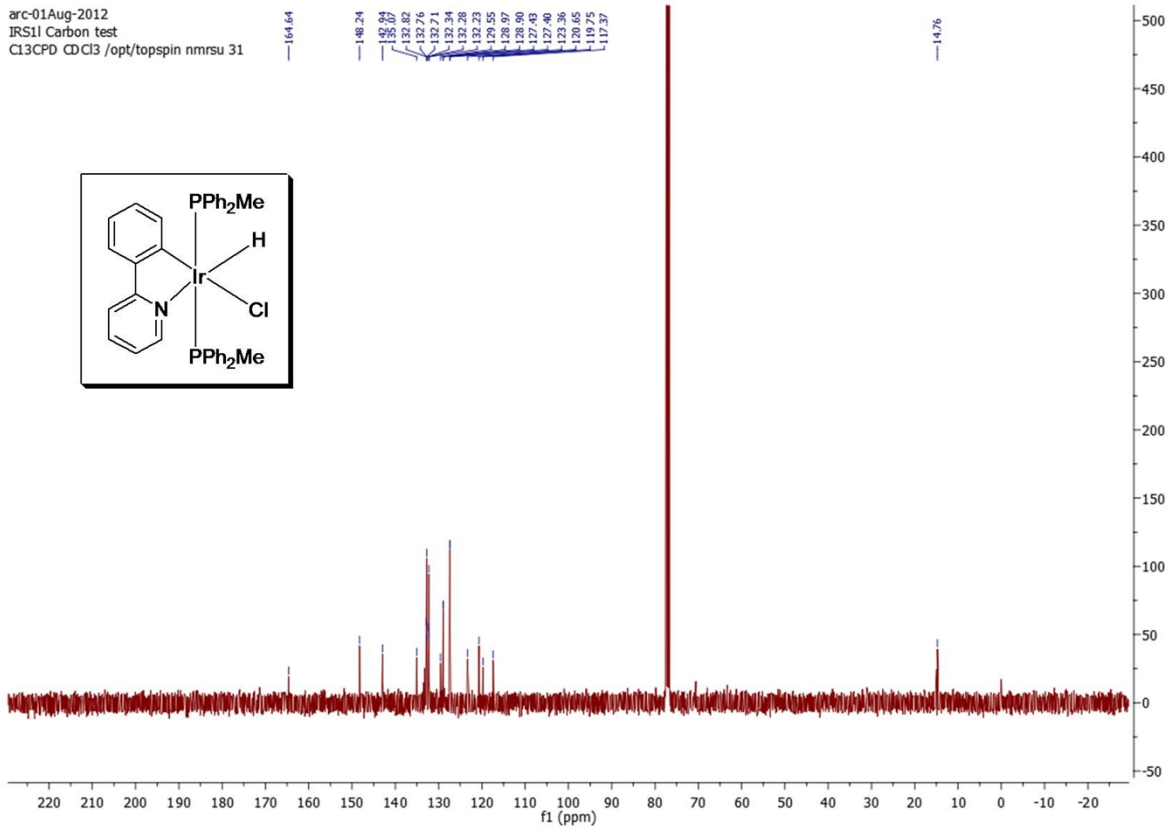
arc-01Aug-2012
IRS1l Carbon test
C13CPD CDCl3 /opt/topspin nmrsu 31
PPh2Me
H
Ir
N
Cl
PPh2Me
f1 (ppm)

b

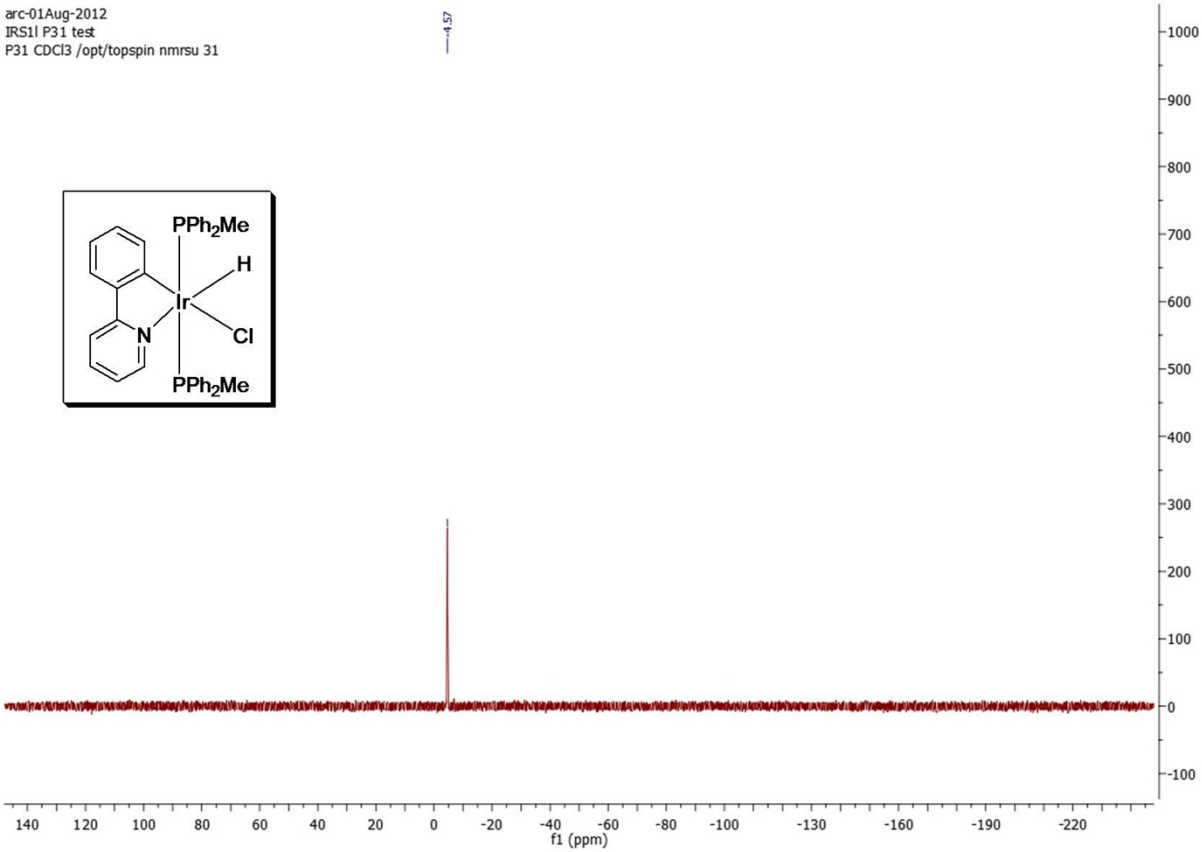
arc-01Aug-2012
IRS1l P31 test
P31 CDCl3 /opt/topspin nmrsu 31
4.57
PPh2Me
H
Ir
N
Cl
PPh2Me
1000
900
800
700
600
500
400
300
200
100
0
-100
140
120
100
80
60
40
20
0
-20
-40
-60
-80
-100
-130
-160
-190
-220
f1 (ppm)

c

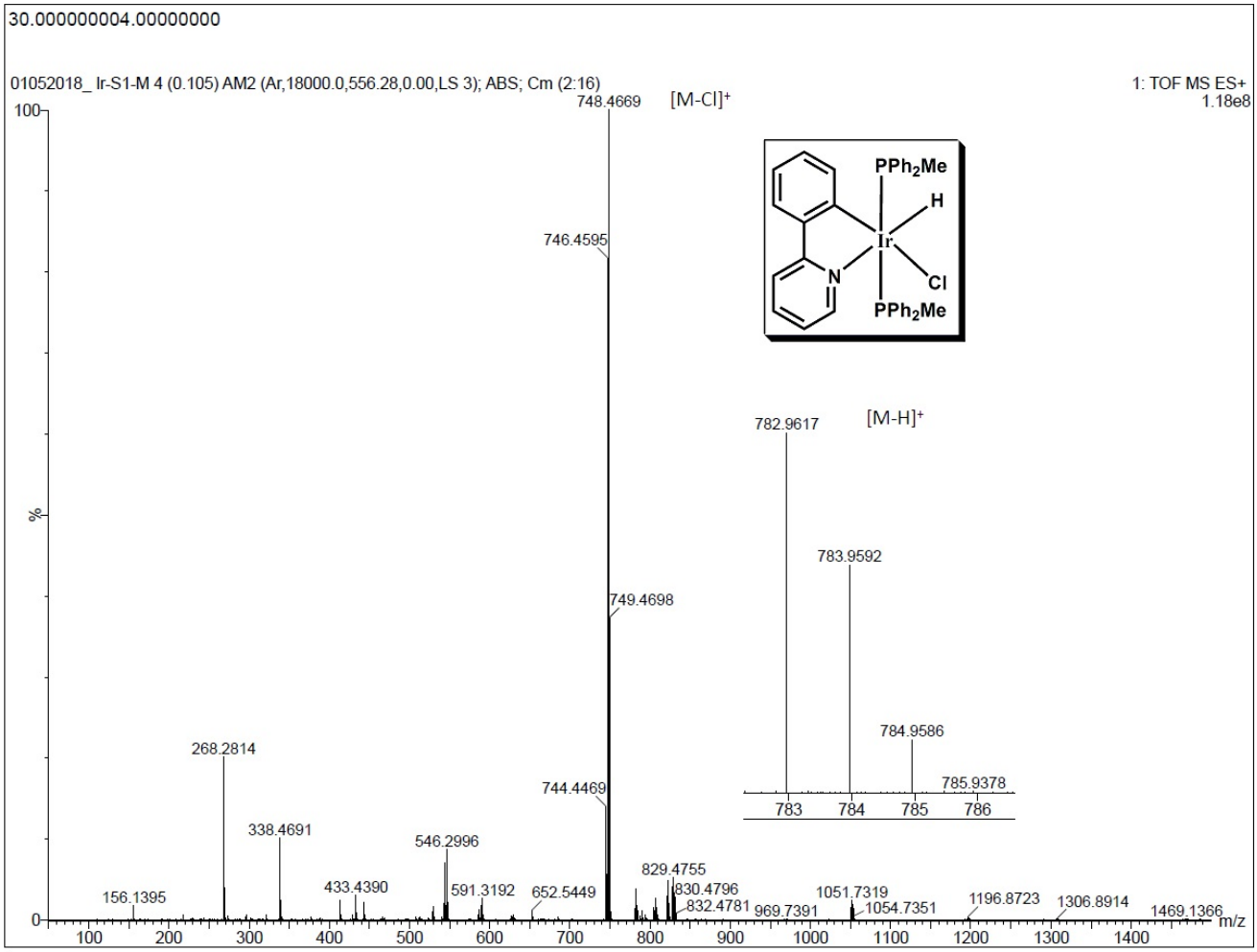

Fig. S11. (^{1}H,^{13}C,^{31}P) NMR spectra are shown in a, b, c and HRMS in d respectively for **7**.

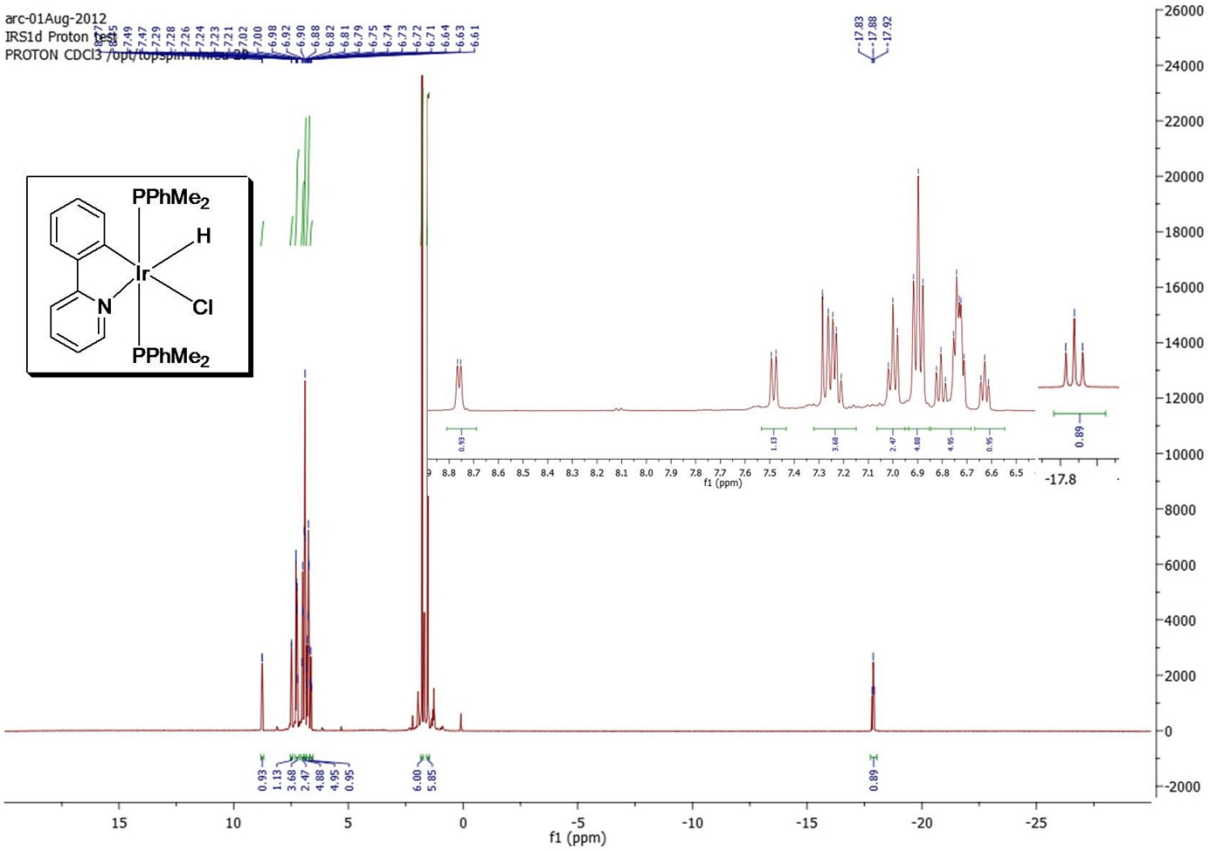
arc-01Aug-2012
IRS1d Proton test
PROTON CDCl3
PPhMe2
H
Ir
N
Cl
PPhMe2
-17.8
f1 (ppm)

a

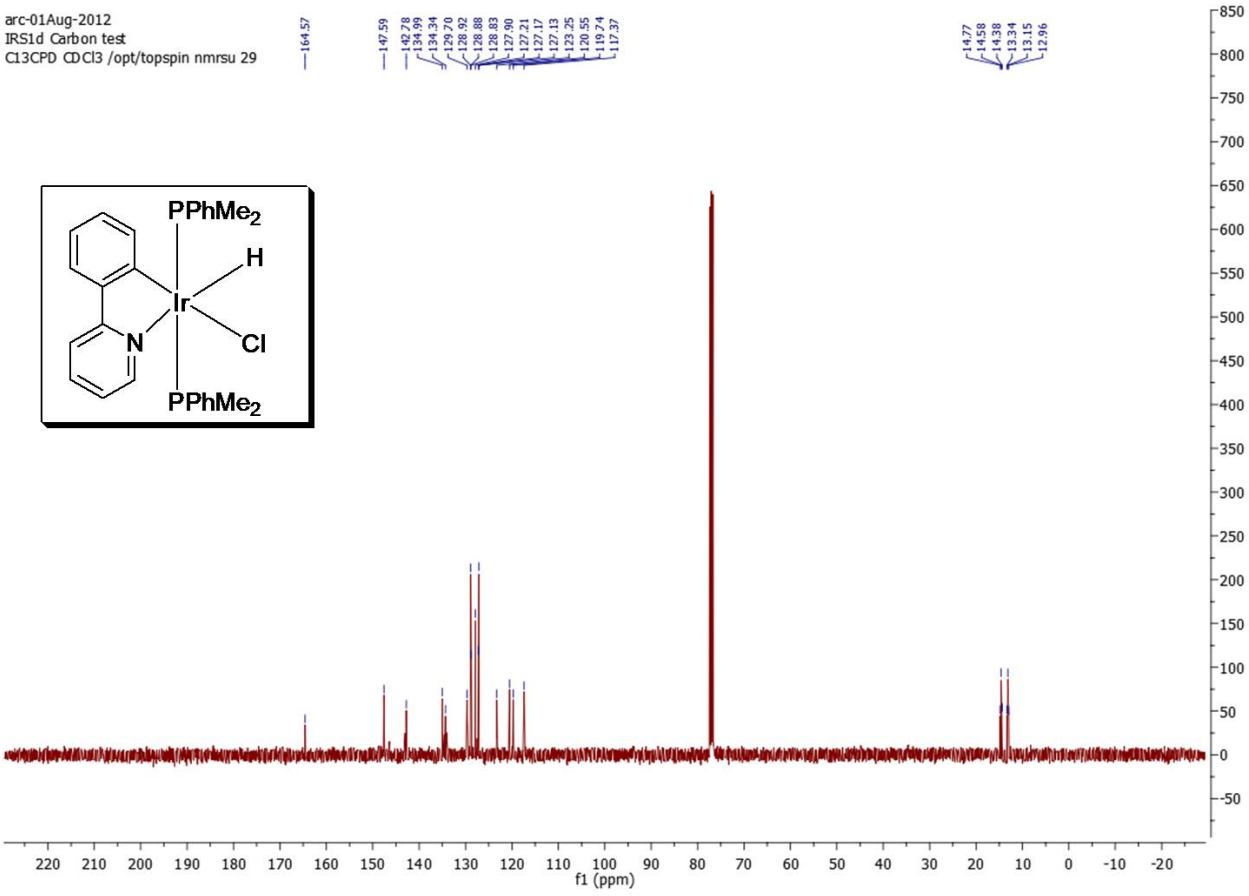
arc-01Aug-2012
IRS1d Carbon test
C13CPD CDCl3 /opt/topspin nmrsu 29
164.57
147.59
142.78
134.99
134.34
129.70
128.92
128.88
128.83
127.90
127.21
127.17
127.13
123.25
120.55
119.74
117.37
14.77
14.58
14.38
13.34
13.15
12.96
PPhMe2
H
Ir
N
Cl
PPhMe2
f1 (ppm)

b

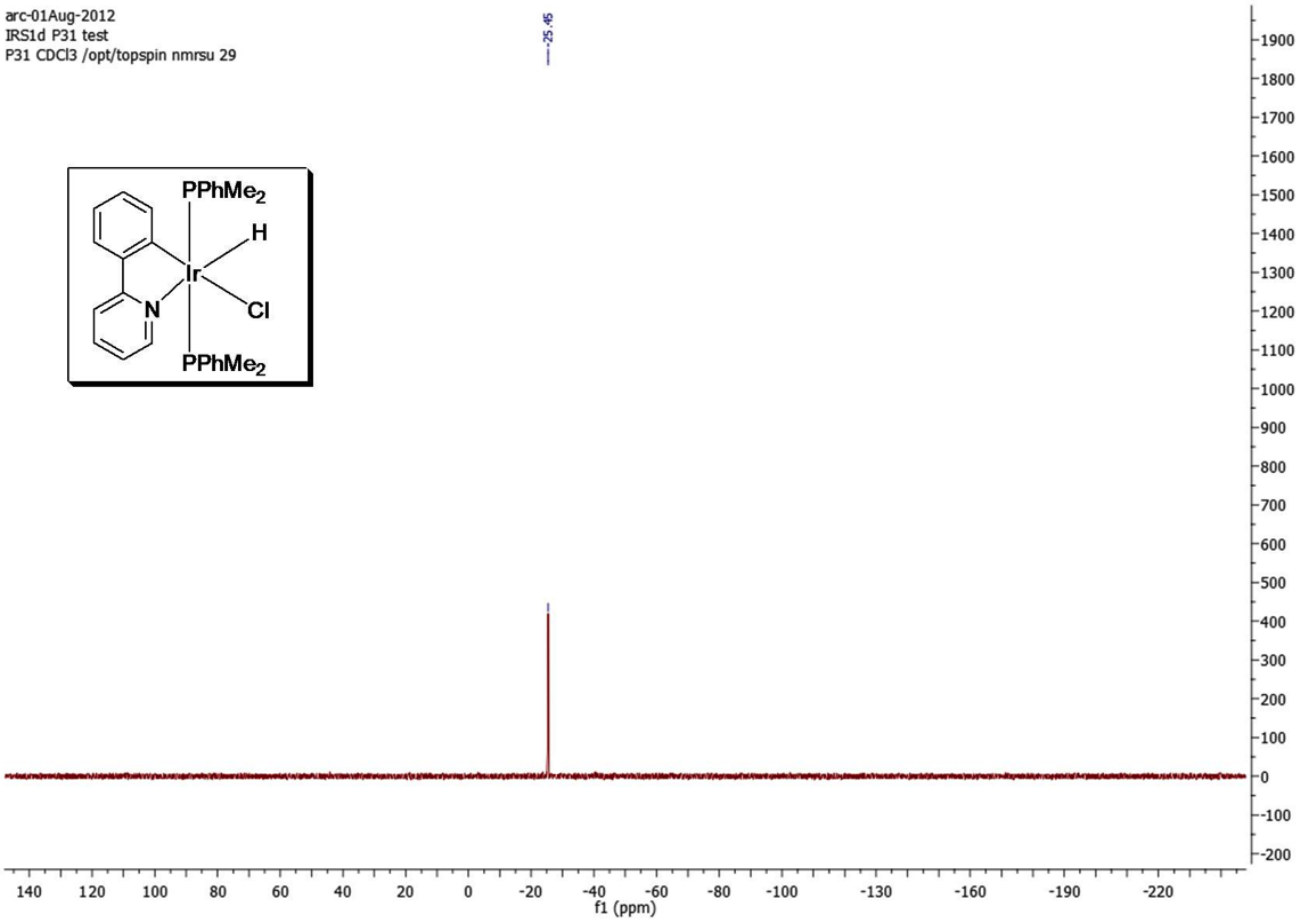
arc-01Aug-2012
IRS1d P31 test
P31 CDCl3 /opt/topspin nmrsu 29
-25.45
PPhMe2
H
Ir
N
Cl
PPhMe2
f1 (ppm)

c

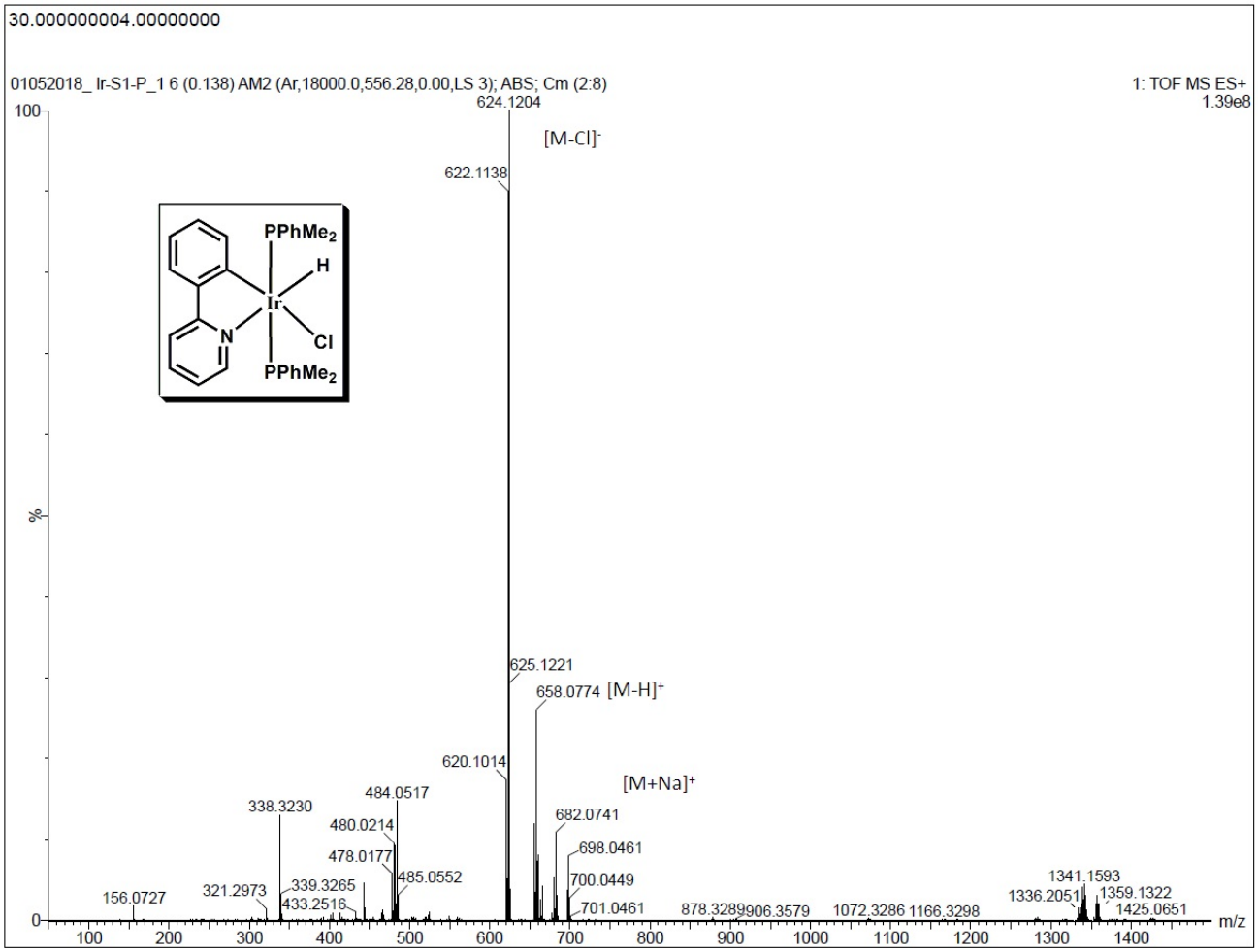

Fig. S12. (^{1}H,^{13}C,^{31}P) NMR spectra are shown in a, b, c and HRMS data in d respectively for **8**.

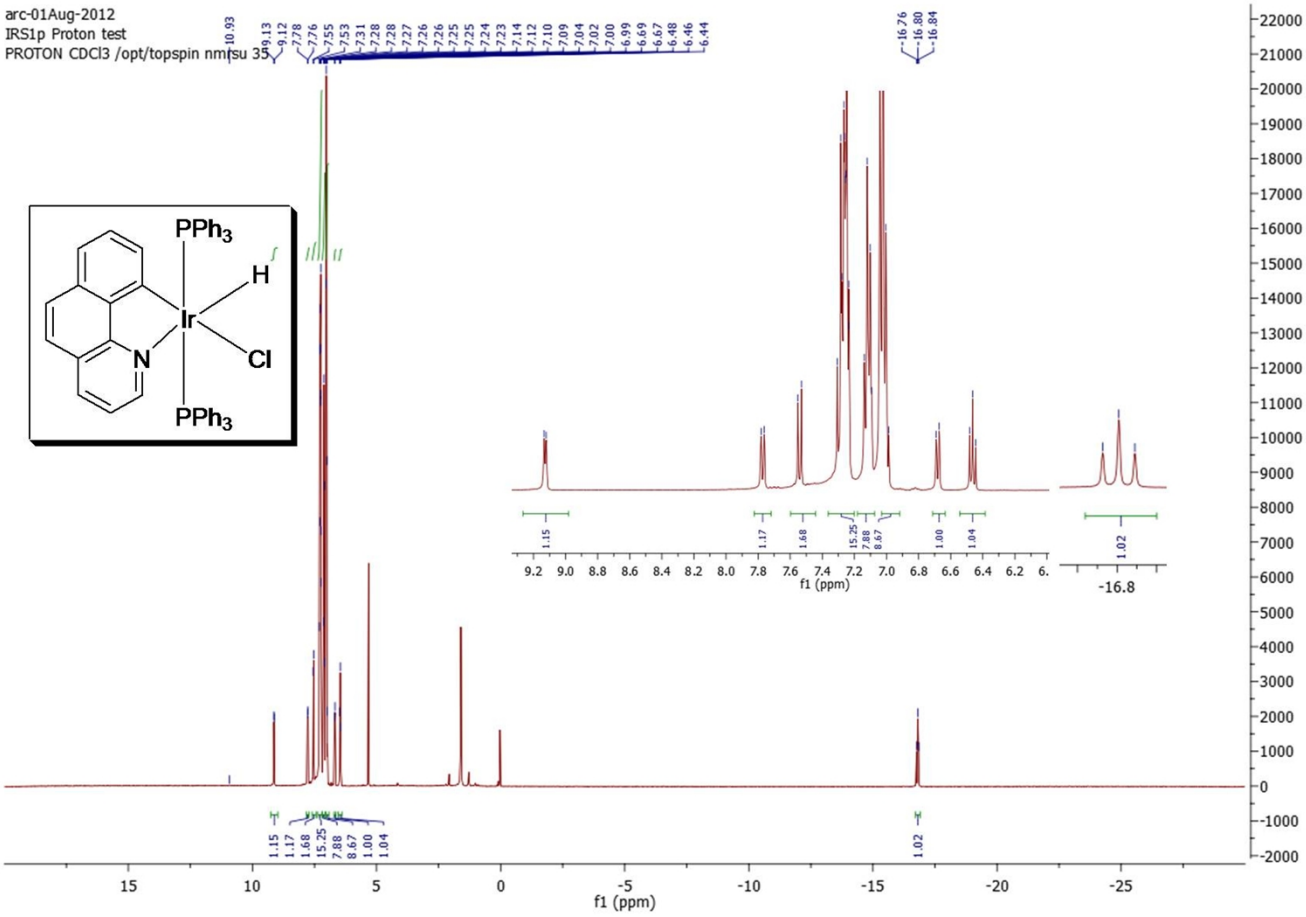
arc-01Aug-2012
IRS1p Proton test
PROTON CDCl3 /opt/topspin nmrsu 35
PPh3
H
Ir
N
Cl
PPh3
f1 (ppm)
-16.8

a

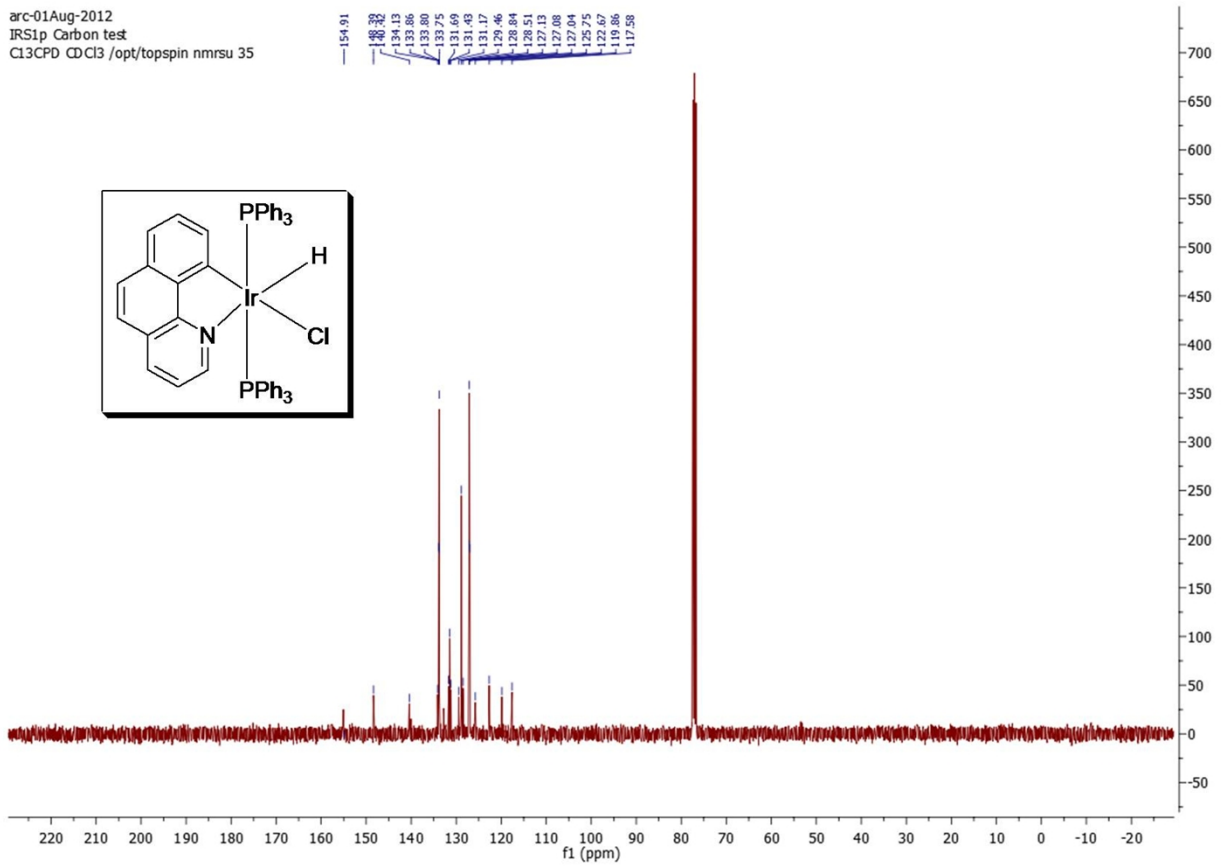
arc-01Aug-2012
IRS1p Carbon test
C13CPD CDCl3 /opt/topspin nmrsu 35
154.91
148.39
140.42
134.13
133.86
133.80
133.75
131.69
131.43
131.17
129.46
128.84
128.51
127.13
127.08
127.04
125.75
122.67
119.86
117.58
PPh3
H
Ir
N
Cl
PPh3
f1 (ppm)

b

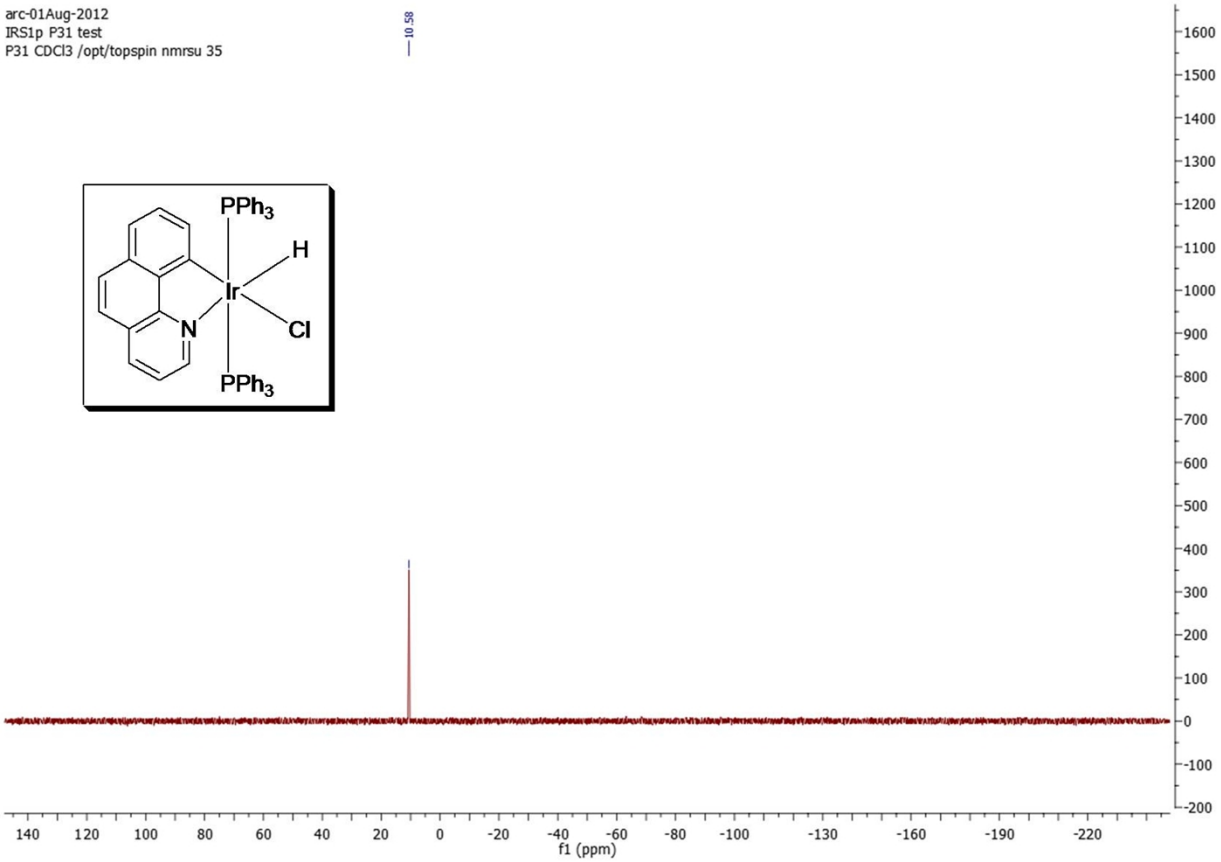
arc-01Aug-2012
IRS1p P31 test
P31 CDCl3 /opt/topspin nmrsu 35
10.58
PPh3
H
Ir
N
Cl
PPh3
f1 (ppm)

c

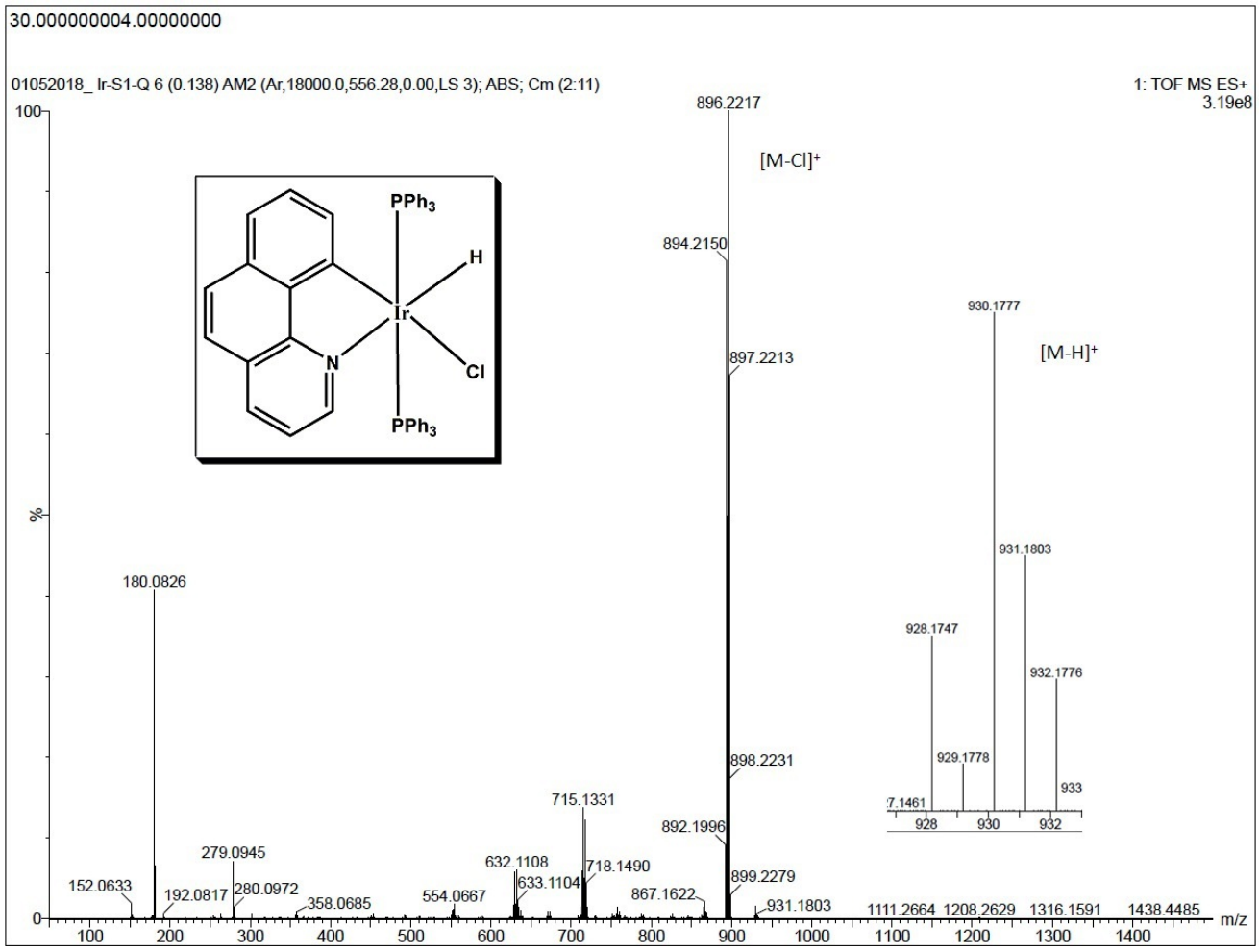

d

Fig. S13. (^{1}H,^{13}C,^{31}P) NMR spectra are shown in a, b, c and HRMS data in d respectively for **9**.

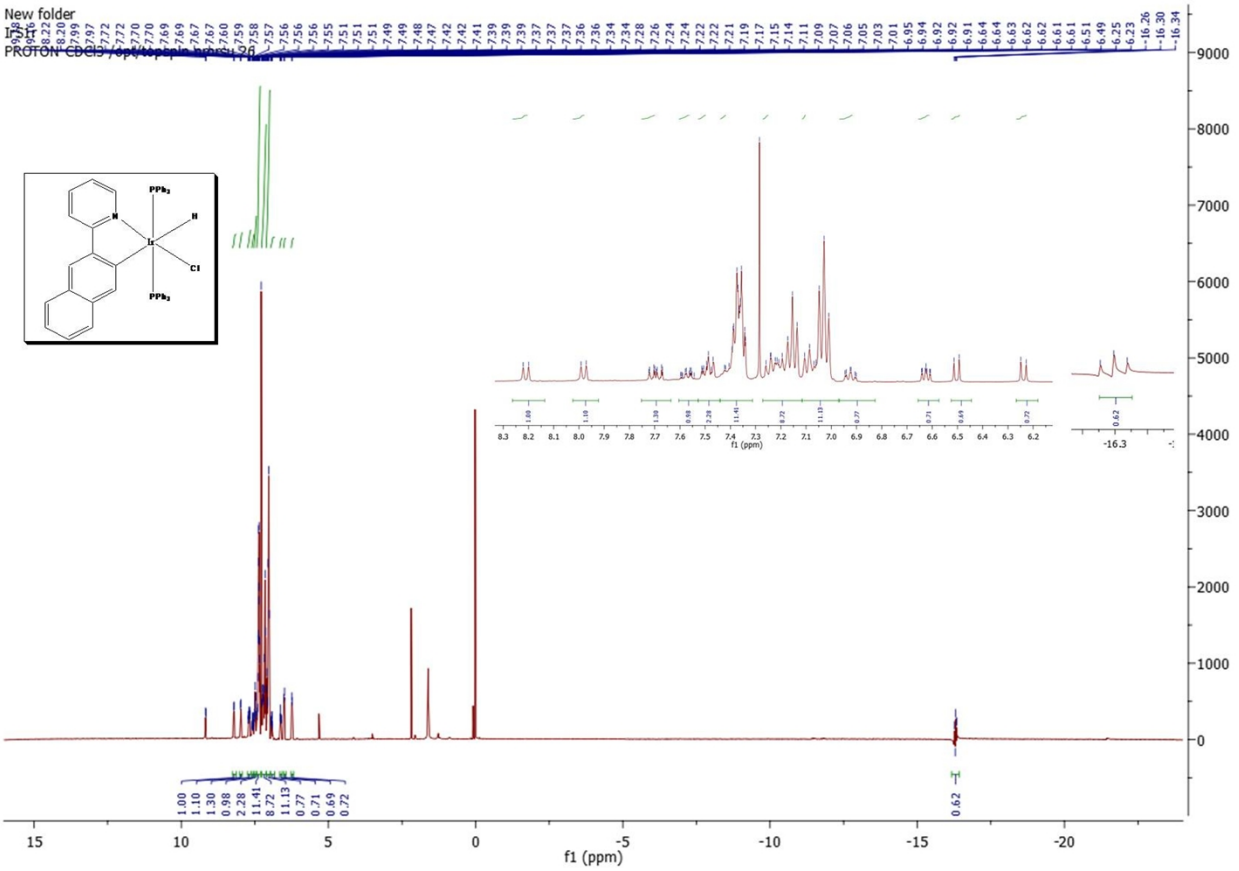
New folder
PPh2
H
Ir
Cl
PPh2
1.00
1.10
1.30
0.98
2.28
11.41
8.72
11.13
0.77
0.71
0.69
0.72
0.62
15
10
5
0
-5
-10
-15
-20
f1 (ppm)
9000
8000
7000
6000
5000
4000
3000
2000
1000
0
-16.3

a

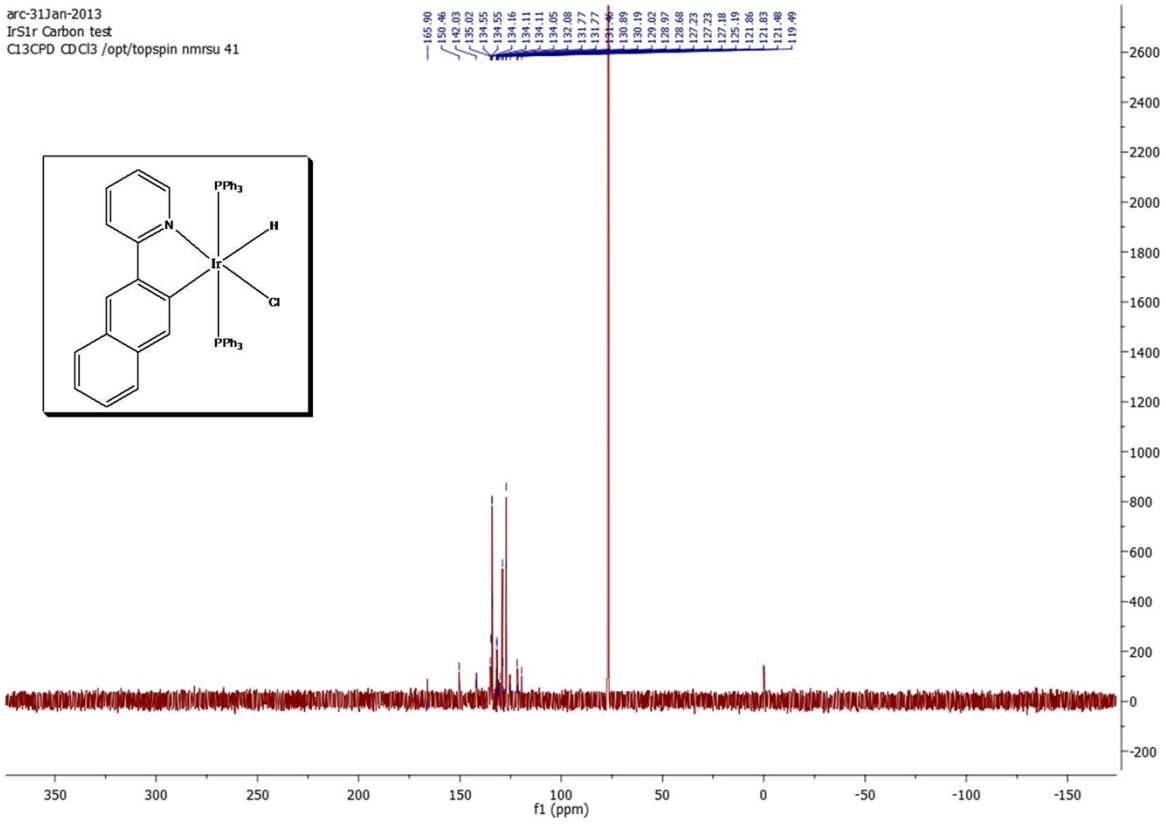
arc-31Jan-2013
IrS1r Carbon test
C13CPD CDCl3 /opt/topspin nmrsu 41
165.90
150.46
142.03
135.02
134.55
134.55
134.16
134.11
134.11
134.05
132.08
131.77
131.77
131.46
130.89
130.19
129.02
128.97
128.68
127.23
127.23
127.18
125.19
121.86
121.83
121.48
119.49
PPh3
N
H
Ir
Cl
PPh3
2600
2400
2200
2000
1800
1600
1400
1200
1000
800
600
400
200
0
-200
350
300
250
200
150
100
50
0
-50
-100
-150
f1 (ppm)

b

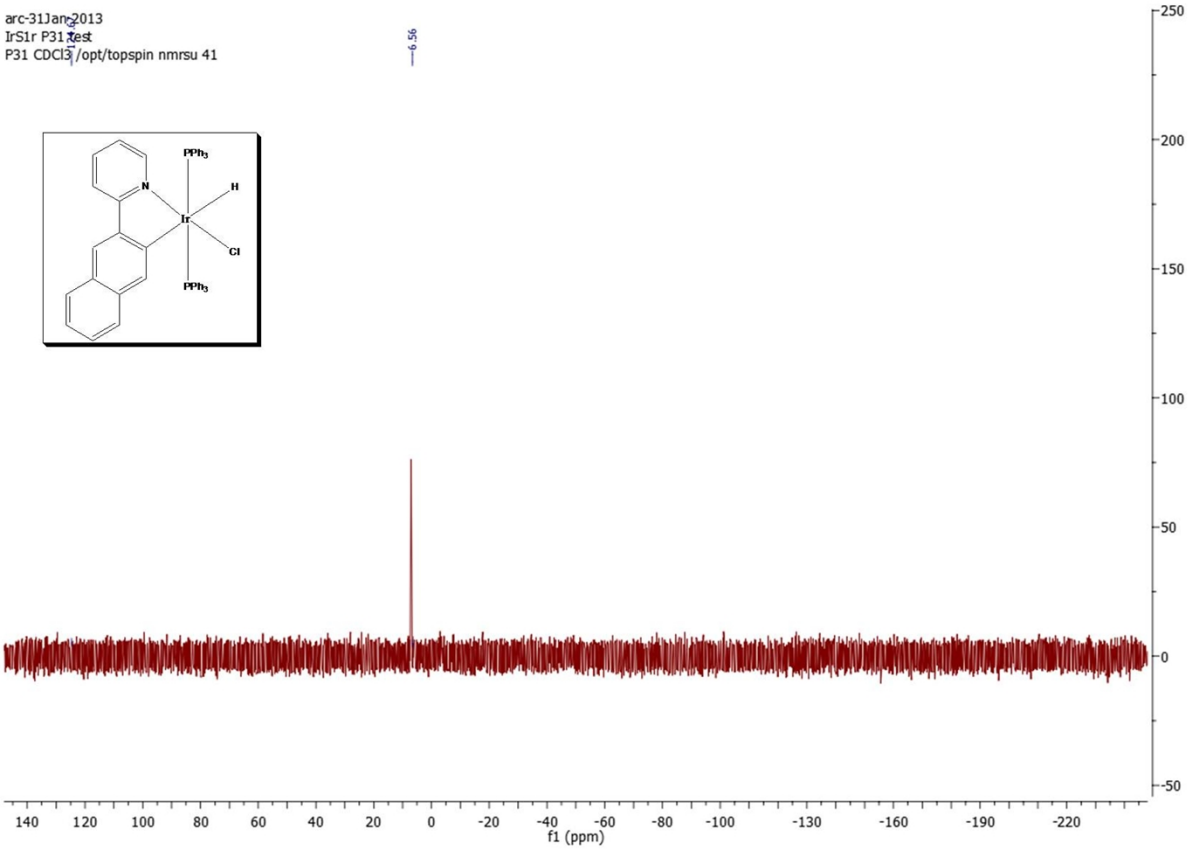

c

Acquisition Parameter

Source Type	ESI	Ion Polarity	Positive	Set Nebulizer	0.3 Bar
Focus	Active	Set Capillary	3700 V	Set Dry Heater	180 °C
Scan Begin	50 m/z	Set End Plate Offset	-500 V	Set Dry Gas	4.0 l/min
Scan End	1500 m/z	Set Collision Cell RF	1500.0 Vpp	Set Divert Valve	Source

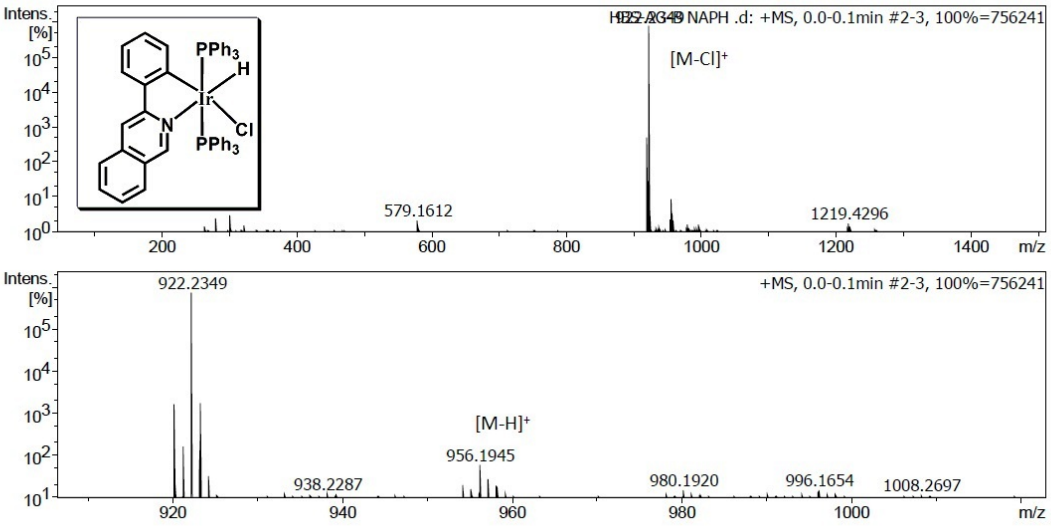

Fig. S14. (^{1}H,^{13}C,^{31}P) NMR spectra are shown in a, b, c and HRMS data in d respectively for **10**.

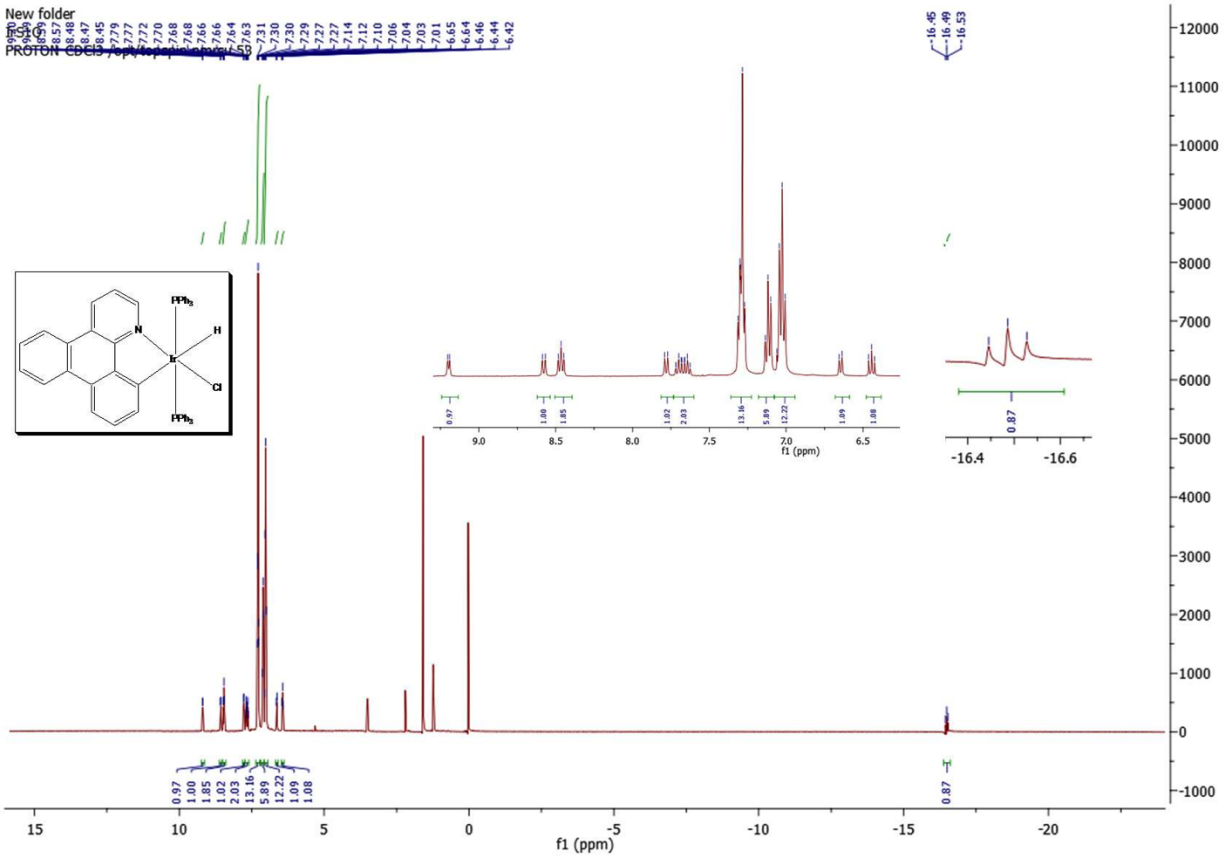

a

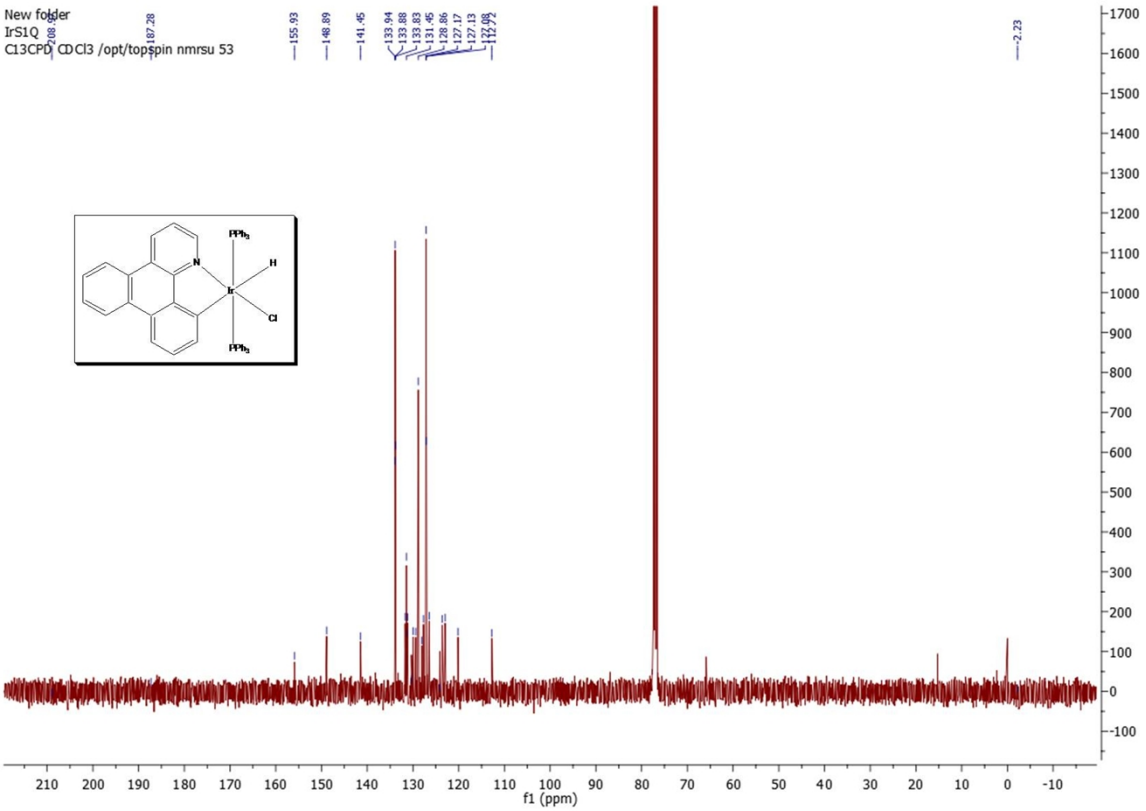
New folder
IrS1Q
C13CPD, CDCl3 /opt/topspin nmrsu 53
155.93
148.89
141.45
133.94
133.88
133.83
131.45
128.86
127.17
127.13
-2.23
PPh3
H
N
Ir
Cl
PPh3
f1 (ppm)

b

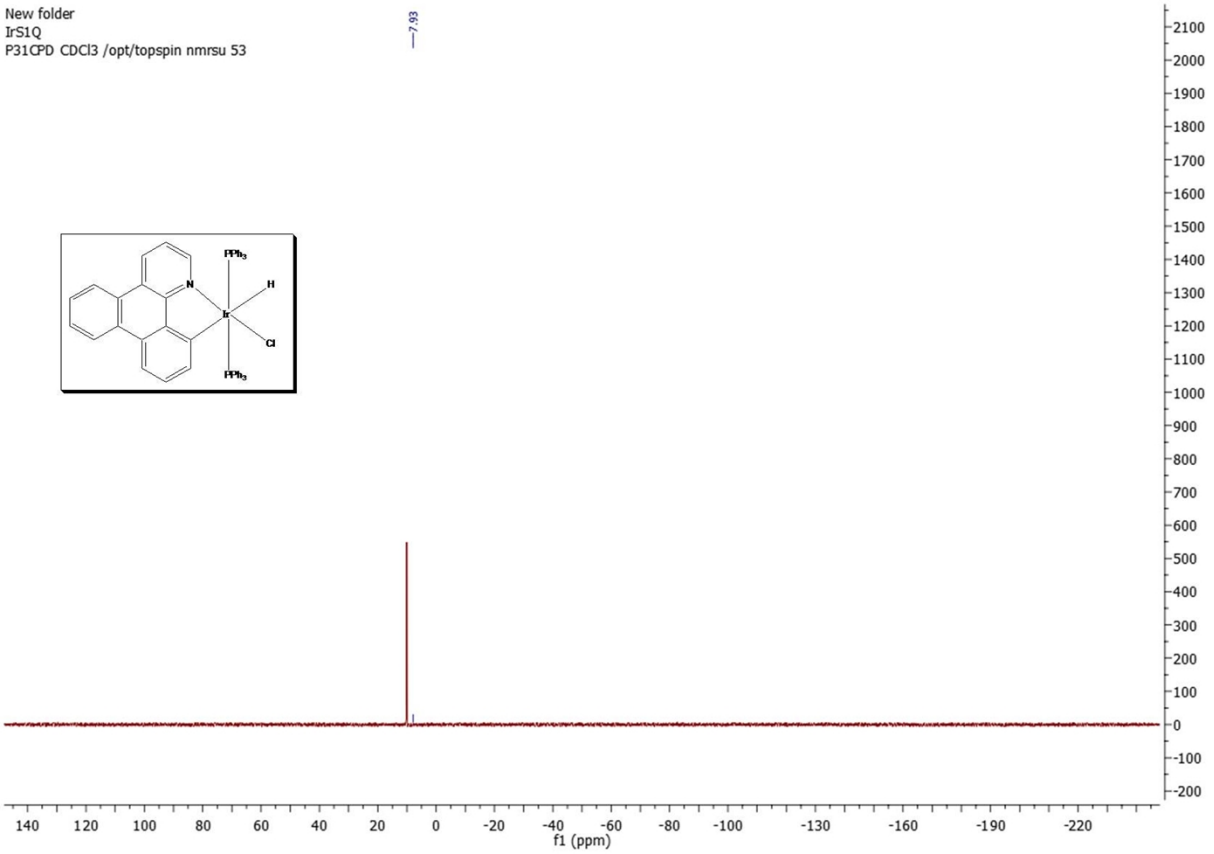
New folder
IrS1Q
P31CPD CDCl3 /opt/topspin nmrsu 53
7.93
PPh3
N
H
Ir
Cl
PPh3
2100
2000
1900
1800
1700
1600
1500
1400
1300
1200
1100
1000
900
800
700
600
500
400
300
200
100
0
-100
-200
140
120
100
80
60
40
20
0
-20
-40
-60
-80
-100
-130
-160
-190
-220
f1 (ppm)

c

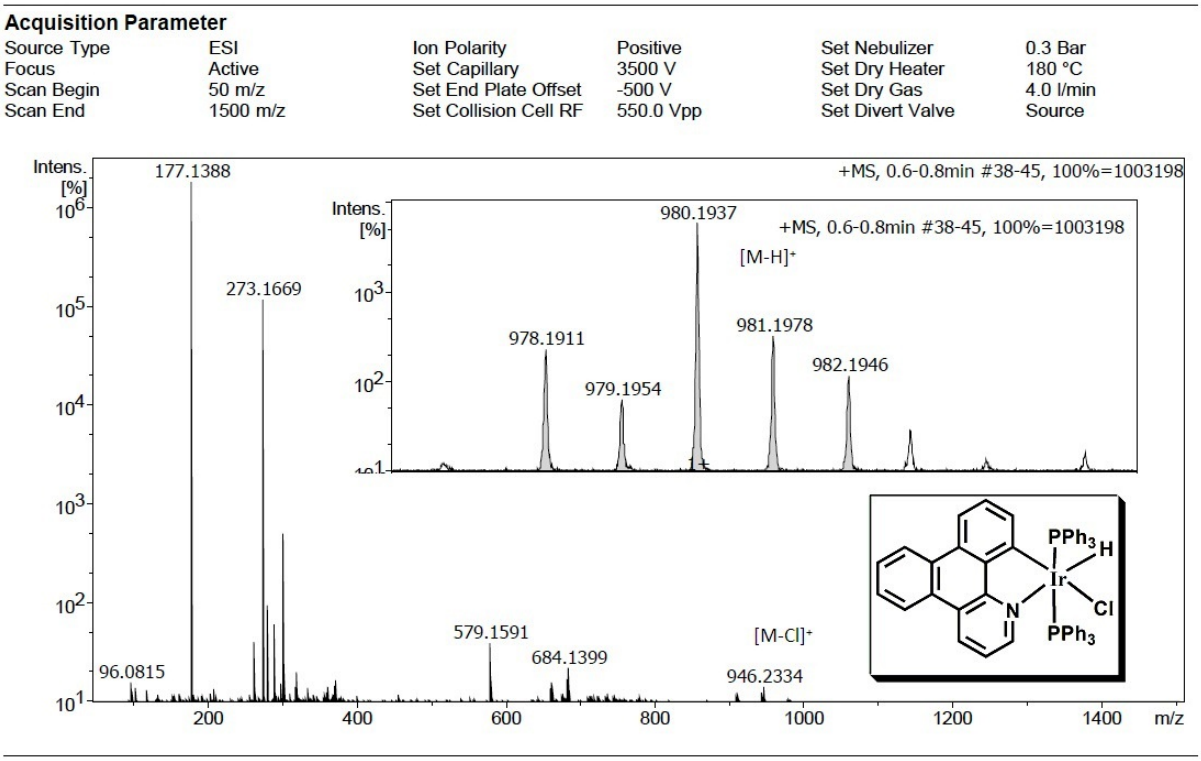

D

Fig. S15. (^{1}H,^{13}C,^{31}P) NMR spectra are shown in a, b, c and HRMS data in d respectively for **11**.

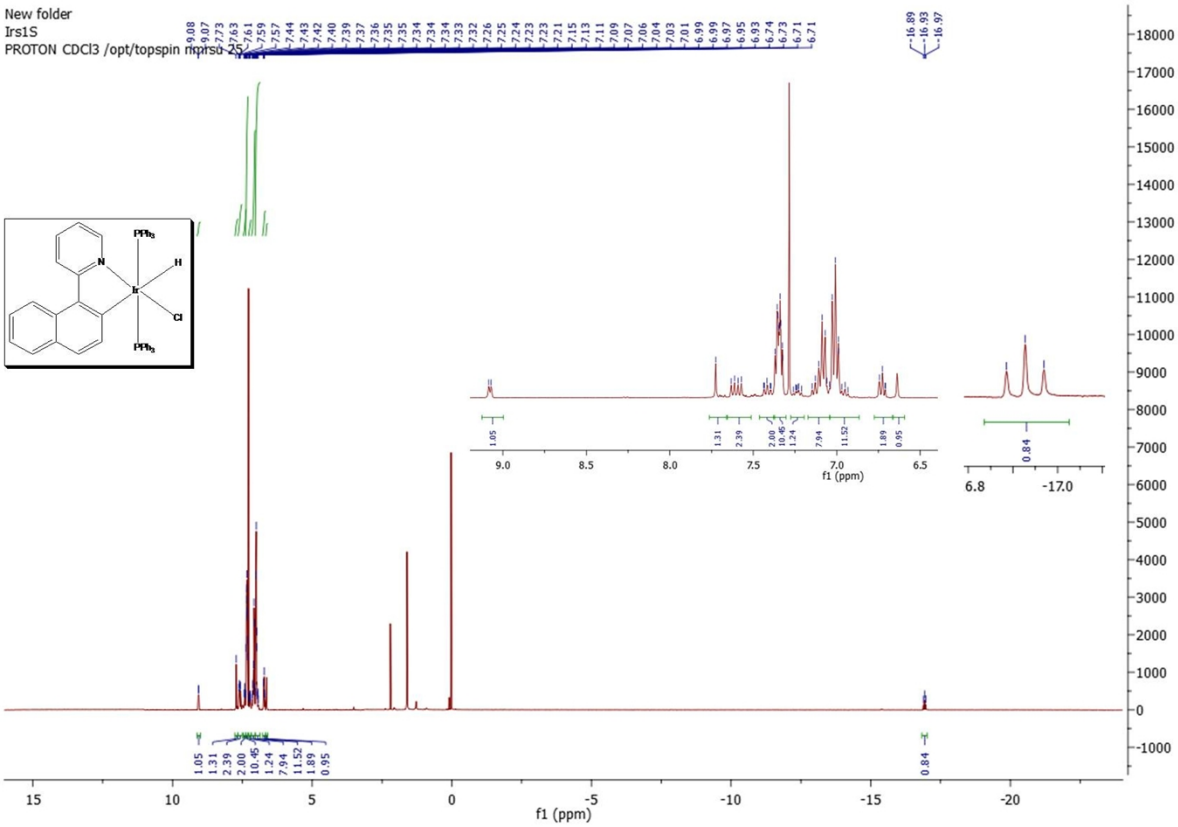
New folder
Irs1S
PROTON CDCl3 /opt/topspin nmrsu 25
f1 (ppm)

a

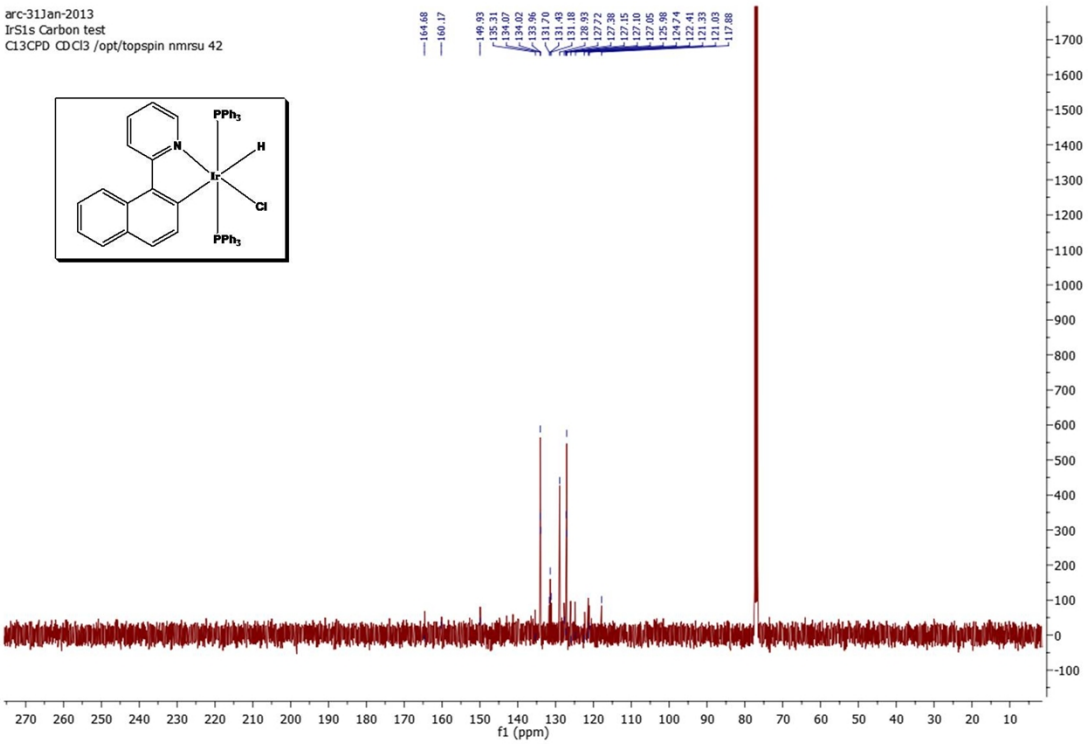
arc-31Jan-2013
IrS1s Carbon test
C13CPD CDCl3 /opt/topspin nmrsu 42
f1 (ppm)

b

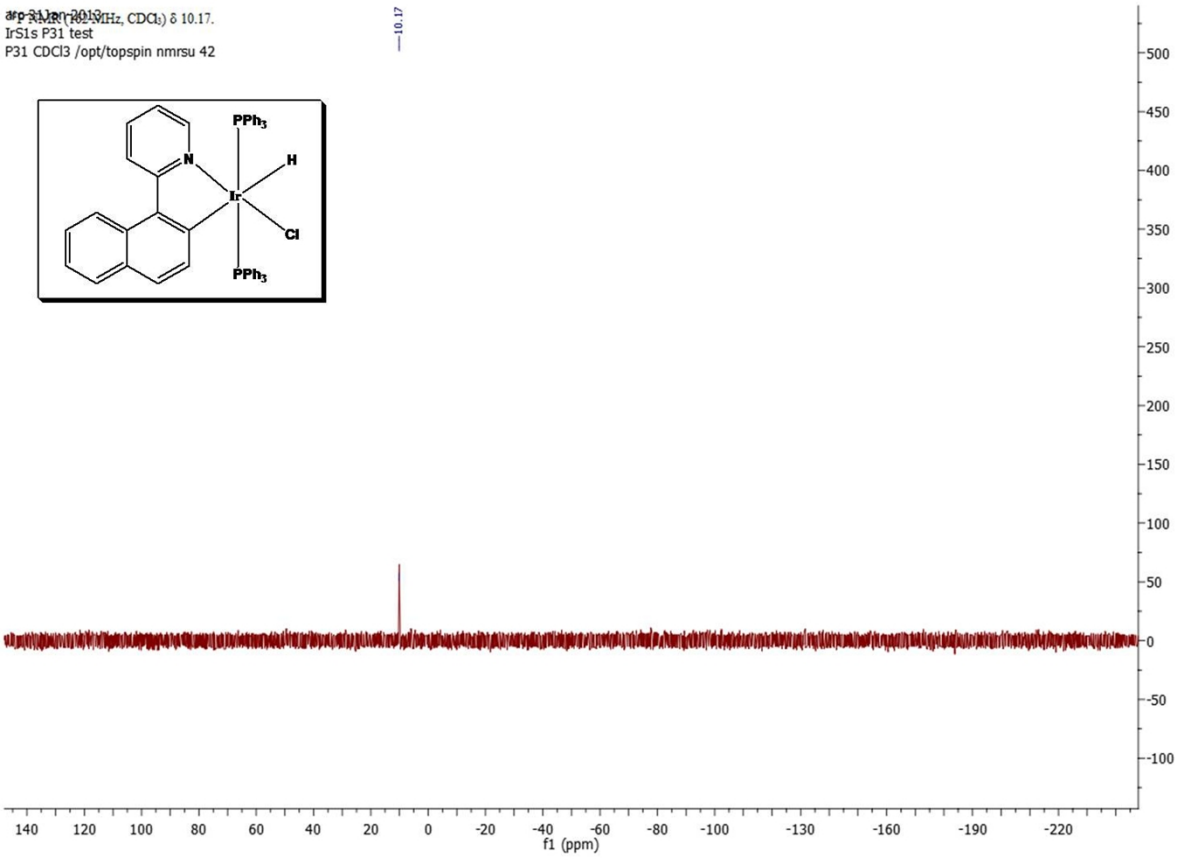
IrS1s P31 test
P31 CDCl3 /opt/topspin nmrsu 42
10.17
PPh3
N
H
Ir
Cl
PPh3
500
450
400
350
300
250
200
150
100
50
0
-50
-100
140
120
100
80
60
40
20
0
-20
-40
-60
-80
-100
-130
-160
-190
-220
f1 (ppm)

c

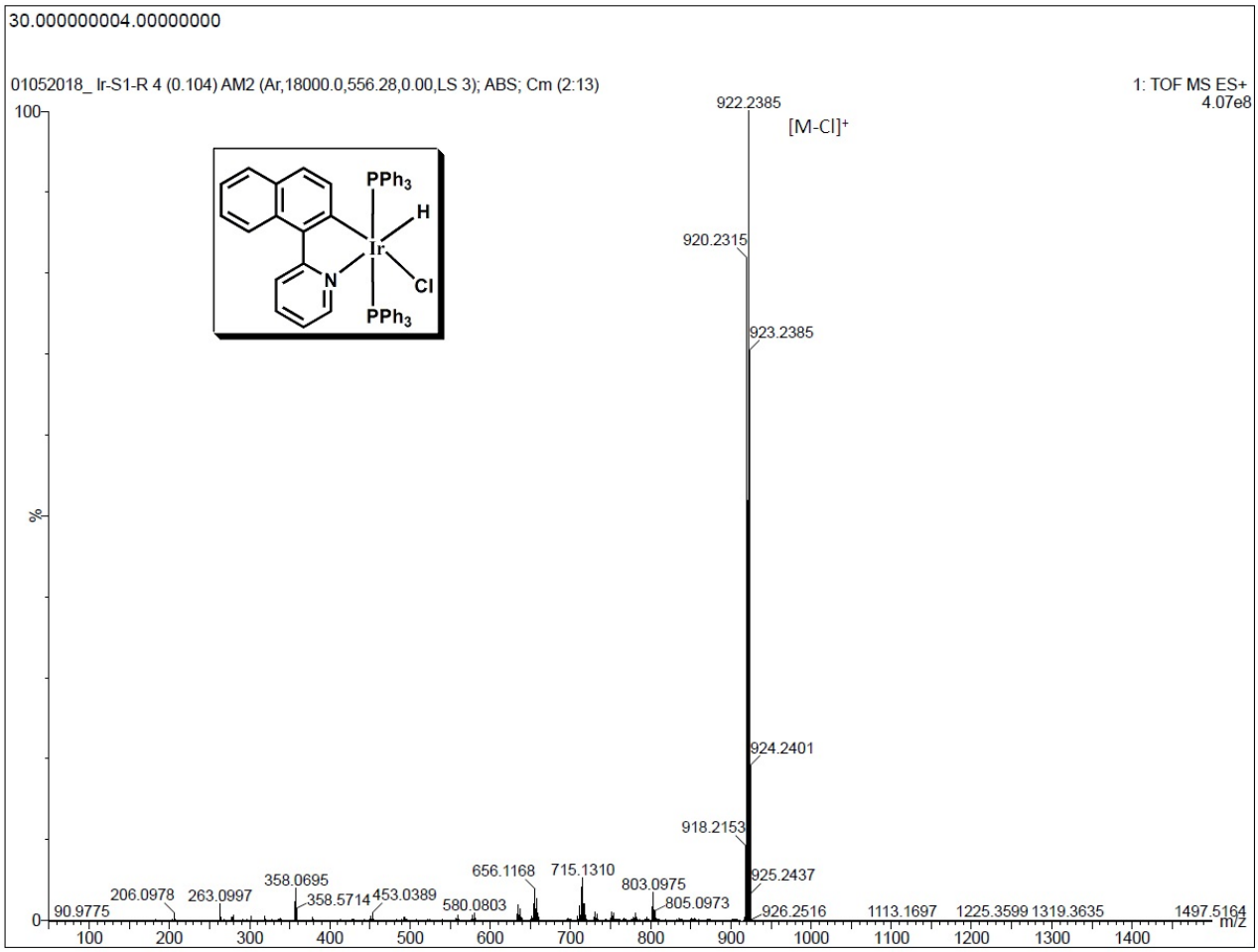

Fig. S16. (^{1}H,^{13}C,^{31}P) NMR spectra are shown in a, b, c and HRMS data in d respectively for **12.**

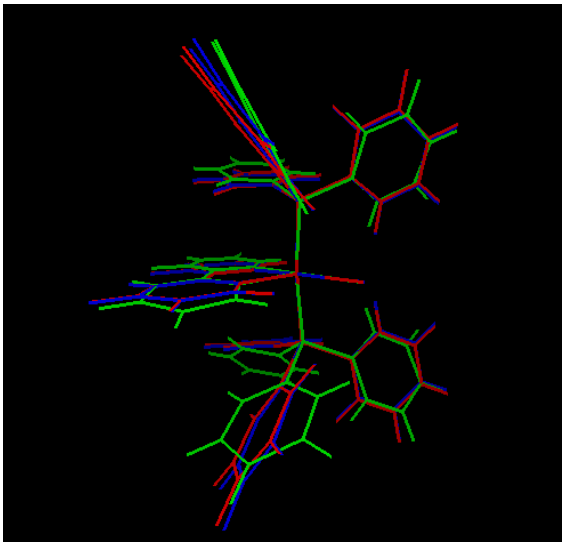

2

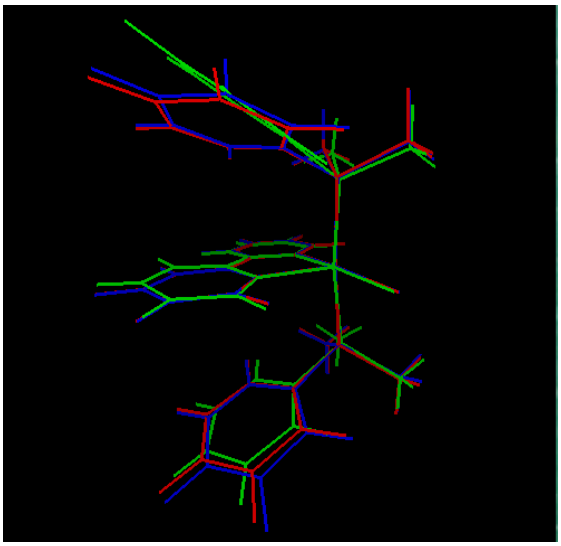

8

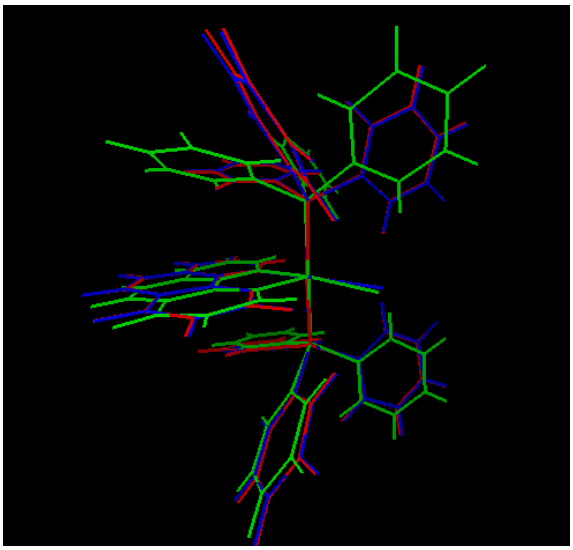

9

Fig. S17. Geometry comparison between the x-ray crystal (green), and the ground state (blue) and lowest triplet (red) optimized geometries in DMC solution of complexes **2**, **8** and **9**.

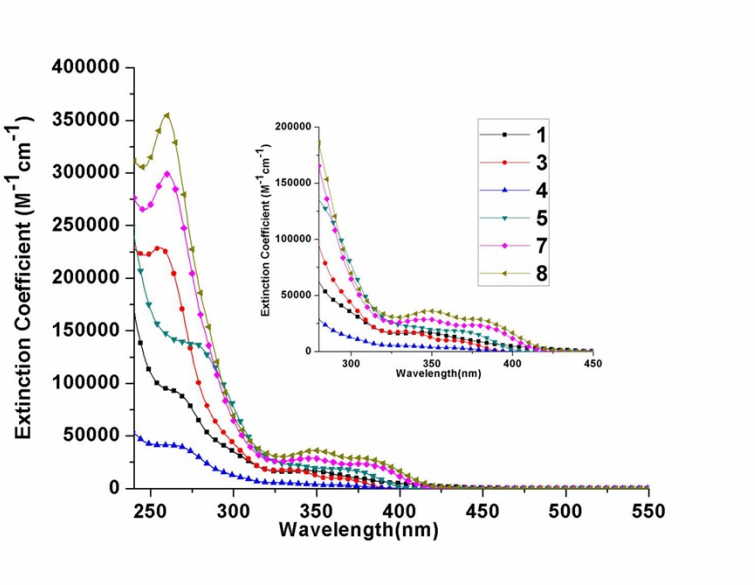

Fig. S18. Solution UV-Vis absorbance spectra (10^{-5}M, DCM) of the complexes, **1-8** [short range spectrum are showed in inset (260 -450 nm)]

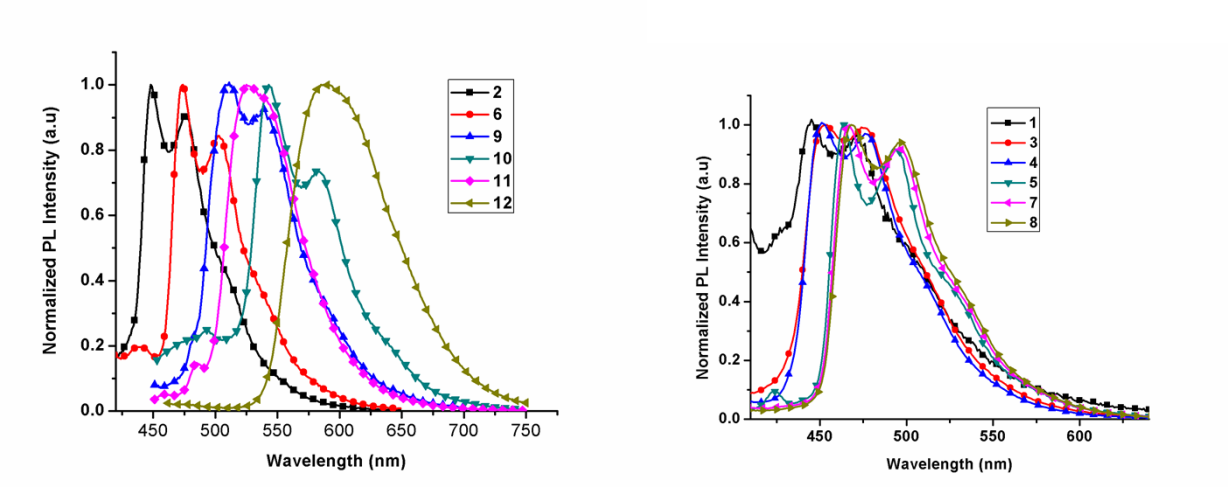

a b

Fig. S19 (a,b) The normalized PL spectra of complex **1-12** in 10^{-4} M DCM.

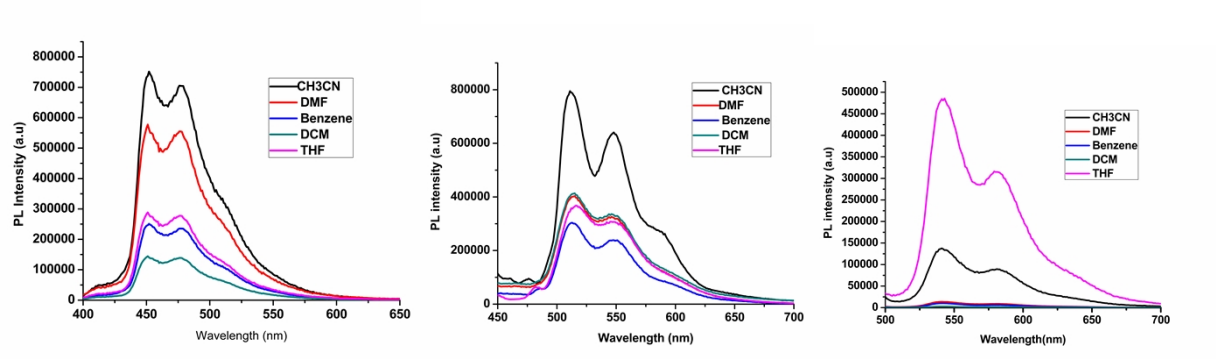

a **b** **c**

Fig. S20. The PL spectra of complexes **2**, **9** and **10** in different solvents with the concentration $1x10^{-4}$ mol.L^{-1}.

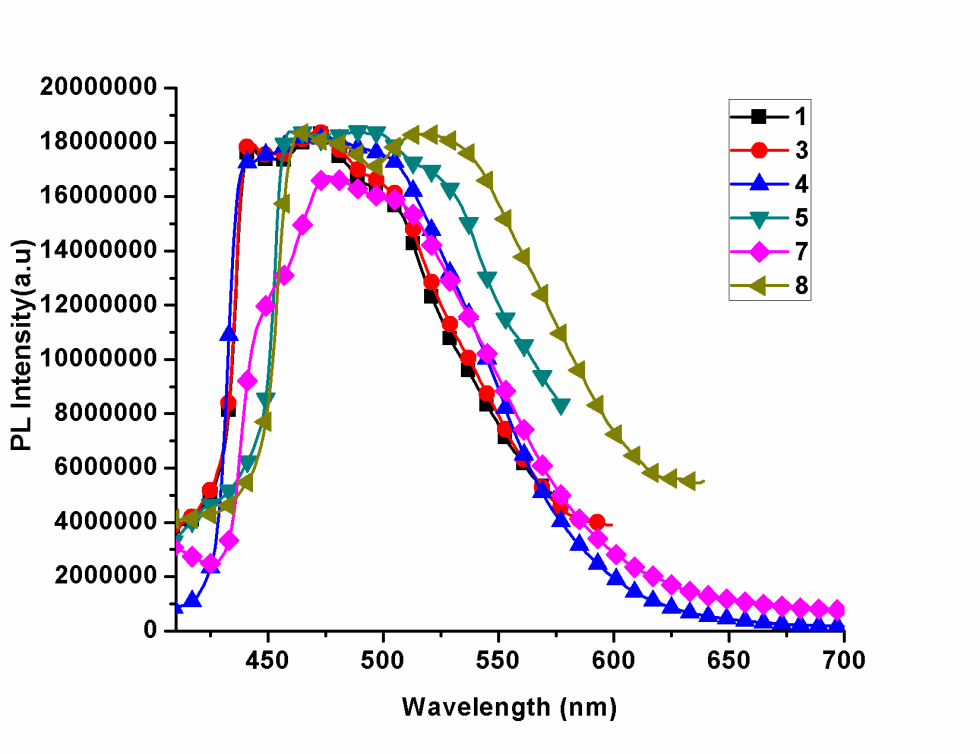

Fig. S21. Solid state PL spectrum for **1-8**, showing the tuning of emission wavelengths

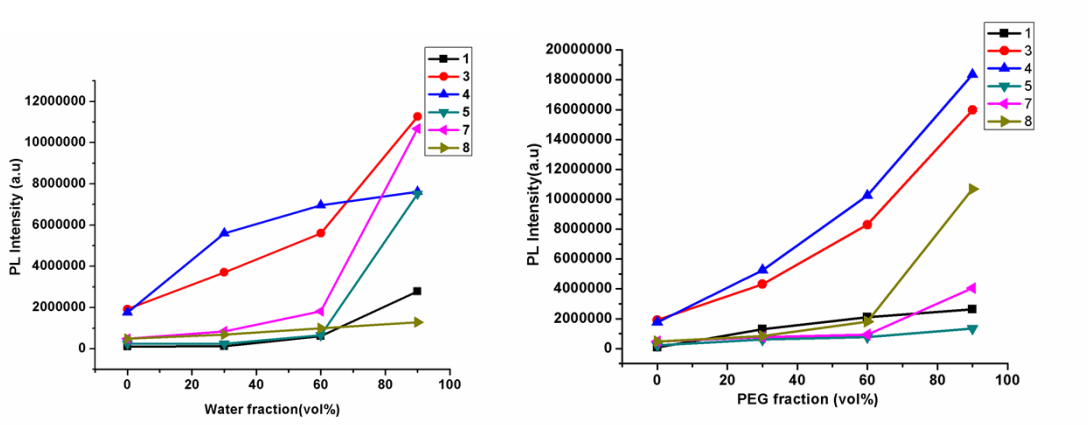

a b

Fig. S22. (a) change in PL intensity of complexes **1, 3, 4, 5, 7** and **8** with changing the water fraction **(b)** change in PL intensity of complexes **1, 3, 4, 5, 7** and **8** with changing the PEG fraction.

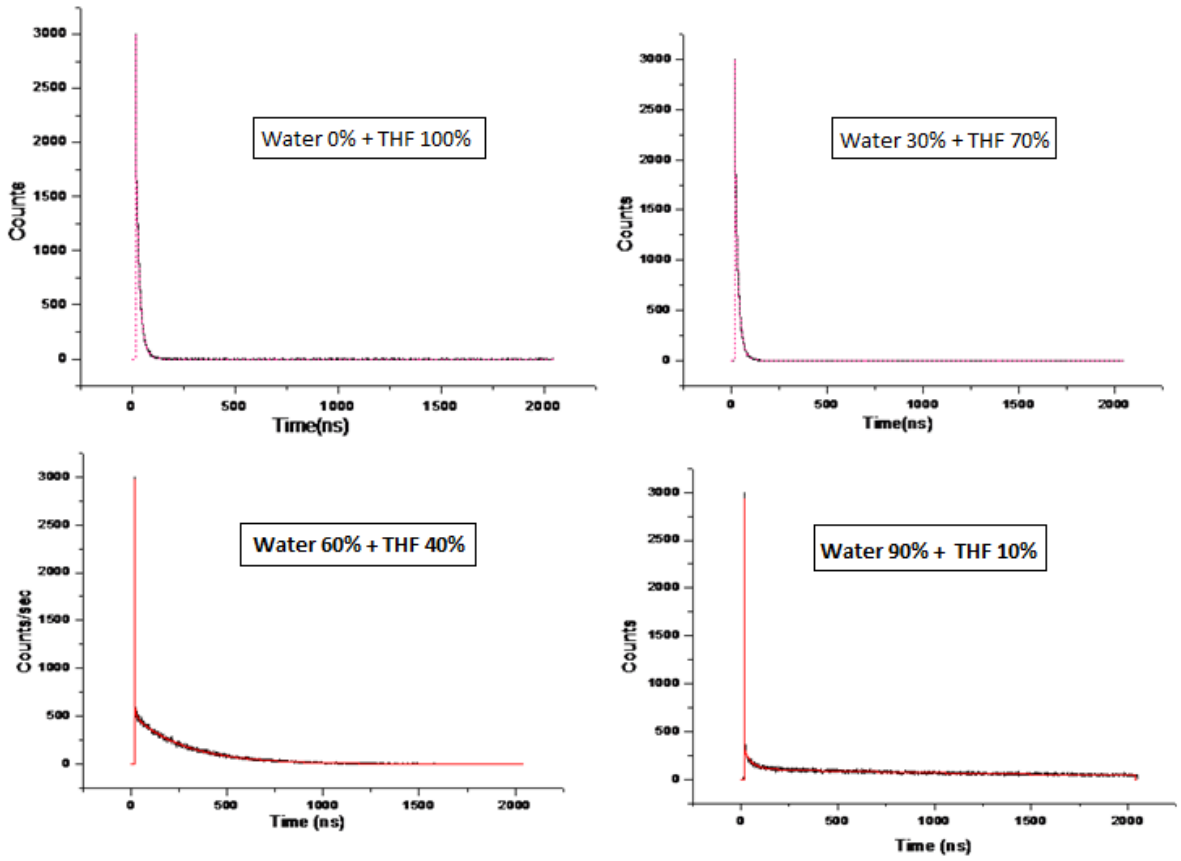

Fig. S23. Photoluminescence life-time decay curves in 0, 30, 60 and 90% water fractions in THF for the complex **6** (0% water was fitted bi exponentially and 30, 60 and 90% were fitted tri expoenentially; red is the fitting curve).

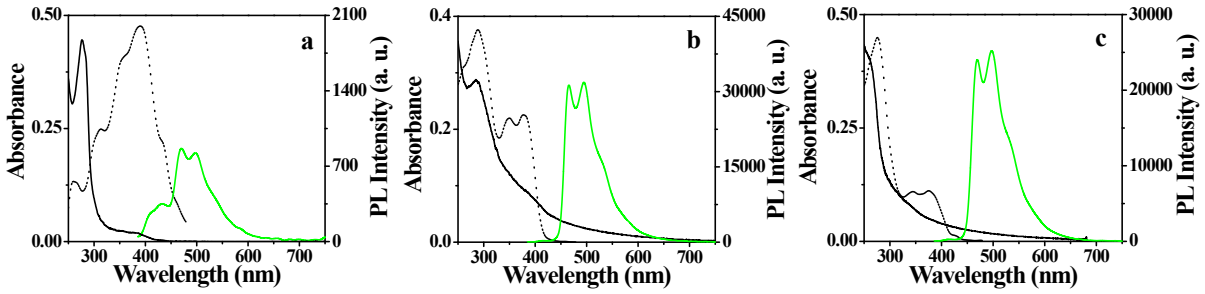

Fig. S24. Absorption, excitation and photoluminescence property of (a) iridium complex in THF (b) aggregated iridium complex in water (c) iridium complex **6** encapsulated PEG-PLA nanoparticles.

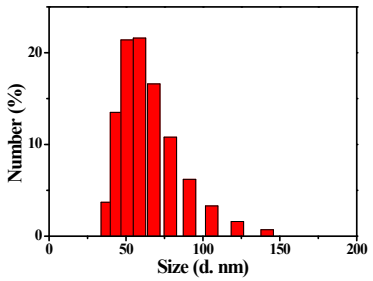

Fig.S25. DLS histogram of PEG-PLA nanoparticles in water.

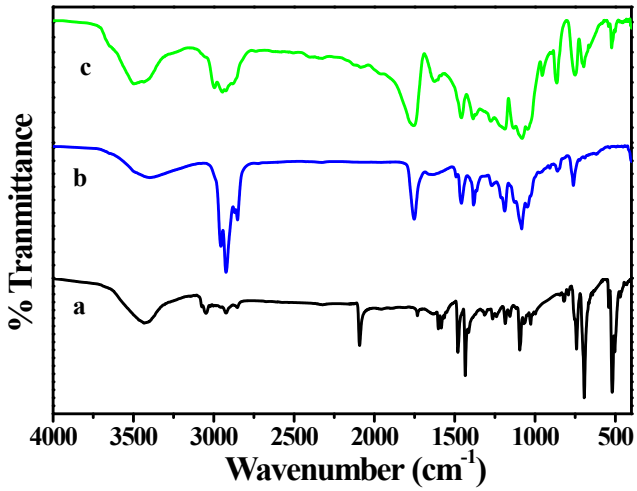

Fig. S26. FTIR spectra of (a) iridium complex **6**, (b) PEG-PLA nanoparticles and (c) iridium complex **6** encapsulated PEG-PLA nanoparticles.

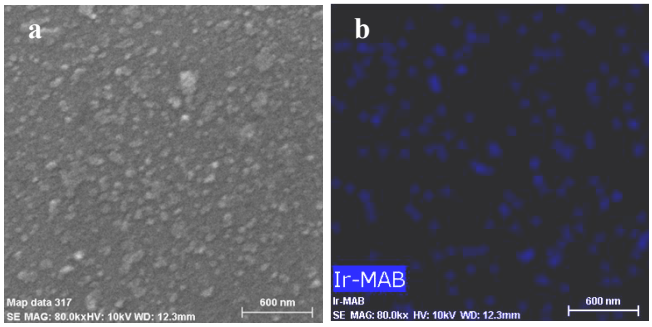

Fig. S27. SEM image of iridium complex **6** encapsulated PEG-PLA particles (a) and the corresponding elemental mapping image of iridium (b).

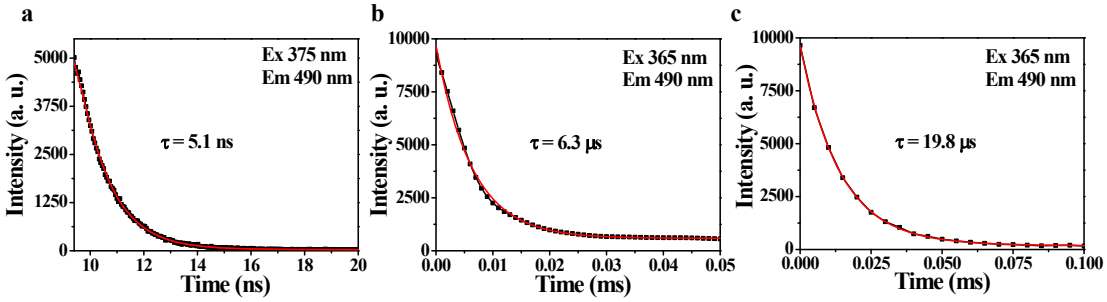

Fig. S28. Luminescent lifetime decay curve of (a) iridium complex in THF (b) aggregated iridium complex in water and (c) iridium complex encapsulated PEG-PLA nanoparticles. Black and red lines correspond to experimental and fitted data respectively.

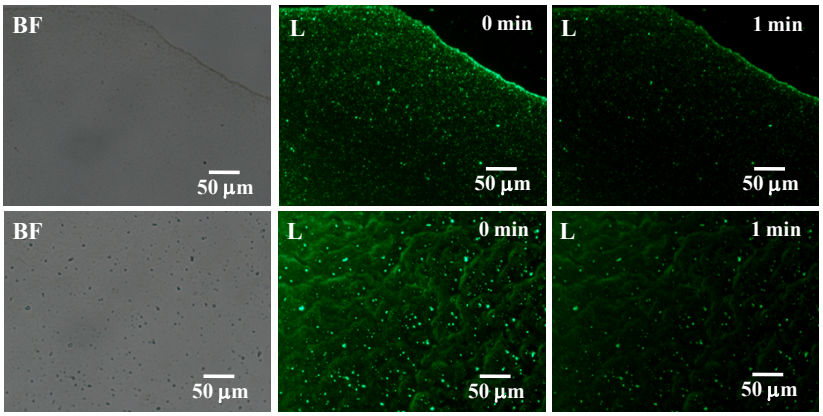

Fig. S29. Bright field (BF) and luminescence(L)image under UV light exposure of the films of iridium complex. Top row represents aggregated iridium complex in water and bottom row represents for iridium complex encapsulated PEG-PLA nanoparticles.

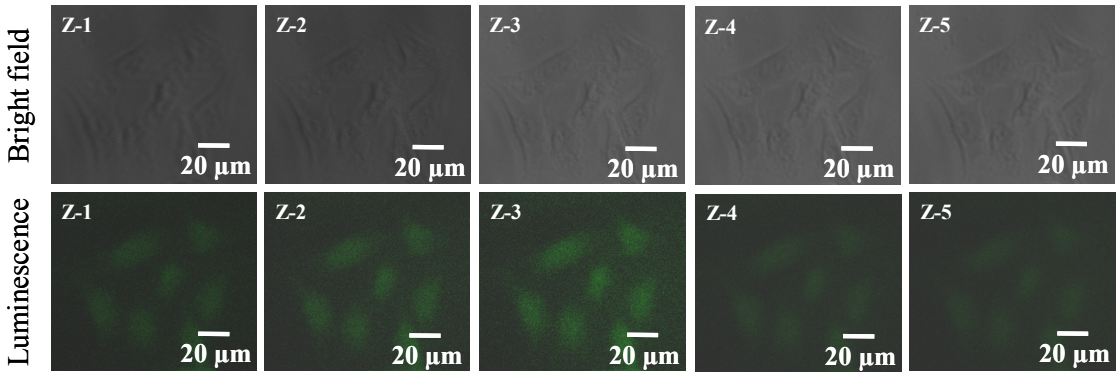

Fig. S30. A series of images of particle labeled HeLa cells using at different Z planes from top to bottom with consecutive Z-axis slices of 3.42 μm each, demonstrating that the particles are located both in cytoplasm and at cell surface.

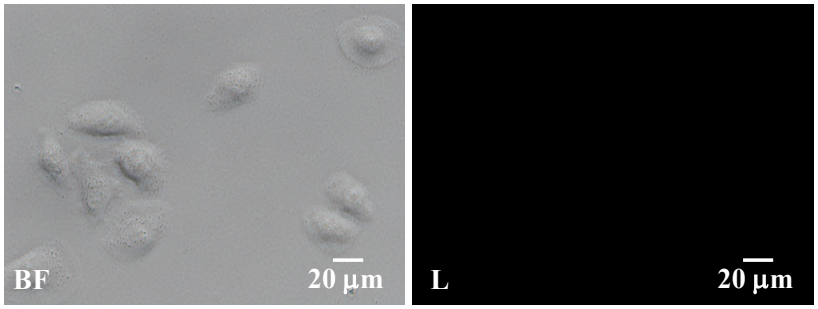

Fig. S31. Bright field (BF) and luminescence (L) image of HeLa cells after incubated with aggregated iridium complex in water for 4 hours.

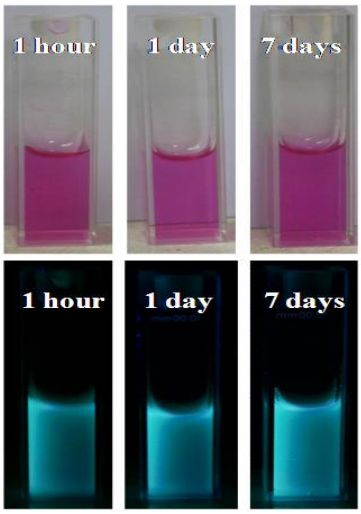

Fig. S32. The digital images of iridium complex **6** encapsulated PEG-PLA particles in cell culture medium without any significant precipitation till 7 days. Particles are mixed with Dulbecco's modifed eagle medium (DMEM) with 10 % fetal bovine serum (FBS) and images are taken after one hour, one day and 7 days. Top and bottom row shows the images of solution under ordinary light and UV light.

Table S1. The time required to produce the intermediates A (i,j,k,l), the complexes (1-12) and the yields of the complexes (1-12).

Reaction Time (h)			
Complex	Intermediate	product	Yield (%)
1	7.0	12	44[a],33[b] (off white solid)
2	5	3	70[a],56[b] (green solid)
3	5	3	53[a] (green solid)
4	6.3	12	31[a] (green solid)
5	7.0	3	38[a] (green solid)
6	4	3	65[a],56[b] (green solid)
7	4	3	45[a] (green solid)
8	6.3	12	36[a] (green solid)
9	4.0	3	60[a],46[b] (green solid)
10	4.0	3	50 [a] (yellow solid)
11	4.0	3	55[a],40[b] (yellow solid)
12	4.0	3	31[a],20[b] (brown solid)

[a]with Na_2CO_3 and [b]without Na_2CO_3

Table S2. Crystal data and structure refinement for 2, 8 and 9.

	2	9	8
Empirical formula	C47H36ClF2IrNP2	C49H39ClIrNP2	IrC27H30ClNP2
Formula weight	942.38	931.4	857.07
Temperature (K)	100.00	296.15	100.00
Crystal system	Orthorhombic	triclinic	orthorhombic
Space group	Pna21	P-1	P212121
Unit cell dimensions	a = 32.2085(4) Å b = 12.2682(1) Å c = 9.6830(1) Å α = β = γ = 90°	a = 10.1170(3) Å b = 12.0586(4) Å c = 16.2142(5) Å α = 100.1390(10) β = 95.3490(10) γ = 94.1500(10)	a = 9.6548(4) Å; b = 15.9271(7)Å; c = 17.1527(7)Å α = β = γ = 90°
Volume (Å3)	3826.14	1930.74(10)	2637.62(19)
Z	4	2	4
Density (Mg/m3)	1.636	1.602	2.158
Absorption coefficient (mm-1)	3.692	3.647	5.330
F(000)	1868	928.0	1632
Crystal size (mm3)	0.2 × 0.2 × 0.1	0.2 × 0.1 × 0.1	0.2 × 0.2× 0.15
Theta range for data collection (°)	2.45 to 37.03	2.56 to 60.06	3.48 to 60.12
Index ranges	0 ≤ h ≤ 54; 0 ≤ k ≤ 20; 0 ≤ l ≤ 16	-13 ≤ h ≤ 14, -16 ≤ k ≤ 16, -22 ≤ l ≤ 22	-12 ≤ h ≤ 13, -22 ≤ k ≤ 21, -24 ≤ l ≤ 24

Reflections collected	10162	33437	24769
Independent reflections	9908 [R(int) = 2.23%]	11275 [R(int) = 0.0176]	7654 [R(int) = 0.0301]
Data / restraints / parameters	10162/1/487	11275/0/491	7654/0/293
Goodness-of-fit on F2	1.062	1.062	0.962
Final R indices [I>2sigma(I)]	R1 = 0.0223, wR2 = 0.0617	R1 = 0.0163, wR2 = 0.0382	R1 = 0.0260, wR2 = 0.0619
R indices (all data)	R1=0.0233, wR2 = 0.0622	R1 = 0.0177, wR2 = 0.0395	R1 = 0.0307, wR2 = 0.0711
Largest diff. peak and hole (e.Å-3)	1.932, -2567	1.44, -0.75	1.961, -0.933

Table S3. Selected Bond lengths [Å] and angles [°] for **2**, **8** and **9.**

Bond distances (Å)	**2**	**9**	**8**
Ir1- C19	1.998(3)	2.0211(15)	(Ir-C27) 2.009(4)
Ir1- N1	2.160(2)	2.1529(13)	2.142(3)
Ir1 - P1	2.3199(6)	2.3251(4)	2.3069(12)
Ir1-P2	2.3278(6)	2.3229(4)	2.2931(12)
Ir1-Cl1	2.4641(7)	2.4748(4)	2.5037(10)

Bond angles (°)	**2**	**9**	**8**

C19 Ir1 N1	78.99(10)	80.30(6)	C27Ir1N1, 79.47(15)
C19 Ir1 P1	91.25(8)	85.80(4)	90.43(12)
N1 Ir1 P1	95.37(6)	92.90(4)	95.91(10)
C19 Ir1 P2	95.38(8)	88.57(4)	C27 Ir1 P2, 90.53(12)
N1 Ir1 P2	91.68(6)	94.62(4)	94.91(10)
P1 Ir1 P2	171.13(2)	169.718(13)	169.13(4)
C19 Ir1 Cl1	176.97(8)	170.64(5)	171.83(13)
N1 Ir1 Cl1	98.14(7)	90.82(4)	C27Ir1Cl1, 92.36(10)
P1 Ir1 Cl1	88.04(2)	97.684(13)	90.67(4)
P2 Ir1 Cl1	85.63(2)	89.211(14)	89.92(4)

Table S4. Selected bond lengths and angles for the ground state optimizedgeometriesin dichloromethane (ε=8.93) of complexes **2**, **6** and **8-12** at the B97-D/6-31+G(d)/LANL2DZ with IEF-PCM computational level.

	Bond distances, Å					Angles (º)		
Complex	Ir-N	Ir-C	Ir-Cl	Ir-H	Ir-P	N-Ir-C	Cl-Ir-H	P-Ir-P
2	2.193	2.007	2.593	1.600	2.345	79.1	91.5	171.1
6	2.201	2.014	2.612	1.601	2.339	79.1	92.4	171.3
8	2.189	2.013	2.618	1.611	2.325	79.1	90.9	175.1
9	2.220	2.018	2.604	1.597	2.340	79.9	92.4	172.5
10	2.050	2.106	2.484	1.673	2.339	80.0	91.7	170.5
11	2.047	2.111	2.485	1.670	2.340	80.0	91.3	171.4
12	2.043	2.101	2.490	1.672	2.340	79.1	91.1	170.2

Table S5. Selected bond lengths and angles for the lowest triplet state optimizedgeometries in dichloromethane (ε=8.93) of complexes **2**, **6** and **8-12** at the B97-D/6-31+G(d)/LANL2DZ with IEF-PCM computational level.

	Bond distances, Å					Angles (º)		
Complex	Ir-N	Ir-C	Ir-Cl	Ir-H	Ir-P	N-Ir-C	Cl-Ir-H	P-Ir-P
2	2.174	1.985	2.555	1.604	2.366	80.8	90.7	172.6
6	2.188	1.980	2.576	1.603	2.363	81.1	91.7	172.9
8	2.181	1.978	2.590	1.613	2.348	81.2	90.9	176.3
9	2.224	1.981	2.573	1.598	2.354	79.7	91.6	173.1
10	2.048	2.081	2.495	1.675	2.342	79.9	91.6	170.3
12	2.065	2.093	2.456	1.665	2.352	79.2	95.3	172.2

Table S6. Comparison between experimental absorption maxima (λ_{exp}) and extinction coefficients to the computed transition energies (λ_{cals}) and oscillator strengths for complexes **2**, **6**, **8**, **9**, **10** and **12** in DCM solution. Computed values obtained at the B3LYP/6-31+G(d)/LANL2DZ level (IEF-PCM).

Complex	λ_{exp} / nm	ε	State	λ_{cals} / nm	strength	Composition
2	430	0.05	T_1	433	-	HOMO → LUMO (56%) HOMO-3 → LUMO (25%)
	-	-	T_2	367	-	HOMO-3 → LUMO (42%) HOMO → LUMO (36%)
	369	1.5	S_1	360	0.05	HOMO → LUMO (97%)
	338	2.3	S_5	310	0.04	HOMO-2 → LUMO (66%) HOMO → LUMO+1 (20%) HOMO-3 → LUMO (11%)
6	445	0.025	T_1	451	-	HOMO → LUMO (68%) HOMO-3 → LUMO (19%)
	-	-	T_2	381	-	HOMO-3 → LUMO (50%) HOMO → LUMO (26%)

	381	0.51	S_1	372	0.07	HOMO → LUMO (97%)
	343	0.65	S_5	312	0.03	HOMO-2 → LUMO (89%)
8	430	0.02	T_1	445	-	HOMO → LUMO (68%) HOMO-3 → LUMO (21%)
	-	-	T_2	376	-	HOMO-3 → LUMO (51%) HOMO → LUMO (27%)
	384	2.7	S_1	368	0.06	HOMO → LUMO (97%)
	349	3.6	S_4	317	0.02	HOMO → LUMO+1 (80%) HOMO-2 → LUMO (16%)
9	-	-	T_1	494	-	HOMO → LUMO (47%) HOMO → LUMO+1 (19%) HOMO-2 → LUMO (13%)
	451	0.04	T_2	442	-	HOMO → LUMO (45%) HOMO → LUMO+1 (37%)
	407	0.71	S_1	400	0.06	HOMO → LUMO (94%)
10	-	-	T_1	553	-	HOMO → LUMO (63%) HOMO-2 → LUMO (16%)
	-	-	T_2	444	-	HOMO-2 → LUMO (62%) HOMO → LUMO (24%)
	424	0.59	S_1	418	0.02	HOMO → LUMO (94%)
	336	5.1	S_3	356	0.21	HOMO-2 → LUMO (86%)
	319	5.5	S_8	328	0.11	HOMO-3 → LUMO (87%)
11	-	-	T_1	465	-	HOMO → LUMO (28%) HOMO-2 → LUMO (17%) HOMO-3 → LUMO+1 (10%) HOMO → LUMO+3 (10%)
	-	-	T_2	442	-	HOMO → LUMO (58%) HOMO → LUMO+1(13%) HOMO-2 → LUMO (13%)

	400	0.27	S_2	393	0.04	HOMO → LUMO (95%)
	331	1.86	S_5	342	0.09	HOMO-1 → LUMO+1 (43%) HOMO-2 → LUMO (29%) HOMO → LUMO+1 (22%)
	331	1.86	S_6	342	0.08	HOMO-1 → LUMO+1 (51%) HOMO-2 → LUMO (25%) HOMO → LUMO+1 (18%)
12	-	-	T_1	567	-	HOMO → LUMO (84%)
	-	-	T_2	425	-	HOMO-2 → LUMO (34%) HOMO-1 → LUMO (33%)
	423	0.4	S_1	419	0.08	HOMO → LUMO (84%) HOMO-1 → LUMO (12%)
	336	0.96	S_5	343	0.11	HOMO-2 → LUMO (77%)

Table S7. Comparison between experimental and calculated emission wavelengths of complexes **2**, **6**, **8**, **9**, **10** and **12** in DMC solution. Computed values obtained at the B3LYP/6-31+G(d)/LANL2DZ level (IEF-PCM).

λ_{em} / nm	**2**	**6**	**8**	**9**	**10**	**12**
calculated	537	563	558	636	714	773
Exp	451, 476	468, 499	468, 497	512, 548	543, 585	589